Covalent and Noncovalent Phthalocyanine–Carbon Nanostructure Systems: Synthesis, Photoinduced Electron Transfer, and Application to Molecular Photovoltaics

Giovanni Bottari,[†] Gema de la Torre,[†] Dirk M. Guldi,[*,‡] and Tomás Torres[*,†,§]

Departamento de Química Orgánica, Universidad Autónoma de Madrid, 28049 Madrid, Spain, IMDEA-Nanociencia, Facultad de Ciencias, Ciudad Universitaria de Cantoblanco, 28049 Madrid, Spain, and Department of Chemistry and Pharmacy and Interdisciplinary Center for Molecular Materials (ICMM), Friedrich-Alexander-Universität Erlangen-Nürnberg, Egerlandstrasse 3, 91058 Erlangen, Germany

Received July 17, 2009

Contents

* To whom correspondence should be addressed. E-mail: tomas.torres@uam.es (T.T.); dirk.guldi@chemie.uni-erlangen.de (D.M.G.).
[†] Universidad Autónoma de Madrid.
[‡] Friedrich-Alexander-Universität Erlangen-Nürnberg.
[§] IMDEA-Nanociencia.

1. Introduction

Photosynthesis is used by nature to convert light energy into chemical energy in some living systems. In such a process, a cascade of very efficient, short-range energy and electron transfer events between well-arranged, light-harvesting organic donor and acceptor pigments takes place within the photosynthetic reaction center, leading to the overall generation of chemical energy from sunlight with near quantum efficiency.[1−8]

During the past decade, a significant effort has been made by the scientific community toward the preparation of synthetic model compounds of natural photosynthetic systems able to convert light into other energy sources,[9] probably fostered by the increasing concerns related to the utilization of fossils fuels for the production of electricity in terms of both availability and environmental issues.

However, considering the structural complexity presented by the natural photosynthetic systems, much of the scientific effort has been devoted toward the preparation and study of structurally simpler systems, with the aim of reproducing some of the fundamental steps occurring in natural photosynthesis, one of the most important being the photoinduced charge separation (CS).[10−12]

Among the chromophores that have been used as molecular components in artificial photosynthetic systems, porphyrinoids, the ubiquitous molecular building blocks employed by nature in natural photosynthesis, have been the preferred and obvious choice, due to their intense optical absorption and rich redox chemistry.[13−20]

Within the large family of porphyrinoid systems, phthalocyanines (Pcs) enjoy a privileged position (Figure 1a). These chromophores, which have a two-dimensional 18-π-electron aromatic system isoelectronic with that of porphyrins (Pors), possess in fact unique physicochemical properties which render these macrocycles valuable building blocks in materials science.[21−32]

Pcs are thermally and chemically stable compounds which present an intense absorption in the red/near-infrared (IR) region of the solar spectrum with extinction coefficients (as high as 200 000 M^{-1} cm^{-1}) and fluorescence quantum yields

10.1021/cr900254z
Published on Web 04/05/2010

Giovanni Bottari (Italy, 1976) graduated in chemistry from the University of Messina, Italy, in 1999. In 2003 he obtained his Ph.D. from the University of Edinburgh, U.K., working in the preparation and study of stimulus-responsive rotaxane-based systems under the supervision of Prof. D. A. Leigh. After that, he joined the group of Prof. T. Torres at the Universidad Autónoma de Madrid (UAM), Spain, as a postdoctoral researcher benefiting from a two-year Marie Curie Intra European Fellowship working on the preparation of phthalocyanine-based molecular and supramolecular systems. Since 2006, G.B. has been a "Ramón y Cajal" Fellow at UAM. His current research interests include the preparation and study of multicomponent, phthalocyanine-based donor−acceptor molecular materials both in solution and on surfaces.

Gema de la Torre was born in Madrid, Spain, and graduated in chemistry from the Universidad Autónoma de Madrid (UAM) in 1992. She obtained her M.Sc. in 1993 and her Ph.D. in 1998 from the same university, working on the chemistry of phthalocyanines under the supervision of Prof. T. Torres. Following two one-year postdoctoral stays with Prof. W. Blau (Trinity College, Dublin, 2000−2001), working on the covalent functionalization of carbon nanotubes, and Prof. N. Martín (Universidad Complutense de Madrid, 2001−2002), working on porphyrin−fullerene ensembles, she joined Prof. T. Torres's group at UAM as Assistant Professor. From 2007 she has held an Associate Professor position in the Organic Chemistry Department at UAM. Her current research interests are the synthesis, nanostructuration, and photophysical and magnetic properties of new phthalocyanine-based materials, including phthalocyanine nanotube ensembles.

Dirk M. Guldi graduated from the University of Cologne (Germany) in 1988, from where he also received his Ph.D. in 1990. Following postdoctoral appointments at the National Institute of Standards and Technology, the Hahn-Meitner Institute Berlin (Germany), and Syracuse University, he joined the faculty of the Notre Dame Radiation Laboratory in 1995. He was promoted a year later from Assistant to Associate Professional Specialist and remained affiliated with Notre Dame until 2004. During this time, he completed his habilitation at the University of Leipzig (Germany) in 1999. Since 2004, he has been a Full Professor at the Institute of Physical Chemistry at the Friedrich-Alexander University in Erlangen (Germany). He was awarded with the Heisenberg-Prize (1999, Deutsche Forschungsgemeinschaft), Grammaticakis-Neumann-Prize (2000, Swiss Society for Photochemistry and Photophysics), JSPS Fellowship (2003, The Japan Society for the Promotion of Science), JPP-Award (2004, Society of Porphyrins and Phthalocyanines), and Elhuyar-Goldschmidt Award (2009, Royal Spanish Chemical Society). He is Editor-in-Chief of *Fullerenes, Nanotubes and Carbon Nanostructures* (since 2001) and a member of the International Advisory Editorial Board of the *Journal of Materials Chemistry*, the *Journal of Photochemistry and Photobiology, A: Chemistry* (since 2004), *Chemical Society Reviews* (since 2005), *Chemical Physics Letters* (since 2007), *Energy and Environmental Science* (since 2008), and *ChemSusChem* (since 2008). He has a track record of more than 300 publications in peer-reviewed scientific journals and has given nearly 250 invited talks. Currently he is chairman of the Fullerenes, Nanotubes and Carbon Nanostructures division of the Electrochemical Society. His research interests are widespread in the field of carbon nanostructures. In particular, primary research activities are in the areas of charge separation in donor−acceptor ensembles and construction of nanostructured thin films for photoenergy conversion.

higher than than those of Pors (Figure 1c), thus representing ideal light-harvesting antenna systems. Moreover, these macrocycles are synthetically versatile compounds, in which the 2 hydrogen atoms of the central cavity can be replaced by more than 70 metals and a variety of substituents can be incorporated in their structure, at the axial and/or peripheral positions of the macrocycle.[33−37] These structural modifications allow tuning of some of the physical parameters of these macrocycles, such as their aggregation status or their reducing/oxidizing characteristics. These features render Pcs ideal molecular components in donor−acceptor (D−A) ensembles where their role is twofold: First, they function as antennas, since they absorb very efficiently light in the visible region of the solar spectrum. Second, once photoexcited, they act as an electron donor for the acceptor moiety.[38−41] These latter characteristics make these macrocycles promising building blocks for their incorporation in photovoltaic and artificial photosynthetic devices.

Similarly, subphthalocyanines (SubPcs) (Figure 1b),[42−44] lower Pc homologues which present an aromatic cone-shaped structure, share with Pcs several fascinating physical properties such as an excellent light-harvesting ability with high extinction coefficients (i.e., as high as 60 000 M^{-1} cm^{-1}) (Figure 1c) and a rich redox chemistry that may be tuned, even easier than in the case of Pcs, by the introduction of different peripheral functional groups.

The great interest in Pcs and SubPcs as molecular building blocks for the construction of artificial photosynthetic systems has led others and us to synthesize and study a wide range of covalent and noncovalent (Sub)Pc-based D−A systems incorporating electroactive acceptor units of diverse nature and redox character such as fullerene, carbon nanotubes (CNTs), perylenediimide (PDI), anthraquinone (AQ), ferrocene (Fc), ruthenium bypyridine complexes, flavin, or Por.

Tomás Torres is currently Full Professor and Head of the Department of Organic Chemistry at the Universidad Autónoma de Madrid, Spain. In addition to various aspects of synthetic and supramolecular chemistry, his current research interests include the synthesis of phthalocyanines and the preparation and study of the photophysical properties of molecular materials based on these compounds. His group, composed of 25 researchers, is also exploring several areas of application of phthalocyanines, including organic and hybrid solar cells, with a focus on nanotechnology. Prof. Torres has published ca. 300 original papers and reviews and has issued 35 patents. He has been awarded the JANSSEN CILAG Prize for Organic Chemistry (2005) by the Royal Society of Chemistry of Spain. In 2009 he was honored as Doctor Honoris Causa by the Ivanovo State University of Chemistry and Technology (ISUCT), Russia.

Among the acceptor units employed for the preparation of such (non)covalent systems, carbon nanostructures such as fullerenes and CNTs deserve a special mention due to their excellent electron acceptor ability, which convert them as perfect molecular partners for photo- and electroactive systems. The extraordinary electron acceptor properties of fullerenes,[45−57] coupled with their small reorganization energy and their ability for promoting ultrafast CS together with very slow charge recombination (CR) features, have prompted the incorporation of these carbon nanostructures in a large number of D−A systems where photoinduced electron transfer (PET) processes and solar energy conversion are sought. Similarly, the outstanding properties of CNTs[58−65] have generated a tremendous interest toward the implementation of this novel carbon allotrope in D−A nanohybrids. CNTs in fact readily accept electrons, which, in turn, might be transported under nearly ideal conditions along its one-dimensional (1-D) tubular axis.

To date, a large variety of covalently linked D−A (Sub)Pc-based conjugates, containing as acceptor units fullerene and CNTs, have been synthesized and their photophysical properties studied in solution and/or in the solid state, revealing the occurrence, in the majority of the cases, of PET events. In such systems, the nature of the bridging spacer has been varied from the electronic (i.e., conjugated/nonconjugated) and/or structural (i.e., rigid/flexible) point of view, with the aim of identifying to which extent these changes would influence the PET dynamics.[40,66]

Supramolecular interactions have also been employed as a tool for the construction of D−A Pc−carbon nanostructure systems with the aim of increasing the lifetime of the photoinduced charge-separated states by taking advantage of the noncovalent nature of the supramolecular system. Several D−A Pc-based supramolecular structures and nanoaggregates have been prepared from appropriately substituted mesomorphic Pcs, by cation complexation of crowned Pcs, or by using hydrogen-bonding, metal−ligand, or D−A interactions.

Although the increasing know-how gained by researchers on studying natural and artificial photosynthetic systems has allowed sophisticated multicomponent Pc- and SubPc-based D−A systems presenting improved charge separation ability in solution to be designed and prepared, the implementation of these molecular systems in efficient solid-state devices still remains a major challenge. In this context, promising results have been obtained by the incorporation of Pcs and SubPcs in photovoltaic devices.[67−71] In particular, Pcs and SubPcs have been incorporated in organic solar cells, either in bulk or in planar heterojuction configurations with carbon nanostructures as acceptor components, which have clearly demonstrated the potential that these macrocycles hold as efficient light-harvesting and donor molecular materials, within the fast-growing and technologically important field of photovoltaics.[72−79] Some of the aforementioned covalently linked Pc−fullerene systems have also been incorporated, with some success, as active components in photovoltaic devices.

Furthermore, the planar, extended, and π-conjugated surface of Pcs opens up the possibility to control, by using supramolecular interactions, the nanoscopic organization of these macrocycles within the active layer of the photovoltaic cell, with the aim of improving the charge transport properties and the performances of the resulting device.

Herein, we review the different synthetic strategies that have been pursued so far for the preparation of D−A Pc− and SubPc−carbon nanostructure systems, having the donor and the acceptor units connected either covalently or by using supramolecular interactions. A photophysical analysis of most of these systems will also be presented with the aim of rationalizing which effect the structural and electronic features of these D−A systems have on the photoinduced electron/energy transfer dynamics. The utilization of Pcs and fullerenes in organic photovoltaics will be also reviewed in

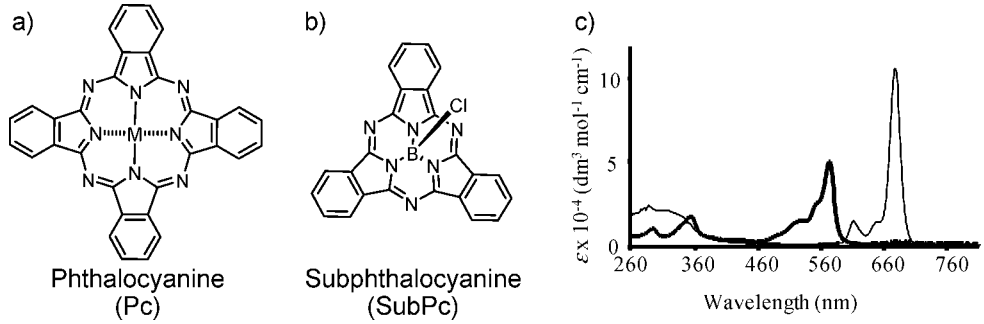

Figure 1. (a) Molecular structures of (a) a Pc and (b) a SubPc. (c) Typical UV/vis absorption spectra of Pcs (thin line) and SubPcs (thick line).

Scheme 1. Synthesis of Pc−C_{60} Fullerene Dyad 1[a]

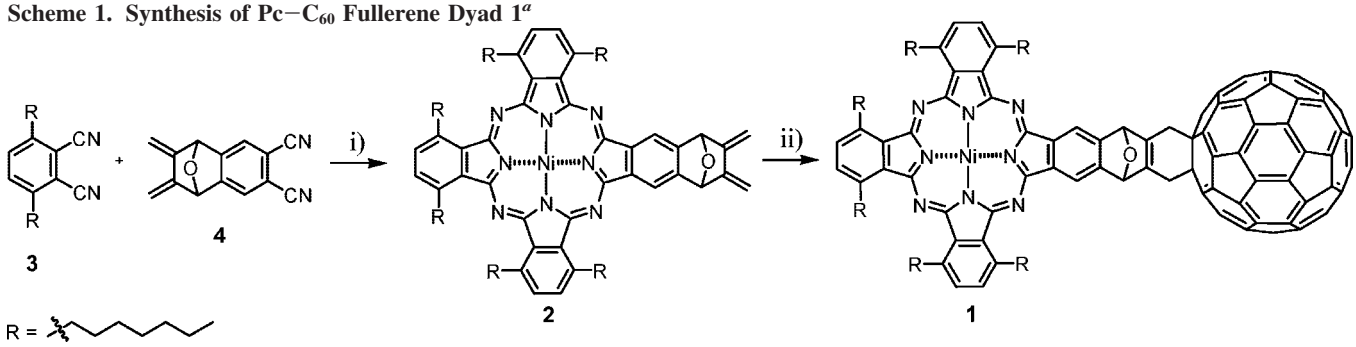

[a] Reagents and conditions: (i) $Ni(OAc)_2$, DBU, 1-pentanol, reflux; (ii) C_{60} fullerene, toluene, reflux.

terms of both the different types of organic solar cell architectures and performance of the devices.

2. Phthalocyanine−Fullerene Donor−Acceptor Systems

2.1. Covalently Linked Phthalocyanine−Fullerene Systems

Among the acceptor units employed for the preparation of D−A Pc-based systems, C_{60} fullerene enjoys a privileged position due to its unique physical properties, the most noteworthy probably being its small reorganization energy associated with PET reactions.

The first report on a molecular system comprising both a Pc and a C_{60} fullerene moiety covalently linked appeared in 1997 by Hanack, Hirsch, and co-workers, who prepared Pc−C_{60} dyad **1** through a Diels−Alder reaction between Ni^{II}Pc **2** bearing two terminal double bonds (i.e., a diene) and C_{60} fullerene (i.e., a dienophile) (Scheme 1).[80,81] The [4 + 2] cycloaddition occurs at a [6,6]-ring junction of the C_{60} fullerene cage, giving rise to the formation of Pc−C_{60} **1**, which was named by the authors "green fullerene" due to the intense green color in solution imparted by the Pc chromophore.

Ni^{II}Pc **2** was prepared in 75% yield by the statistical condensation of 3,6-diheptylphthalonitrile (**3**) and phthalonitrile **4** in the presence of nickel(II) acetate and a catalytic amount of 1,8-diazabicyclo[5.4.0]undec-7-ene (DBU). Electrochemistry measurements carried out on **1** showed five reversible reduction peaks, which were assigned by spectroelectrochemistry to be either fullerene- or Pc-based, the first reduction peak at −0.41 V being fullerene-centered, as reflected by the appearance of an absorption at 1074 nm characteristic of the fullerene monoanion species. However, these measurements showed that the reduction potentials of both the Pc and the fullerene moieties in **1** do not change significantly compared to those of the respective parent compounds (i.e., **2** and a C_{60} fullerene monoadduct lacking the Pc moiety), thus ruling out any ground-state electronic communication between the two electroactive subunits in **1**.

The third-order nonlinear optical properties of a Cu^{II}Pc−C_{60} Diels−Alder adduct analogue of **1** have also been investigated, giving rise to high second-order hyperpolarizability values.[82] Moreover, it has been found that nanoparticle dispersions of this Cu^{II}Pc−C_{60} dyad exhibit enhanced optical limiting performances[83] and nonlinear absorption enhancement.[84]

Since that first report, a large number of covalently linked Pc−C_{60} systems (i.e., dyads, triads, tetrads, etc.) have been reported. A compound frequently used for the preparation of several of these Pc−C_{60} systems is tri-*tert*-butyliodo-Pc **5**, either metalated (i.e., **5a**,**c**) or in its free base form (i.e., **5b**), which has established itself as an interesting building block for the preparation of such D−A systems (Scheme 2). Compounds **5a**−**c** can be prepared via statistical condensation of 4-*tert*-butylphthalonitrile (**6**) and 4-iodophthalonitrile (**7**) using lithium metal (**5b**) or a metal salt (**5a**,**c**) as the templating reagent. There are several factors that have contributed to the extensive use of Pc **5** for the preparation of D−A Pc-based systems such as the possibility to prepare it in reasonable yields (>20%) and its easy purification. Moreover, the *tert*-butyl groups that decorate the macrocycle periphery in **5** confer to this molecule high solubility and help to reduce the strong self-aggregation tendency typical of the Pcs. Besides the above-mentioned points, probably the most important feature of Pc **5** is the presence of an iodine atom directly attached to the Pc framework, which allows the easy functionalization of this macrocycle with, virtually, any functional group through the use of metal-catalyzed reactions.

Pcs **5a**−**c** have been used as starting compounds for the preparation of Pc−C_{60} dyads **8a**−**c** (Scheme 2).[85,86] The synthesis of these dyads involves a palladium-catalyzed Stille coupling reaction of Pcs **5** with tributylvinyltin, affording tri-*tert*-butylvinyl-Pcs **9** in excellent yields (≥88%). The latter Pcs are then oxidized by using a polymer-supported osmium tetroxide and sodium periodate in tetrahydrofuran (THF) (or ozone at −78 °C in dichloromethane), affording formyl-Pcs **10** in good yields (≥70%) (8−10% via the ozonolysis route). Finally, the 1,3-dipolar cycloaddition reaction of azomethine ylides, generated in situ from formyl-Pcs **10** and *N*-methylglycine, to C_{60} fullerene (also known as the "Prato reaction") allowed Pc−C_{60} dyads **8** to be obtained in reasonable yields (i.e., 40% (**8a**), 43% (**8b**), 41% (**8c**)). Such a reaction, which results in the formation of a pyrrolidine group, represents one of the synthetic strategies most used nowadays for the functionalization of fullerenes.

An alternative synthetic route for the preparation of Pc−C_{60} dyad **8a** has also been pursued. This procedure involves the preparation of 4-vinylphthalonitrile from 4-iodophthalonitrile (**7**), followed by the oxidative cleavage of the vinyl functionality to obtain 4-formylphthalonitrile (**11**). The latter compound was then reacted with C_{60} fullerene in the presence of *N*-methylglycine to afford the fullerene-containing phthalonitrile **12**, which was subsequently condensed with 4-*tert*-butylphthalonitrile (**6**) in the presence of zinc(II) chloride, affording Pc−C_{60} dyad **8a** in low yield. UV/vis studies on dyads **8a**−**c** revealed, in all cases, a small,

Scheme 2. General Reaction Conditions for the Preparation of Pc−C_{60} Dyads 8a−c[a]

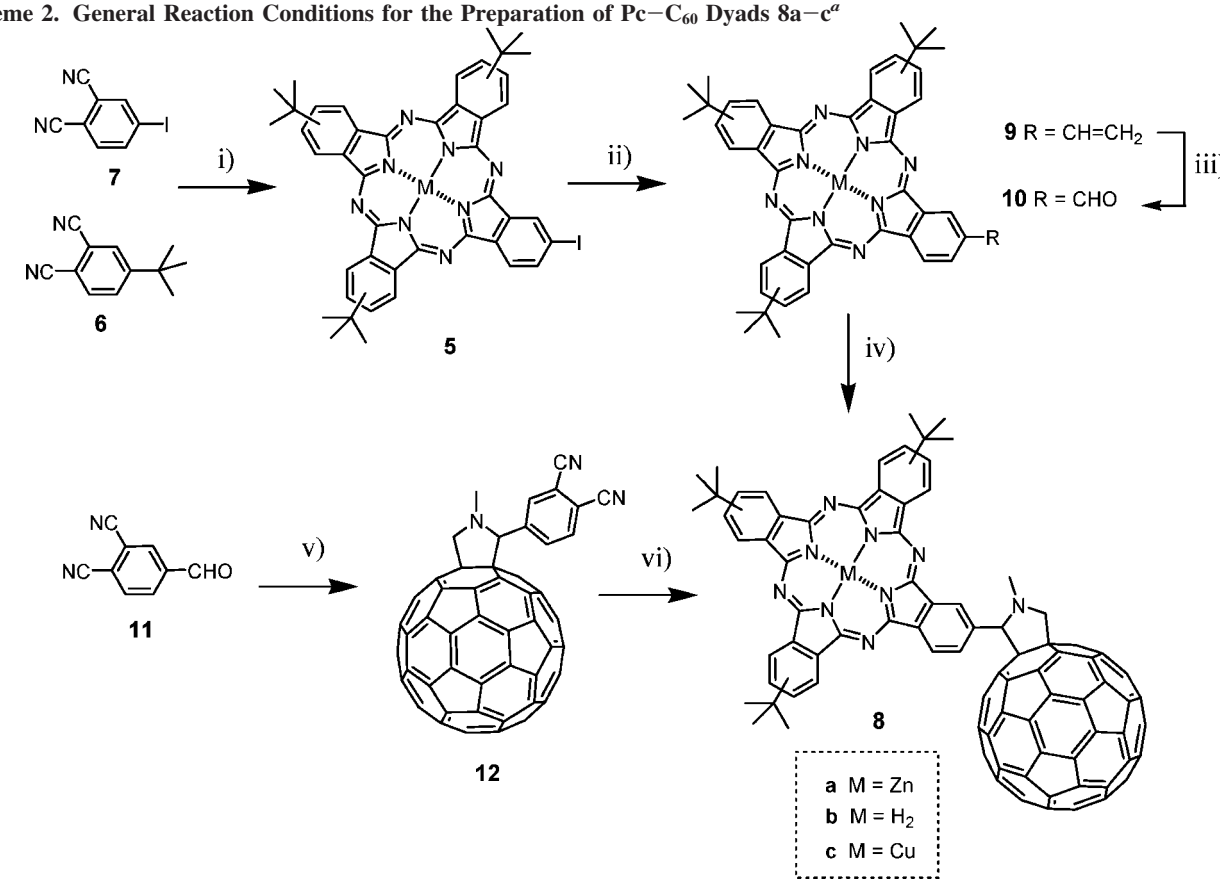

[a] Reagents and conditions: (i) $ZnCl_2$ for **5a** or $Cu(AcO)_2$ for **5c**, (dimethylamino)methanol (DMAE), reflux, argon; for **5b**, lithium, 1-pentanol, amyl alcohol, reflux, argon; (ii) tributylvinyltin, $Pd(PPh_3)_4$, toluene, 100 °C; (iii) OsO_4, $NaIO_4$, THF, room temperature (rt); (iv) C_{60} fullerene, *N*-methylglycine, toluene, reflux; (v) C_{60} fullerene, *N*-methylglycine, toluene, reflux; (vi) only for **8a**, 4-*tert*-butylphthalonitrile (**6**), $ZnCl_2$, DMAE/*o*-DCB, reflux.

ground-state electronic communication between the two spatially close, active units (i.e., Pc and C_{60}).

Electrochemical investigation showed that the Pc-based oxidation and reduction potentials were positively shifted in the dyads **8a**,**b** in comparison to the redox potentials of some reference compounds (i.e., Pcs **10a**,**b** and a fullerene derivative lacking the Pc moiety). Conversely, the C_{60}-based reduction potentials for **8a**,**b** were negatively shifted with respect to those of a fullerene derivative reference compound, thus inferring some degree of ground-state intra- and/or intermolecular interactions between the electron-donating Pc to the electron-accepting fullerene moiety.

A thorough analysis on the photophysical properties (i.e., steady-state and time-resolved fluorescence measurements and transient absorption measurements) of dyads **8a**−**c** in solution was also carried out, confirming the occurrence of

Scheme 3. General Reaction Conditions for the Preparation of Pc−C_{60} Dyad 13[a]

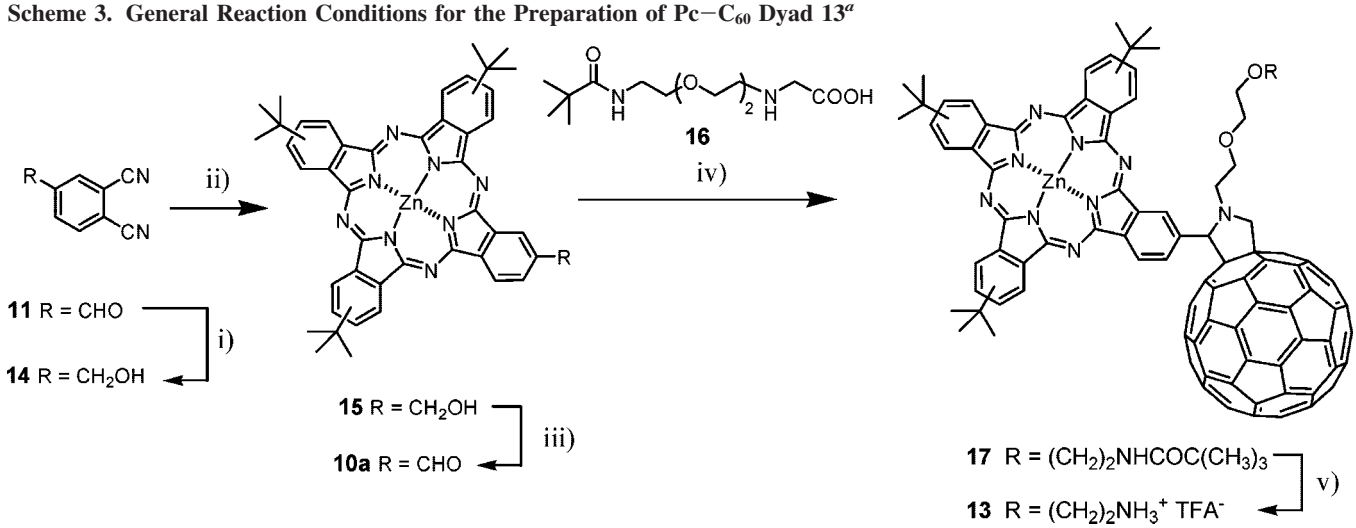

[a] Reagents and conditions: (i) $NaBH_4$, ethanol, rt; (ii) 4-*tert*-butylphthalonitrile (**6**), $Zn(OAc)_2$, DMAE, reflux; (iii) SO_3−pyridine complex, NEt_3, dry dimethyl sulfoxide, argon, 50 °C; (iv) C_{60} fullerene, *tert*-butylcarbamate-protected, N-functionalized glycine **16**, toluene, reflux; (v) trifluoroacetic acid, CH_2Cl_2, rt.

Scheme 4. Synthesis of $Zn^{II}Pc-C_{60}$ Conjugates 18−20[a]

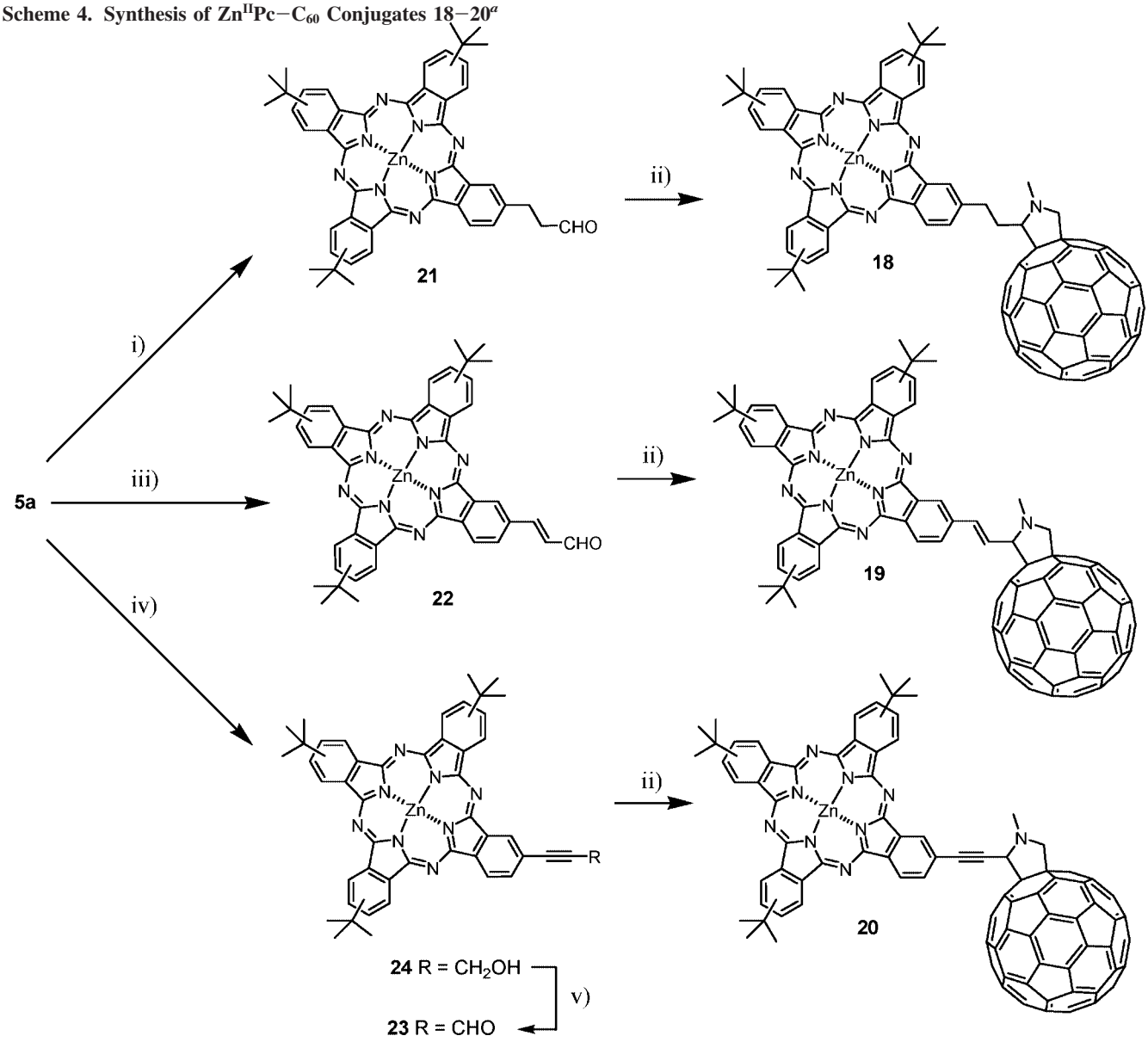

[a] Reagents and conditions: (i) allylic alcohol, $Pd(OAc)_2$, $NaHCO_3$, Bu_4NCl, DMF, 30 °C; (ii) C_{60} fullerene, *N*-methylglycine, toluene, reflux; (iii) acrolein, $Pd(OAc)_2$, $NaHCO_3$, Bu_4NCl, DMF, 20 °C; (iv) propargyl alcohol, $Pd(PPh_3)_2Cl_2$, CuI, THF, NEt_3, rt; (v) pyridinium chlorochromate, CH_2Cl_2,rt.

PET events,[86,87] a phenomenon that has been proved to be almost ubiquitous in the covalently linked $Pc-C_{60}$ systems and that will be extensively discussed in the photophysical part of this review.

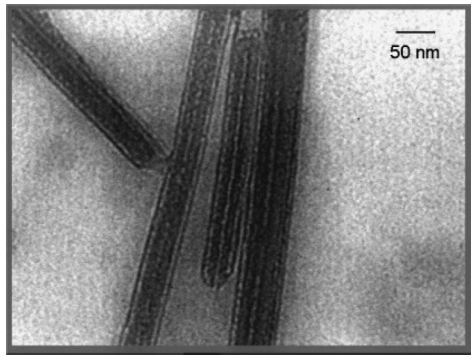

Figure 2. TEM image of the nanotubules formed by $Pc-C_{60}$ dyad **13** in water. Reprinted from ref 88. Copyright 2005 American Chemical Society.

A $Pc-C_{60}$ analogue of **8a** has also been reported, in which the methyl group on the fulleropyrrolidine moiety has been replaced with a polyethylene glycol group terminated with an ammonium function (Scheme 3).[88] In this case, a novel synthetic route was undertaken for the preparation of the aldehyde-containing Pc **10a**, the precursor of $Pc-C_{60}$ dyad **13**. The synthesis of dyad **13** starts with a statistical crossover condensation of 4-*tert*-butylphthalonitrile (**6**) and 4-(hydroxymethyl)phthalonitrile (**14**) (the latter one prepared via reduction of 4-formylphthalonitrile (**11**)) in the presence of $Zn(OAc)_2$, leading to the hydroxymethyl-functionalized $Zn^{II}Pc$ **15**, which was isolated in 22% yield. Pc **15** was then subjected to an oxidative treatment with an excess of a SO_3−pyridine complex in the presence of NEt_3 in dry dimethyl sulfoxide, affording formyl-Pc **10a** in 84% yield (using this method, formyl-Pc **10a** is obtained in a higher yield compared to that from the route involving the oxidation of vinyl-Pc **9**[85]). Compound **10a** was then reacted with *tert*-butylcarbamate-protected, N-functionalized glycine **16** in the presence of C_{60} fullerene to afford $Pc-C_{60}$ dyad **17**, in which

Scheme 5. Synthesis of the Structurally Rigid Pc−C_{60} Conjugate 25[a]

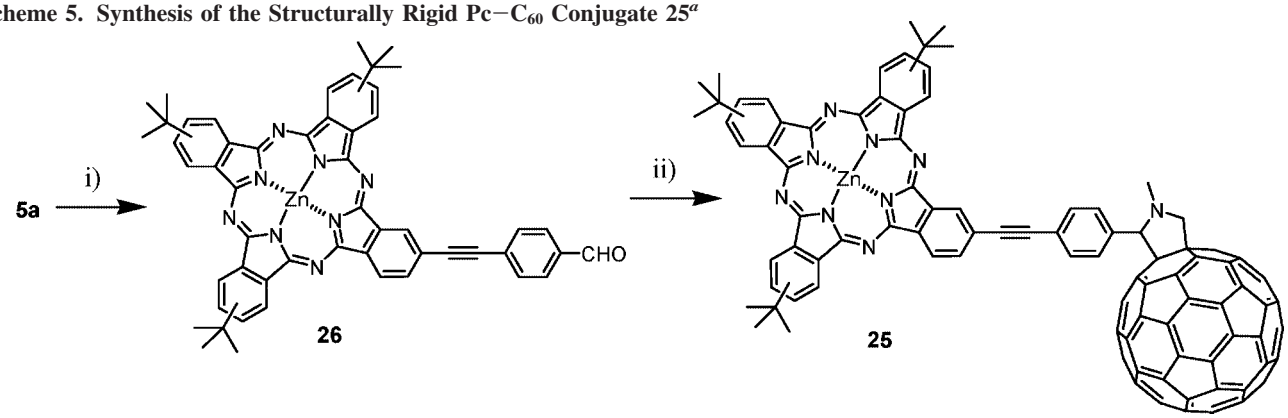

[a] Reagents and conditions: (i) 4-ethynylbenzaldehyde, CuI, $PdCl_2(PPh_3)_2$, NEt_3, dry toluene, reflux; (ii) C_{60} fullerene, *N*-methylglycine, dry toluene, reflux.

the carbamate protecting group was finally converted into an ammonium group by treatment with an excess of trifluoroacetic acid to afford salt **13**.

Transmission electron microscopy (TEM) studies revealed that the amphiphilic Pc−C_{60} dyad salt **13**, when dispersed in water, is able to form perfectly ordered 1-D nanotubules, due to a combination of solvophobic and $\pi-\pi$ stacking interactions (Figure 2). Similar 1-D nanostructures have been obtained using a Por−C_{60} dyad system.[89]

Pc **5a** has been used as well as the common starting compound for the preparation of the series of Pc−C_{60} conjugates **18**−**20** (Scheme 4).[90] These dyads, bearing different spacers (i.e., single (**18**), double (**19**), or triple (**20**) bonds) between the Pc and C_{60} fullerene, have been prepared with the aim of studying how the nature of the spacer influences the stabilization of the photogenerated radical ion pair states.

To prepare the aforementioned Pc−C_{60} dyads, the corresponding aldehyde-containing Pcs **21**−**23** were prepared. Pc **23** was obtained by reacting Pc **5a** via a Sonogashira cross-coupling reaction with propargyl alcohol in the presence of NEt_3 and a catalytic amount of $Pd(PPh_3)_2Cl_2$ and CuI, yielding compound **24** in 63% yield. Subsequent oxidation of **24** with pyridinium chlorochromate led to Pc **23** in 47% yield. In the case of Pc **22**, the initial synthetic strategies considered for its preparation (i.e., direct reduction of the triple bond functionality of **23** or Heck reaction of Pc **5a** with acrolein acetal) proved to be unsuccessful. A Heck-modified, Jeffery protocol was found to be the most straightforward and high-yielding procedure for the preparation of Pc **22**. This compound was prepared in 91% yield by palladium-catalyzed vinylic substitution of acrolein on Pc **5a** in the presence of $NaHCO_3$, Bu_4NCl, and a catalytic amount of $Pd(OAc)_2$. Similar reaction conditions were used for the preparation of Pc **21**, which was obtained in 76% yield by Heck arylation of allylic alcohol with Pc **5a**.

The three formyl-containing Pcs **21**−**23** were finally subjected to 1,3-dipolar cycloaddition with C_{60} fullerene and *N*-methylglycine in refluxing toluene to afford conjugates **18**−**20** in 20%, 23%, and 21% yields, respectively. Detailed photophysical investigations of compounds **18**−**20** revealed, for all three dyads, the occurrence of an intramolecular electron transfer dynamic that evolves from the photoexcited Pc macrocycle to the electron-accepting C_{60} moiety. Complementary time-dependent density functional theory calculations supported the spectral assignment seen in the differential absorption spectra for the $ZnPc^{\bullet+}$ radical cation and the $C_{60}^{\bullet-}$ radical anion.

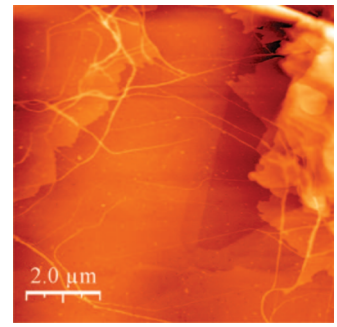

Figure 3. AFM topographic image of Pc−C_{60} dyad **25** drop-cast onto highly oriented pyrolytic graphite ([**25**] = 10^{-5} M). Reprinted with permission from ref 91. Copyright 2008 Wiley-VCH.

Recently, a structurally rigid, triple bond containing Pc−C_{60} dyad (**25**) that bears some structural resemblance to conjugate **20** has been prepared starting from Pc **5a** (Scheme 5).[91] Similarly to the case of **24**, a palladium-catalyzed Sonogashira coupling reaction between Pc **5a** and ethynylbenzaldehyde has been used to directly attach a triple bond group to the Pc ring, resulting in the formation of formyl-Pc **26** in 92% yield. This latter compound was then reacted under the standard Prato reaction conditions, affording dyad **25** in 36% yield. The organization properties of this covalently linked conjugate **25** on highly ordered pyrolytic graphite and graphite-like surfaces were also investigated by using different microscopic techniques (i.e., atomic force microscopy (AFM) and conductive AFM). These studies showed that, on such surfaces, the D−A ensemble **25** is able to self-organize, forming fibers and films (Figure 3). The electrical properties of these supramolecularly assembled nanostructured architectures were also probed, obtaining outstanding electrical conductivity values, which were found to be related to the extremely high degree of molecular order of the Pc−C_{60} conjugates within the nanostructures.

The structurally rigid Pc−C_{60} dyad **27**, in which the two active components are separated by a [2.2]paracyclophane unit, has also been prepared from Pc **5a**, which was coupled via a palladium-catalyzed Heck-type coupling reaction with [2.2]paracyclophane **28** to yield **29** in 64% yield (Scheme 6).[92] Compound **27** was finally obtained in a 35% yield by Prato reaction of the aldehyde-containing Pc **29** with C_{60} fullerene in the presence of *N*-methylglycine. Photophysical studies on this dyad confirmed the occurrence of a photoinduced dynamic process, which resulted in the formation of a long-lived charge-separated state.

Scheme 6. Synthesis of Pc−C_{60} Conjugate 27[a]

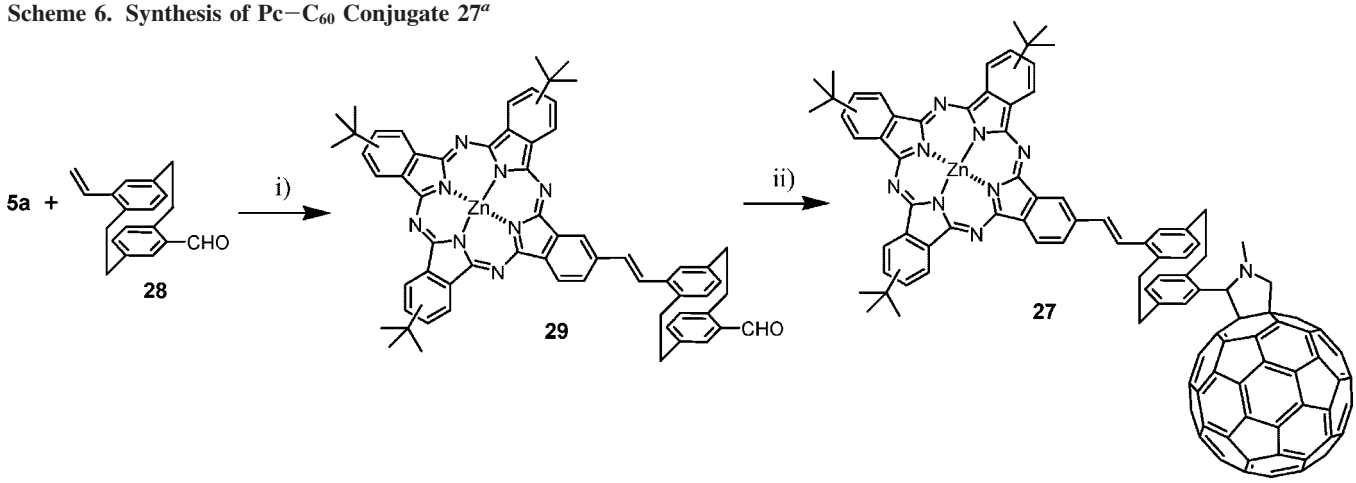

[a] Reagents and conditions: (i) $Pd(OAc)_2$, NEt_3, DMF, tetrabutylammonium bromide; (ii) C_{60} fullerene, *N*-methylglycine, *o*-DCB, reflux.

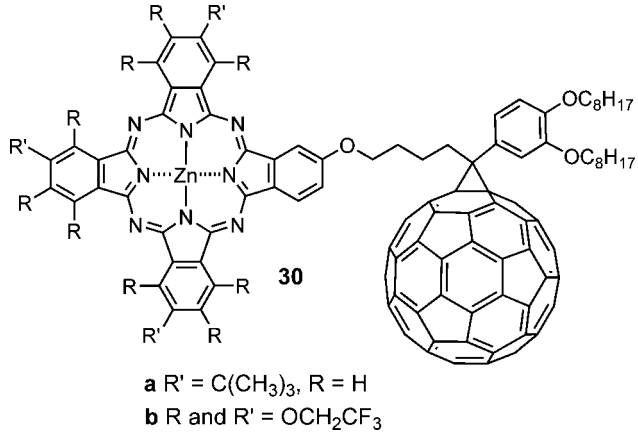

Figure 4. Molecular structure of Pc−C_{60} dyads **30a**,**b**.

Recently, two Pc−C_{60} dyads (**30a**,**b**) have been prepared, in which a fullerene moiety has been connected covalently to a Pc bearing either *tert*-butyl (i.e., **30a**) or trifluoroethoxy (i.e., **30b**) groups at its peripheral positions (Figure 4).[93] Both dyads were obtained starting from a common fullerene derivative bearing a terminal phthalonitrile moiety that was then reacted with 3-*tert*-butylphthalonitrile or a persubstituted, trifluoroethoxy-coated phthalonitrile, leading to Pc−C_{60} dyads **30a** and **30b**, respectively. Electrochemical and spectroscopic studies on both dyad systems revealed that whereas in the case of ensemble **30a** the occurrence of an efficient intramolecular PET process was detected, dyad **30b** did not show any sign of electronic communication between Pc and C_{60}. This result is presumably due to the strong electron-withdrawing nature of numerous trifluoroethoxy groups in **30b**, which lead the Pc to become an acceptor with an electron-accepting property equivalent to that of fullerene.

Dyads comprising both a double-decker lanthanide(III) bis(phthalocyaninato) and a C_{60} moiety (i.e., [Ln^{III}(Pc)(Pc′)]−C_{60} (Ln = Sm, Eu, Lu) **31a**−**c**) have also been synthesized (Scheme 7).[94] The sandwich complexes **31a**−**c** were obtained by means of a stepwise procedure from unsymmetrically substituted free base Pc **32**,[95] which was first transformed into the monophthalocyaninato intermediate [Ln^{III}(acac)(Pc)] (Ln = Sm, Eu, Lu; acac = acetylacetone) and further reacted with 1,2-dicyanobenzene in the presence of DBU to yield [Ln^{III}(Pc)(Pc′)] **33a**−**c**. The final synthetic step involved the reaction of these unsymmetrically functionalized heteroleptic sandwich complexes **33a**−**c** with a fulleropyrrolidine carboxylic acid derivative using a dicyclohexylcarbodiimide (DCC) protocol, obtaining conjugates **31a**−**c** in approximately 50% yields.

^{1}H NMR spectra of the bis(phthalocyaninato) complexes **33a**−**c** and dyads **31a**−**c** could be obtained by adding hydrazine hydrate to solutions of the complexes in [D_7]DMF, a treatment that converts the free radical double-deckers into the respective protonated species. UV/vis spectroscopy of these dyads in THF displayed the absorption bands of both constituents (i.e., the double-decker Pc and C_{60} derivative), but no evidence of ground-state interactions could be appreciated. The lack of ground-state electronic interactions between the two electroactive units was also confirmed by cyclic voltammetry studies on **33a**−**c** and dyads **31a**−**c** in THF. These studies showed that the electrochemical behavior of dyads **31a**−**c** was almost the superposition of the redox peaks of both components, namely, the double-decker Pc and C_{60} fullerene.

With the aim of studying the possible stabilization of the photoinduced charge-separated state in a D−A supramolecular triad, an electron-deficient, symmetrically substituted Pd^{II}Pc (**34**) and a Pc−C_{60} dyad (**35a**), bearing a phenylethenyl unit separating the Pc and the C_{60} units, were prepared (Figure 5).[96] Heck coupling reaction of an iodo-substituted Zn^{II}Pc bearing six peripheral *n*-butyloxy substituents with 4-vinylbenzaldehyde in the presence of NEt_3, tetrabutylammonium bromide, and a catalytic amount of $Pd(OAc)_2$ yielded a formyl-substituted Pc, which was subjected to the standard Prato reaction conditions to obtain Pc−C_{60} dyad **35a**. On the other hand, the electron-deficient octakis(propylsulfonyl)Pd^{II}Pc **34** was prepared by refluxing a diiminoisoindoline precursor in a mixture of dimethylformamide (DMF) and *o*-dichlorobenzene (*o*-DCB) in the presence of $Pd(OAc)_2$. Also for compound **35a**, as already seen before for some Pc−C_{60} fullerene dyads, some degree of ground- and excited-state electronic communication between the Pc and the fullerene units could be observed as inferred by electrochemical investigation (i.e., the alkoxy-substituted Pc unit becomes more difficult to oxidize when it is covalently connected to a C_{60} unit) and photophysical measurements (i.e., the considerable decrease in fluorescence quantum yields and fluorescence lifetimes of **35a** with respect to a Pc reference compound). The formation of a D−A supramolecular complex (**34**/**35a**) in solution was inferred by the changes in the absorption and fluorescence spectra of Pc−C_{60}

Scheme 7. Synthesis of Double-Decker Lanthanide(III) Bis(phthalocyaninato)−C_{60} Dyads 31a−c[a]

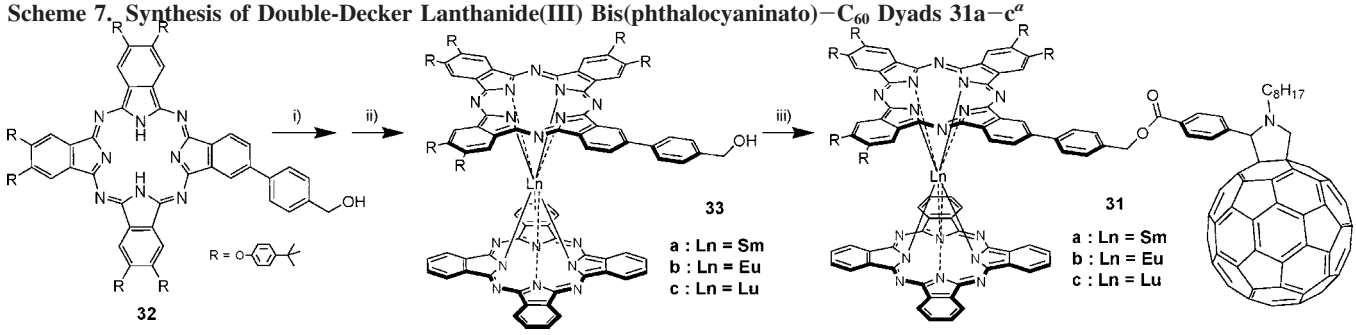

[a] Reagents and conditions: (i) $[Ln^{III}(acac)_3]\cdot nH_2O$, *o*-DCB, 170 °C (Ln = Sm, Eu, Lu; acac = acetylacetone); (ii) dicyanobenzene, DBU, *o*-DCB/1-pentanol, 160 °C; (iii) 4-(1′-octyl-3′,4′-fulleropyrrolidin-2′-yl)benzoic acid, DMAP, DCC, THF, rt.

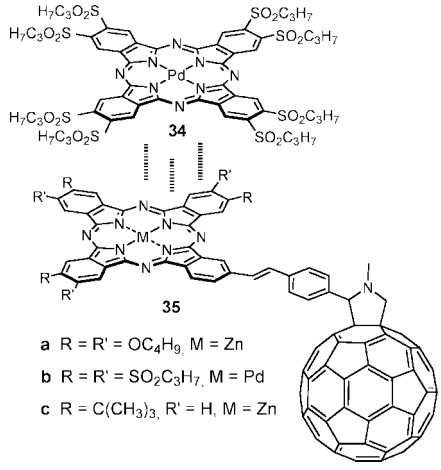

Figure 5. Molecular structures of Pc−C_{60} dyads **35a−c** and electronically complementary Pc **34**.

dyad **35a** during the titration with symmetric Pc **34**, whereas the Job plot method was used to ascertain the 1:1 stoichiometry of the **34/35a** supramolecular triad. A numerical analysis of the titration data revealed an association constant (K_a) for the supramolecular complex **34/35a** of $\sim 5 \times 10^5$ M^{-1} in $CHCl_3$ as a result of the strong D−A $\pi-\pi$ stacking interactions between the electron-deficient, alkylsulfonyl-substituted Pc **34** and the electron-rich, alkoxy-substituted Pc **35a**.

Very recently, the first examples of mesogenic Pc−C_{60} dyads (**36a−d**) have been reported in which Pcs bearing three swallowtail alkoxy groups have been covalently connected to a 1-(3-carboxypropyl)-1-phenyl-[6,6]-C_{61} (PCBM) moiety (Scheme 8).[97] The synthetic strategy used to prepare these dyads relies on the preparation of two different monosubstituted phthalonitriles, one bearing two long, lipophilic alkyl chains and the other one terminated with an acetyl protecting group [i.e., (methoxyethoxy)methyl (MEM)]. Statistical condensation of these two phthalonitriles in Li/1-pentanol at reflux afforded Pcs **37a−d** in 13−24% yield after column chromatography. The MEM protective group in Pcs **37a−d** was then quantitatively removed to give Pcs **38a−d** upon treatment with pyridinium tosylate (PPTS) in *tert*-butyl alcohol. In the final synthetic step, reaction between Pcs **38a−d** and a fullerene derivative containing a carboxylic acid (prepared by acid-catalyzed hydrolysis of the commercially available PCBM) following the dicyclohexylcarbodiimide (DCC)/(*N*,*N*-dimethylamino)pyridine (DMAP) protocol afforded the corresponding Pc−C_{60} dyads **36a−d** in yields up to 45%.

Scheme 8. Synthesis of Mesogenic Pc−C_{60} Dyads 36a−d[a]

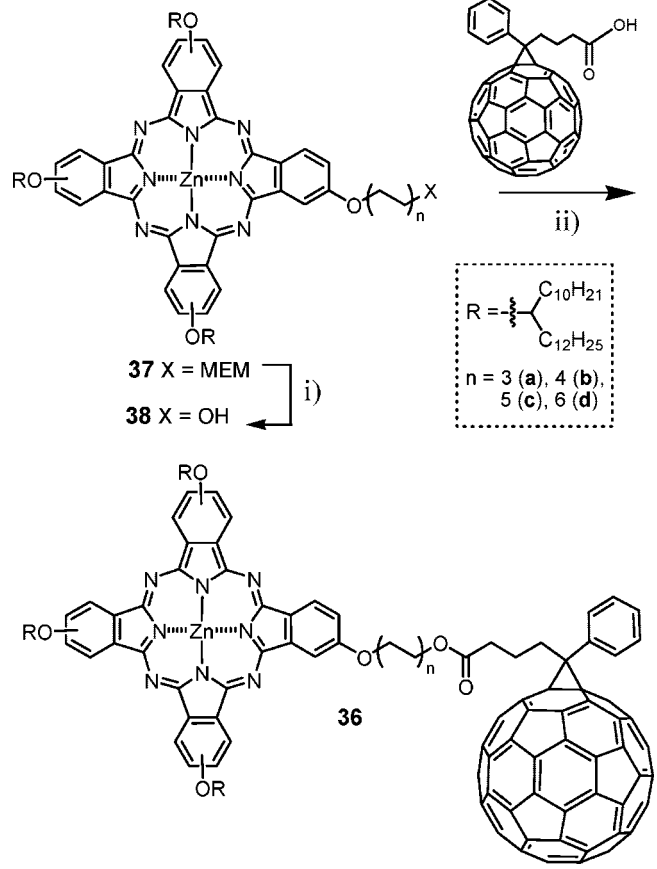

[a] Reagents and conditions: (i) PPTS, *tert*-butyl alcohol; (ii) DCC/DMAP, *o*-DCB, 0 °C.

Cyclic voltammetry measurements of **36a**,**d** in CH_2Cl_2 showed that (i) the voltammograms of these dyads effectively correspond to the superposition of those for PCBM and a symmetrically substituted Pc reference compound and (ii) the wave potentials do not change upon elongation of the spacer between the donor and the acceptor units. These observations, together with the UV/vis data, suggest the absence of intramolecular charge transfer in the ground state for dyads **36a−d**. Preliminary investigation of Pc−C_{60} dyads **36a−d** by polarized optical microscopy (POM) showed that the length of the spacer between the Pc and the fullerene moieties considerably influences the thermotropic properties of the material.

The formation of $\pi-\pi$ stacking interactions between Pc units has also been recently exploited for the incorporation of D−A Pc−C_{60} dyads in a liquid crystalline phase. The

Scheme 9. Synthesis of the Crown Ether-Containing Pc−C_{60} Conjugate 39[a]

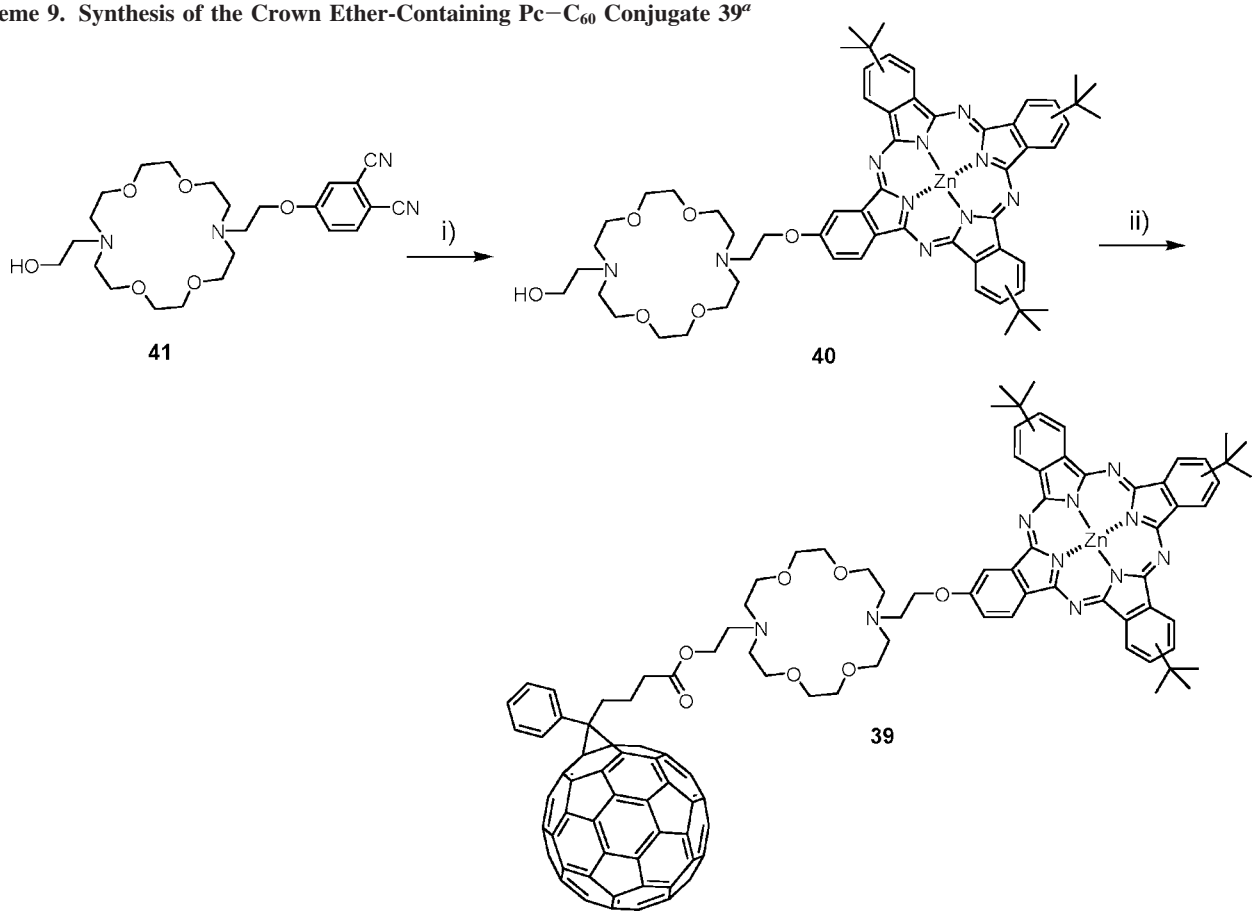

[a] Reagents and conditions: (i) 4-*tert*-butylphthalonitrile (**6**), $Zn(OAc)_2$, DMAE, reflux; (ii) PCBM, 1-hydroxybenzotriazole, dicyclohexylcarbodiimide, 4-(dimethylamino)pyridine, bromobenzene.

strategy consisted of blending a nonmesogenic Pc−C_{60} dyad (**35a**, **35b**, or **35c**) with a mesogenic, symmetrically substituted octakis(hexadecylthio)Zn^{II}Pc. The two Pc−C_{60} dyads **35b**,**c** have been prepared following the same synthetic procedure used for the preparation of Pc−C_{60} dyad **35a**, starting from the respective monoiodo-substituted Pc derivatives.[98] Equimolecular mixtures of octakis(hexadecylthio)Zn^{II}Pc and dyads **35a**−**c** resulted in the formation of hexagonal columnar mesophases in which the liquid crystal columns are composed of alternating stacks of the mesogenic Pc and Pc−C_{60} dyads **35a**−**c**, as suggested by X-ray diffraction studies. The use of blends, in which a mesogen is able to induce mesomorphism on a nonmesogenic Pc-based functional material, represents an interesting strategy for the incorporation of photoactive, D−A Pc−C_{60} fullerene systems in a liquid-crystalline architecture. Such an approach in fact overcomes the synthetic problems related to the preparation and isolation of mesogenic, unsymmetrically substituted Pc compounds from the other Pcs obtained in the statistical condensation reaction.

A flexible azacrown macrocycle has also been used as a linker between a Pc and C_{60} fullerene in **39** with the aim of studying the effect of possible ion-induced conformational changes on the electronic communication between the active units (Scheme 9).[99] The synthesis of dyad **39** requires the preparation of the azacrown-substituted Pc **40**, which is obtained in a 21% yield by statistical crossover condensation of 4-*tert*-butylphthalonitrile (**6**) and phthalonitrile **41**, the latter one obtained via *ipso* substitution of 4-nitrophthalonitrile with *N*,*N*′-bis(hydroxyethyl)diaza-18-crown-6 using potassium carbonate as the base. The final Pc−C_{60} dyad **39** is obtained in 30% yield through the coupling between PCBM and unsymmetrical Pc **40**, in the presence of 1-hydroxybenzotriazole, dicyclohexylcarbodiimide, and 4-(dimethylamino)pyridine in bromobenzene as the solvent. UV/vis analysis on dyad **39** revealed that neither the nature of the solvent nor the presence of alkali-metal cations had any effect on the aggregation properties of the dyad and that the C_{60} moiety did not have any influence on the electronic properties of the Pc ring. Complementary experiments measuring the kinetics after the addition of potassium salts to a solution of dyad **39** showed no significant changes in the excited-state dynamics in accordance with the UV/vis experiments. Similar conclusions were gathered from the electrochemical analysis of the cyclic voltammograms of **39** upon addition of Na^+ or K^+, which led to negligible shift effects in the peak potentials and peak separations.

Among the different methodologies developed for the covalent functionalization of fullerenes, the Bingel−Hirsch reaction between a fullerene and a malonate derivative, often incorporating a halide atom, generated in situ in a mixture of base and tetrachloromethane or iodine, represents one of the most versatile ones.[100] The mechanism of this reaction involves the abstraction of an acidic malonate proton by a base (usually DBU), thus generating a carbanion (or enolate) which readily reacts with one of the fullerene double bonds in a nucleophilic addition. This attack in turn generates a carbanion located on the fullerene which ultimately displaces

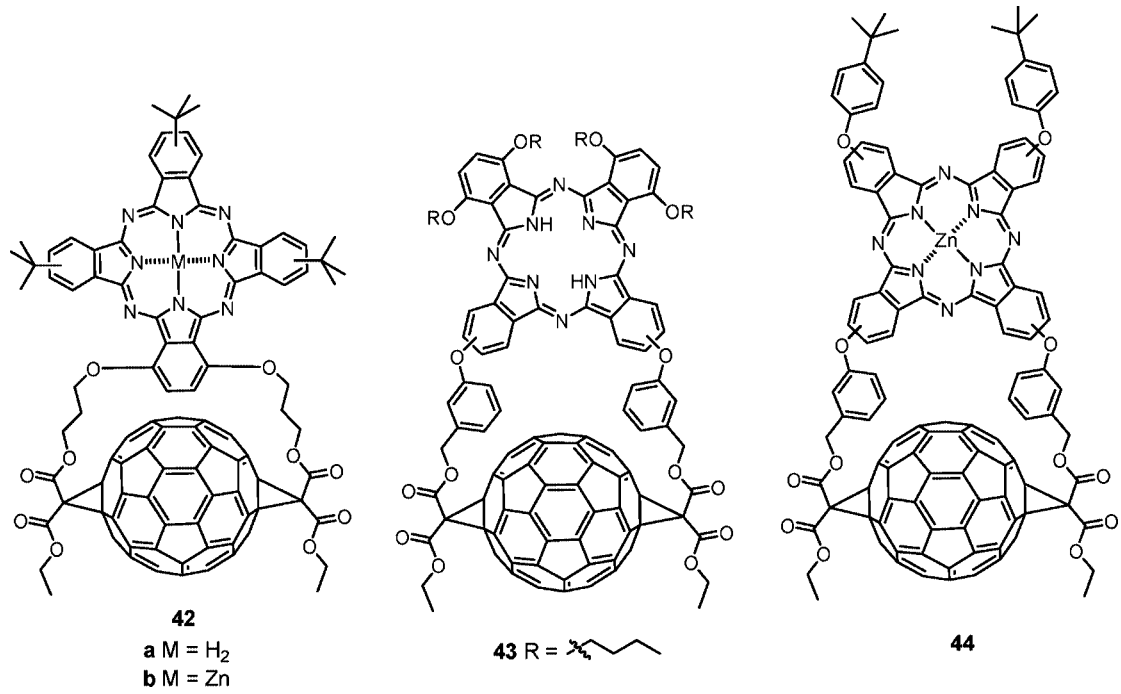

Figure 6. Molecular structures of Pc−C_{60} fullerene dyads **42**−**44**.

the halogen atom in an intramolecular, nucleophilic aliphatic substitution, giving rise to the formation of a cyclopropane ring.

In this context, some Pc−C_{60} fullerene dyads (**42**−**44**) have been constructed using this synthetic strategy (Figure 6).[101] The synthesis of these dyads involves the preparation of Pcs, differently substituted depending on the target dyad, each of them carrying at their periphery two pendent malonate groups. These bismalonate-containing Pcs, which were prepared by reaction of the corresponding Pcs bearing two hydroxyl functions with ethylmalonyl chloride, are then used in a double Bingel−Hirsch-type reaction with C_{60} fullerene in the presence of I_2 and DBU, thus affording the respective Pc−C_{60} fullerene dyads **42**−**44**. The photophysical properties of these systems have been determined to elucidate to which extent the geometrical restrictions imposed by the double addition on the fullerene scaffold, which would set the Pc and the C_{60} fullerene moieties in spatial proximity, would influence the occurrence of PET processes.[101,102]

More recently, alternating multilayer films of PDI with either Pc−C_{60} dyad **42a** or a free base Pc were prepared by the Langmuir−Schäfer method.[103] In such films, the presence of the two chromophores PDI and Pc increases the spectral range of the film photoactivity.

Molecular ensembles constituted by multiple Pc donor and/or C_{60} fullerene acceptor units have also been prepared with the aim of further stabilizing the photogenerated excited states and/or making more efficient the light-harvesting process. Recently, a Pc−C_{60} ensemble (**45**) constituted by

Scheme 10. Synthesis of Pc−$(C_{60})_2$ Triad 45[a]

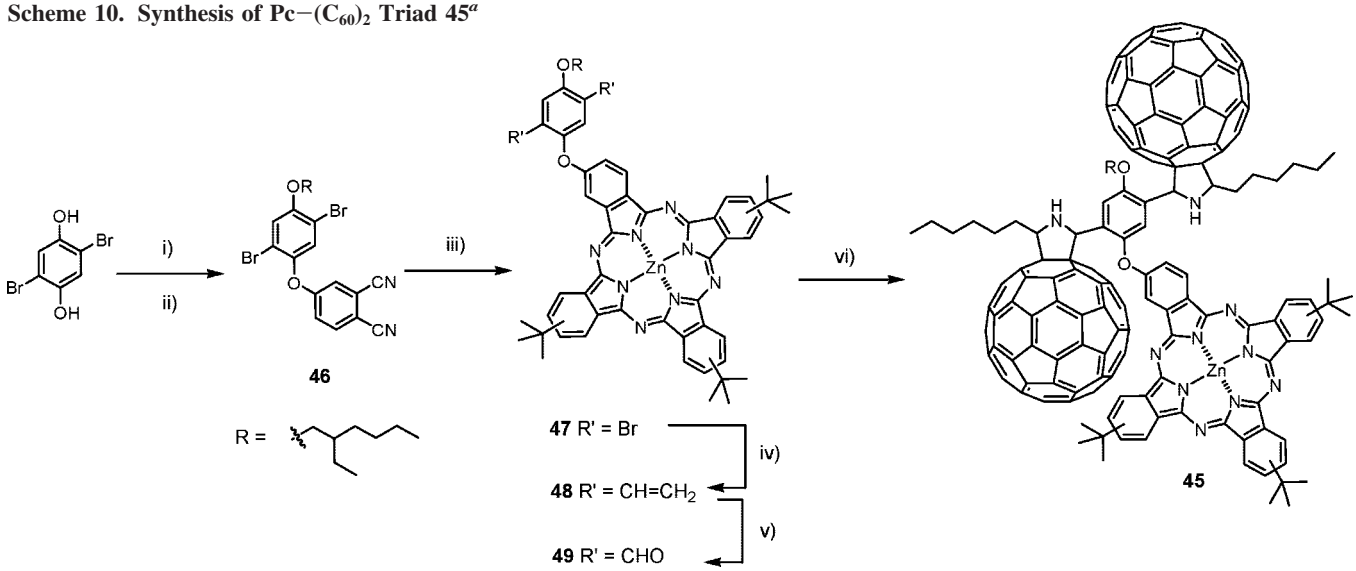

[a] Reagents and conditions: (i) 4-nitrophthalonitrile, K_2CO_3, DMF, argon, rt; (ii) 2-ethyl-1-hexyl bromide, K_2CO_3, DMF, argon, 100 °C; (iii) 4-*tert*-butylphthalonitrile (**6**), $ZnCl_2$, DMAE, argon, reflux; (iv) tributylvinyltin, $Pd(PPh_3)_4$, dry toluene, argon, 100 °C; (v) OsO_4 (1%, w/w, in poly(vinylpyridine)), saturated aqueous solution $NaIO_4$, THF, rt; (vi) C_{60} fullerene, hexylglycine, dry toluene, reflux, argon.

Scheme 11. Synthesis of Pc_3-C_{60} Fullerene Tripod 50[a]

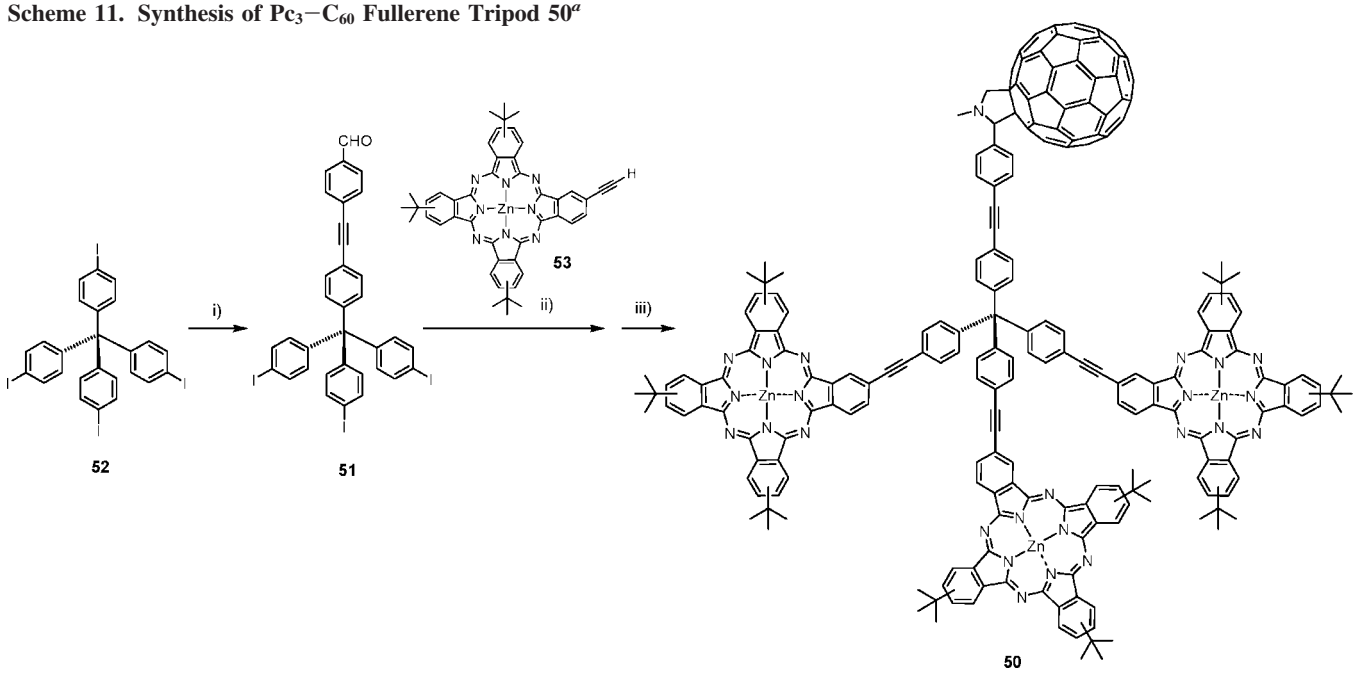

[a] Reagents and conditions: (i) 4-ethynylbenzaldehyde, $Pd(PPh_3)_2Cl_2$, CuI, NEt_3, THF, rt; (ii) Pc **53**, Pd_2(dibenzylideneacetone)$_3$, $AsPh_3$, NEt_3, THF, rt; (iii) C_{60} fullerene, *N*-methylglycine, toluene, reflux.

one Pc and two C_{60} fullerene acceptor units covalently connected between them has been prepared (Scheme 10).[104]

The synthesis of triad **45** starts with the preparation of substituted phthalonitrile **46** by *ipso* substitution of 4-nitrophthalonitrile with 2,5-dibromohydroquinone, followed by alkylation with 2-ethyl-1-hexyl bromide (62% yield over two steps). The crossover condensation of compound **46** with 4-*tert*-butylphthalonitrile (**6**), in the presence of $ZnCl_2$, afforded Pc **47** (23% yield), which was subsequently subjected to a double Stille coupling reaction using an excess of vinyltributyltin and $Pd(PPh_3)_4$ to obtain Pc **48**. The two terminal alkenes of **48** were then oxidized with an OsO_4/$NaIO_4$ mixture in THF, affording diformyl-Pc **49** (61% yield over the two steps). In situ generation of the azomethine ylides from diformyl derivative **49**, followed by a double [3 + 2] cycloaddition reaction with 2 equiv of C_{60} fullerene, afforded triad **45** in 47% yield.

En route toward the preparation of novel electron D−A conjugates, a multinuclear Pc_3-C_{60} fullerene tripodal architecture (**50**) containing a tetraphenylmethane core has been recently reported (Scheme 11).[105] The synthesis of conjugate **50** was carried out starting with the preparation of compound **51** obtained by Sonogashira cross-coupling reaction of 4-ethynylbenzaldehyde over one of the four iodophenyl groups of **52**. Compound **51** was then subjected to a threefold cross-coupling reaction with the ethynyl-containing Pc **53** to give a formyl-containing, tripod precursor which was then

Scheme 12. Synthesis of $Pc_2-(C_{60})_2$ Tetrad 54[a]

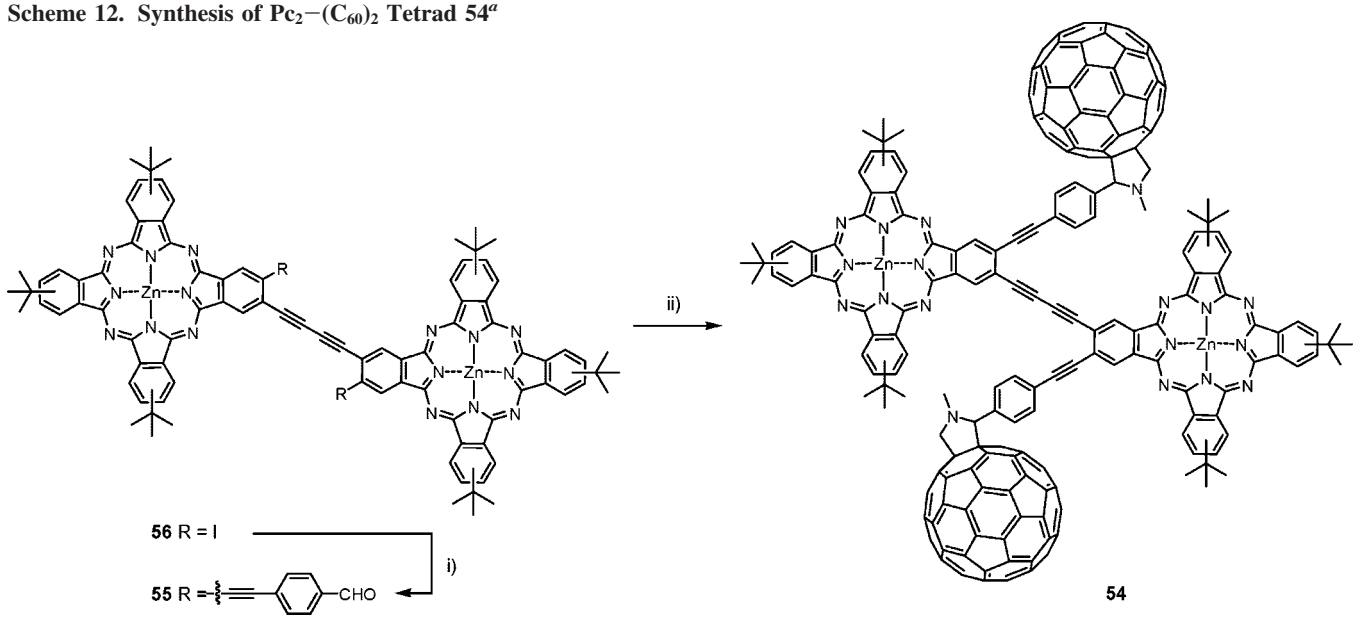

[a] Reagents and conditions: (i) 4-ethynylbenzaldehyde, $Pd(PPh_3)_2Cl_2$, CuI, NEt_3, THF, rt; (ii) Pd_2(dibenzylideneacetone)$_3$, $AsPh_3$, NEt_3, THF, rt; (iii) C_{60} fullerene, *N*-methylglycine, toluene, reflux.

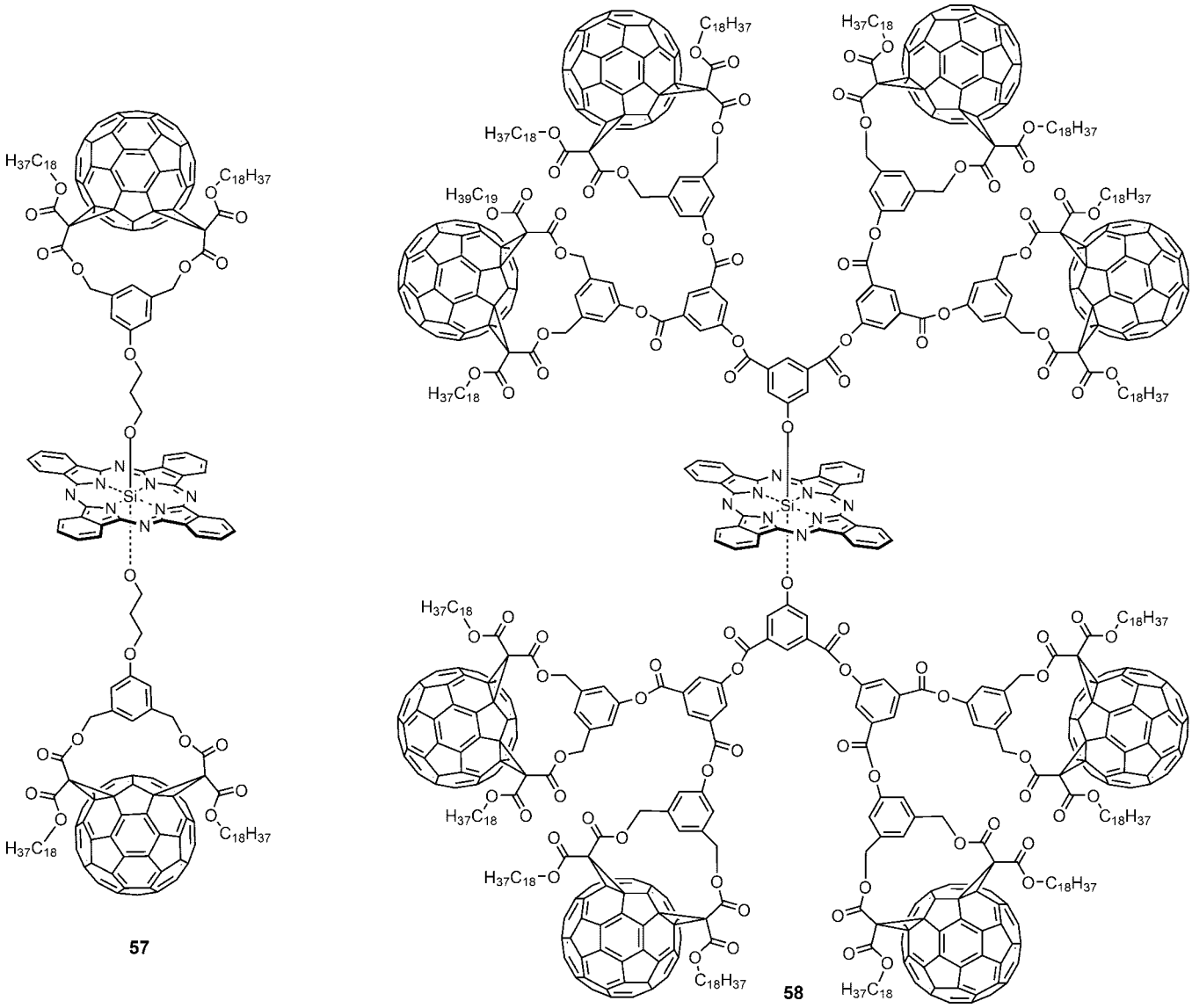

Figure 7. Molecular structures of Si^{IV}Pcs bearing two axial fullerene moieties (**57**) and two axial fullerodendrimers (**58**).

reacted under the standard Prato reaction conditions to obtain tetrad **50** in 22% yield.

An ensemble containing two Pc macrocycles and two C_{60} fullerene units (i.e., **54**) has also been recently reported (Scheme 12).[106] The synthetic strategy toward conjugate **54** consisted in the preparation of the formyl-containing Pc precursor **55**, the latter one prepared from the diiodo-Pc **56**[107] via Sonogashira cross-coupling reactions with 4-ethynylbenzaldehyde. The diformyl-Pc **55** was then reacted under the standard Prato reaction conditions to afford the $Pc_2-(C_{60})_2$ tetrad **54**. Photophysical analysis of ensemble **54** revealed relatively short charge-separated-state lifetimes, probably due to the close proximity of the Pc and the C_{60} subunits in the nanoconjugate. The tight contact between the donor and the acceptor moieties could in fact lead to a through-space deactivation dynamics, which could prohibit the feasibility of forming long-lived radical ion pair states.

The formation of silicon−oxygen bonds has also been used as a means to obtain $Pc-C_{60}$ ensembles, where the C_{60} units are placed at the axial position of the Si^{IV}Pc macrocycle. In this context, an example is represented by Si^{IV}Pc **57**, which bears two axial fullerene substituents (Figure 7).[108] The synthesis of this ensemble involves the reaction of a $Si^{IV}Cl_2$Pc with a C_{60} fullerene bisadduct bearing an alcohol functionality. The structural shape of this triad presenting two bulky C_{60} fullerenes in the axial positions permits achievement of the steric isolation of the Pc macrocycle by diminishing the Pc−Pc intermolecular interactions. Electrochemical studies revealed that the first reduction of the Pc moiety in compound **57** was more anodic than that of a reference compound lacking the C_{60} fullerene axial ligand. This observation was rationalized in terms of the strong electron-withdrawing effect of the two axial fullerene substituents, which led to the stabilization of the first reduced state of the Pc. However, the first oxidation of the Pc moiety in **57**, as well as the first reduction potential of C_{60}, remained the same with respect to that of the reference compounds. Using related dendritic, bisadduct-type C_{60} derivatives, Si^{IV}Pc-containing fullerodendrimers bearing up to eight axial fullerene subunits (i.e., **58**) have been synthesized with the aim of stabilizing the photogenerated radical ion pair state (Figure 7).[109]

A structurally simpler $C_{60}-Si^{IV}Pc-C_{60}$ triad (**59**) with a short $C_{60}-Pc$ plane distance has been prepared by reaction of *p*-formylbenzoic acid with tetra-*tert*-butyl-$Si^{IV}PcCl_2$, followed by a double Prato reaction with C_{60}

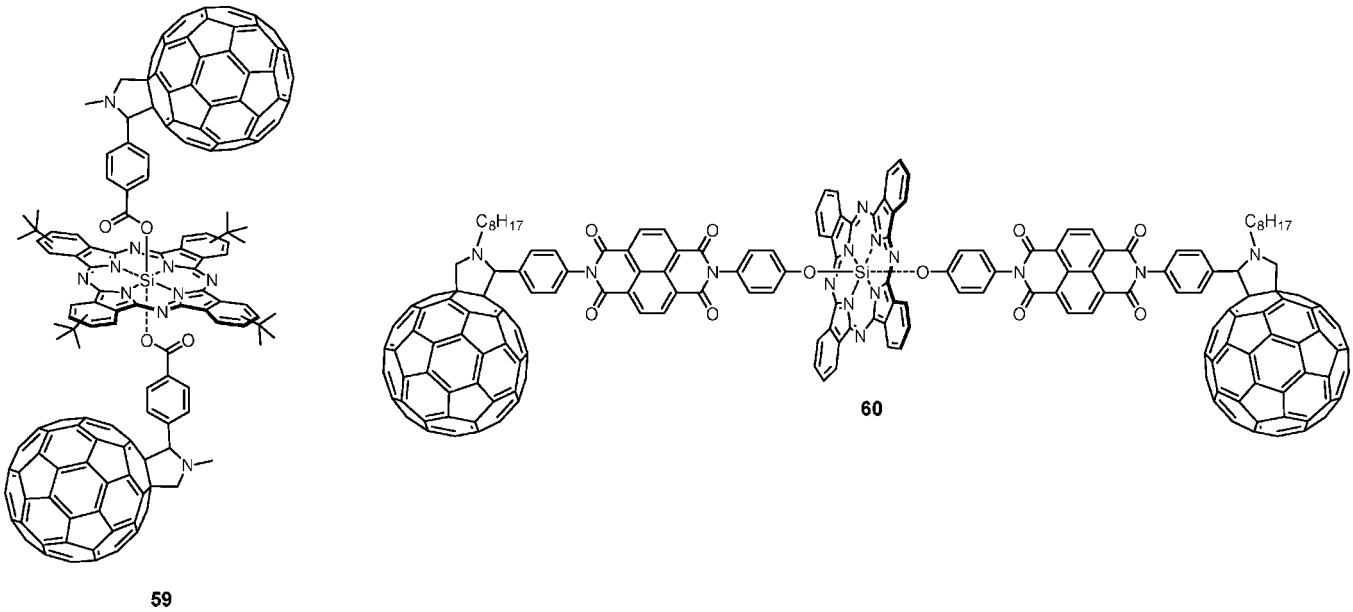

Figure 8. Molecular structures of Si^{IV}Pcs bearing axial fullerene (**59**) and 4,5,8-naphthalenenediimide (NDI)−C_{60} (**60**) moieties.

Scheme 13. Synthesis of Pc−C_{60} Polymers 61[a]

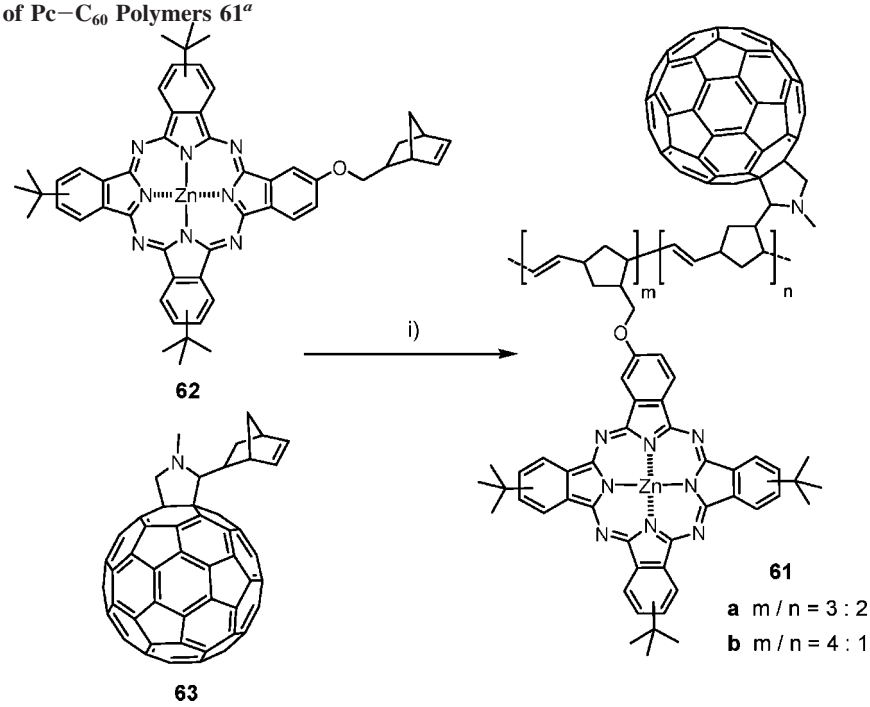

[a] Reagents and conditions: (i) Grubbs catalyst [1,3-dimesityl-4,5-dihydroimidazol-2-ylidene)(tricyclohexylphosphine)$Cl_2RuCH(C_6H_5)$] (2%), toluene, rt.

fullerene (Figure 8).[110] Other Si^{IV}Pc-based triads containing either two trinitrofluorenone or two trinitrodicyanomethylenefluorene moieties in the Pc axial position have also been synthesized.[111] More recently, a Si^{IV}Pc-based pentad (**60**) comprising two different electron-accepting entities, namely, NDI and C_{60}, has been constructed following the same methodology, that is, the reaction between the $Si^{IV}PcCl_2$ and a hydroxyl-functionalized, C_{60} fullerene, NDI derivative (Figure 8).[112]

On the other hand, molecular systems based on a polynorbornene framework (i.e., **61a,b**) bearing several electroactive Pc and C_{60} pendent units have also been reported.[113] These polymeric systems were prepared in good yields from Pc **62** and C_{60} derivative **63**, both containing a norbornene moiety, by ring-opening-metathesis polymerization in the presence of a Grubbs catalyst (Scheme 13).

Statistical condensation of 4-*tert*-butylphthalonitrile (**6**) and a phthalonitrile bearing a pendent norbornene group allowed for the preparation of the polymer precursor **62**, whereas compound **63** was obtained via a Prato reaction of C_{60} fullerene with *N*-methylglycine and a norbornene bearing an aldehyde functionality. Two copolymers (**61a** and **61b**) were prepared, presenting a distinct ratio between C_{60} fullerene and Pc units (2:3 and 1:4, respectively) as a function of the relative molar ratio of the fulleropyrrolidine− and Pc−norbornene monomers **61a** and **61b** in the reaction mixture.

Scheme 14. Synthesis of Pc-Containing, $M_3N@C_{80}$-Based (M = Y, Sc) Dyads 64 and 65[a]

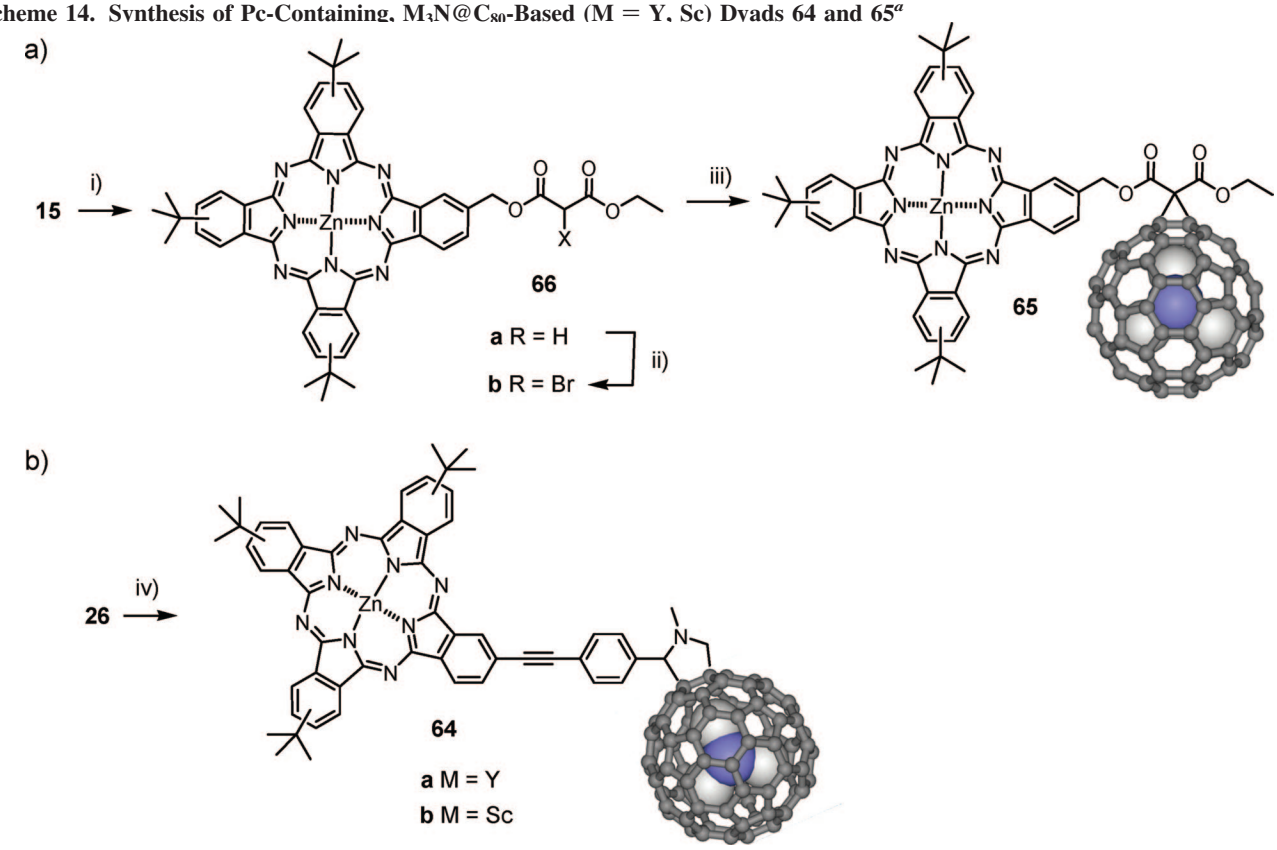

[a] Reagents and conditions: (a) (i) 3-chloro-3-oxopropionate, NEt_3, CH_2Cl_2, argon, rt; (ii) CBr_4, DBU, CH_2Cl_2, argon, 0 °C; (iii) I_h $Y_3N@C_{80}$, DBU, *o*-DCB, argon; (b) (iv) *N*-methylglycine, I_h $Y_3N@C_{80}$ (for **64a**) or I_h $Sc_3N@C_{80}$ (for **64b**), anhydrous toluene/anhydrous *o*-DCB, reflux.

Partially pyrrole ring reduced Pc analogues such as azachlorins, macrocyclic species which present a significant chemical instability with respect to Pcs, have also been covalently connected to C_{60} fullerene by the mixed condensation of an appropriately substituted phthalonitrile and a C_{60} fullerene derivative bearing two adjacent cyano groups.[114] In such molecular dyads and triads, electronic communication between the azachlorin and C_{60} fullerene moieties was demonstrated on the basis of UV/vis absorption, magnetic circular dichroism, electrochemical, and quantum chemical methods.

More recently, a tetraazachlorin−C_{60} fullerene conjugate containing three 15-crown-5 units as substituents has been synthesized, and the electronic and supramolecular structure modulations in the presence of cations such as Na^+ or K^+ have been studied.[115] A system structurally related to the tetraazachlorin−C_{60} fullerene conjugate, in which the three crown ether macrocycles at the chlorin periphery have been substituted for *tert*-butyl groups, has also been prepared.[116] UV/vis absorption studies on this conjugate show a red shift from the corresponding absorption of a related chlorin derivative lacking the fullerene moiety, indicating, in the former dyad, interactions between the macrocycle and C_{60}. Electrochemical studies of the tetraazachlorin−C_{60} dyad in polar solvents show that the first oxidation potential is centered on the Pc moiety, whereas the first reduction potential is associated with C_{60}, suggesting that the lowest unoccupied molecular orbital (LUMO) localizes on the fullerene moiety in polar solvents.

The preparation of Pc-based D−A dyads in which the Pc units have been covalently linked to trimetallic nitride templated endohedral metallofullerenes has also been reported.[117] These metallofullerenes, one of the latest entries within the family of fullerene compounds, are constituted by a carbon cage encapsulating a trimetallic nitride cluster and since their first synthesis in 1999[118] have been the focus of increasing interest. Trimetallic nitride templated endohedral metallofullerenes present several advantages with respect to C_{60} fullerene, such as larger absorptive coefficients in the visible region of the electromagnetic spectrum and lower highest occupied molecular orbital (HOMO)−LUMO energy gaps, while preserving, similar to C_{60}, a remarkable electron-accepting ability.

In this context, a series of $M_3N@C_{80}$-based (M = Y, Sc) dyads containing a Pc macrocycle (as well as some other acceptor units such as Fc or extended tetrathiafulvalene) have been prepared via Prato (**64**) or Bingel−Hirsch (**65**) reactions (Scheme 14). The synthesis of compounds **64a**,**b** involves a 1,3-dipolar cycloaddition reaction of a Pc-containing azomethine ylide (generated in situ from Pc **26**) on either $Y_3N@C_{80}$ or $Sc_3N@C_{80}$ endohedral fullerenes, leading to **64a** and **64b**, respectively. Unfortunately, the attempts made to prepare the Pc-substituted, pyrrolidine-containing $M_3N@C_{80}$ (M = Y, Sc) dyads proved to be unsuccessful in the case of $Sc_3N@C_{80}$, whereas in the case of $Y_3N@C_{80}$ the desired product **64a** could be isolated in low yield. These findings seem to indicate a considerable instability of these Pc-based dyads, not observed in their C_{60}-based counterparts. On the other hand, the synthesis of compound **65** involves the preparation of Pc derivative **66a** containing a malonate unit by reacting Pc **15** with 3-chlorooxopropionate. The latter compound was then monobrominated to obtain **66b**, which was successively reacted with $Y_3N@C_{80}$ in the presence of DBU (in the case of the trimetallic nitride templated endohedral fullerene chemistry, it is not possible to generate the halomalonate precursor directly in situ as commonly done

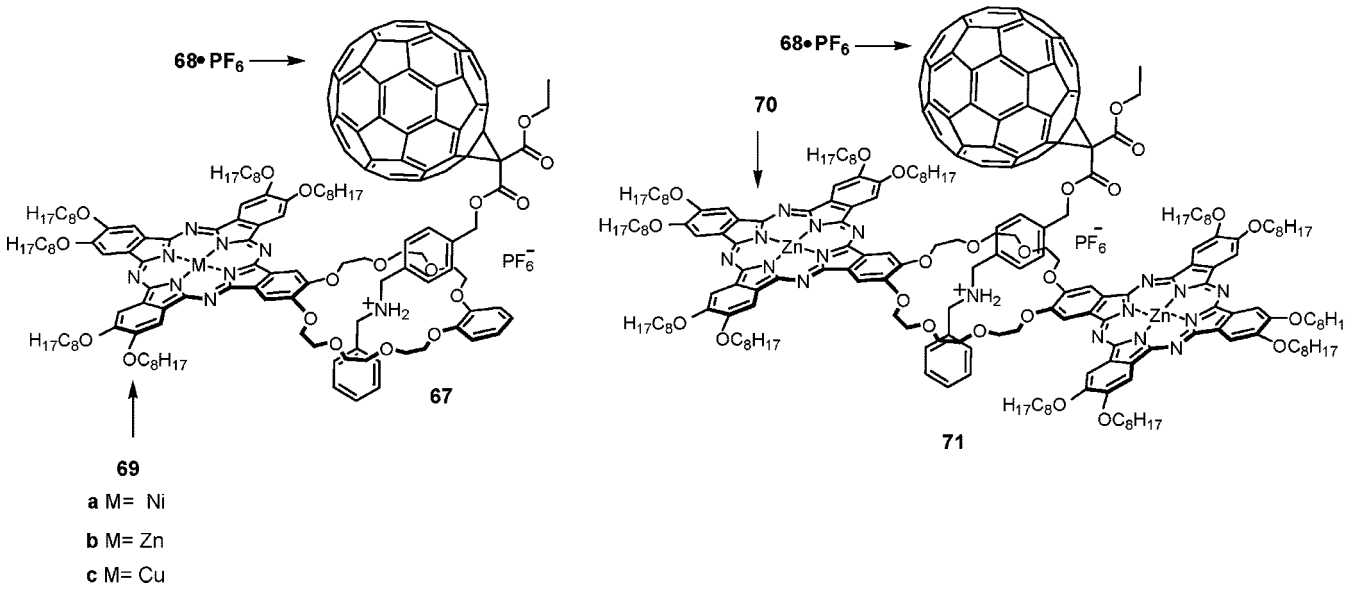

Figure 9. Molecular structures of [2]pseudorotaxane Pc−C_{60} dyads **67a**−**c** and Pc_2−C_{60} triad **71**.

in the Bingel−Hirsch reaction, since the presence of either I_2 or CBr_4 would oxidize the endohedral fullerene). Dyad **65** could be isolated, but it proved to be not stable and decomposed in $CHCl_3$ solution during the purification process. The formation and degradation of dyad **65** was followed by high-pressure liquid chromatography, which allowed identification of the two major degradation products, a $Y_3N@C_{80}$−monoethyl malonic acid adduct and Pc **15**. The two decomposition products of dyad **65** are the result of a hydrolysis process, probably promoted by the close proximity of the endohedral fullerene.

2.2. Phthalocyanine−Fullerene Supramolecular Systems

The preparation of D−A Pc-based systems in which the active components spontaneously assemble via noncovalent interactions is a promising strategy for the construction of functional systems. Such noncovalent systems are expected to give rise to efficient and long-lived photoinduced CS processes, thus representing an attractive alternative to their covalently linked counterparts. To date, several Pc−C_{60} fullerene-based supramolecular systems have been prepared by hydrogen-bonding, metal−ligand coordination, or cation−crown ether supramolecular interactions, among others.

In 2002, the first example of a Pc−C_{60} fullerene pseudorotaxane-like complex (i.e., **67**) was reported (Figure 9).[119] The supramolecular complex **67** consists of two components: a C_{60} derivative (**68**) bearing a secondary dibenzylammonium moiety and a Pc macrocycle (**69**) peripherally substituted with a dibenzo-24-crown-8 unit. The latter compound was prepared by statistical crossover condensation of 4,5-bis(octyloxy)-phthalonitrile and a dibenzo-24-crown-8 macrocycle containing two adjacent cyano groups on one of the benzene units.

The two components **69a**, **69b**, or **69c** and **68** self-assemble in chloroform solutions by threading of the dibenzylammonium chain of the C_{60}-containing molecule through the crown ether ring of Pc **69a**, **69b**, or **69c**, as demonstrated by ^{1}H NMR experiments. In fact, resonance peaks assigned to (i) the two free components and (ii) the 1:1 complex could be observed due to the unusually slow host−guest exchange on the ^{1}H NMR time scale at rt, which allowed determination of the stoichiometry and the association constant of the complex ($K_a = 1.53 \times 10^4$ M^{-1}) by integration of the signals of the species at equilibrium. However, UV/vis titration experiments of a dilute solution of **69a** in CH_2Cl_2 did not show a significant change in the Pc absorption upon addition of an equimolar amount of the fullerene derivative **68**, thus indicating negligible electronic communication between the two active units in the ground state. Similarly, electrochemical analysis on the fullerene reduction waves upon addition of the crown ether Pc **69b** did not show substantial changes, thus suggesting that the complexation does not influence the reduction properties of the fullerene component. The absence of measurable electronic interactions between the two components in **67** could be due to the distance between the electroactive units, which can adopt several conformations within the complex as revealed by molecular modeling studies.

Maintaining the same recognition motif employed above for the preparation of Pc−C_{60} dyad complex **67** (i.e., ammonium−crown ether interactions), but increasing this time the number of Pc units around the crown ether ring from 1 (i.e., **69**) to 2 (i.e., **70**), allowed for the construction of the Pc_2−C_{60} supramolecular triad **71** (Figure 9).[120]

Directional, Watson−Crick hydrogen-bonding interactions have also been used recently as a recognition motif for the assembly of Pc−C_{60} dyad **72**, constituted by a cytidine-substituted Pc (**73**) and a fulleropyrroline (**74**) bearing a guanosine moiety (Figure 10).[121] UV/vis studies on Pc **73** revealed that this molecule undergoes self-assembly as a result of both $\pi-\pi$ interactions and cytidine−macrocycle interactions. The resulting aggregates can be disrupted upon addition of C_{60} fullerene derivative **74**, in which the guanosine nucleic acid base serves to tie up the cytidine functionality of **73** through base-pairing interactions, although other disrupting mechanisms such as direct interaction of the guanosine moiety in **74** with the metal center of **73** should also be considered. Moreover, the addition of **74** to a dichloromethane solution of cytidine-functionalized Pc **73** leads to a nonlinear decrease in the fluorescence intensity of this latter chromophore, suggesting that photoinduced intracomplex CS takes place within ensemble **72**. Fluorescence titration studies also allowed determination of the binding constant between the two components **73** and **74** in

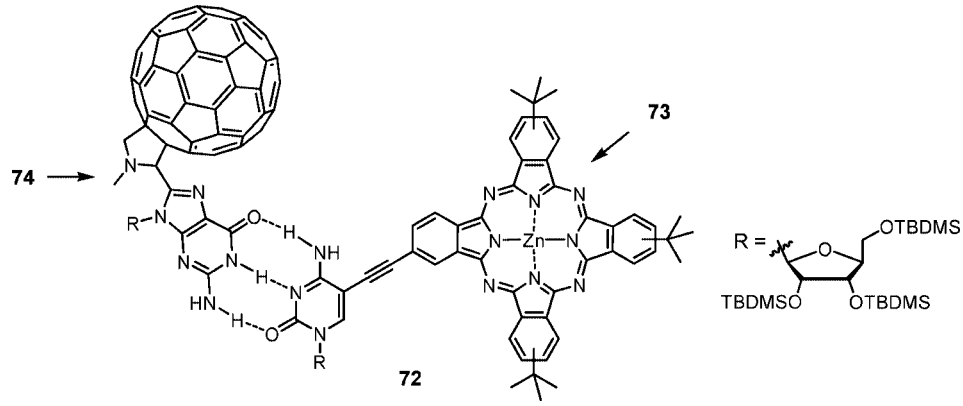

Figure 10. Molecular structure of Pc−C_{60} dyad **72** assembled through Watson−Crick hydrogen-bonding interactions.

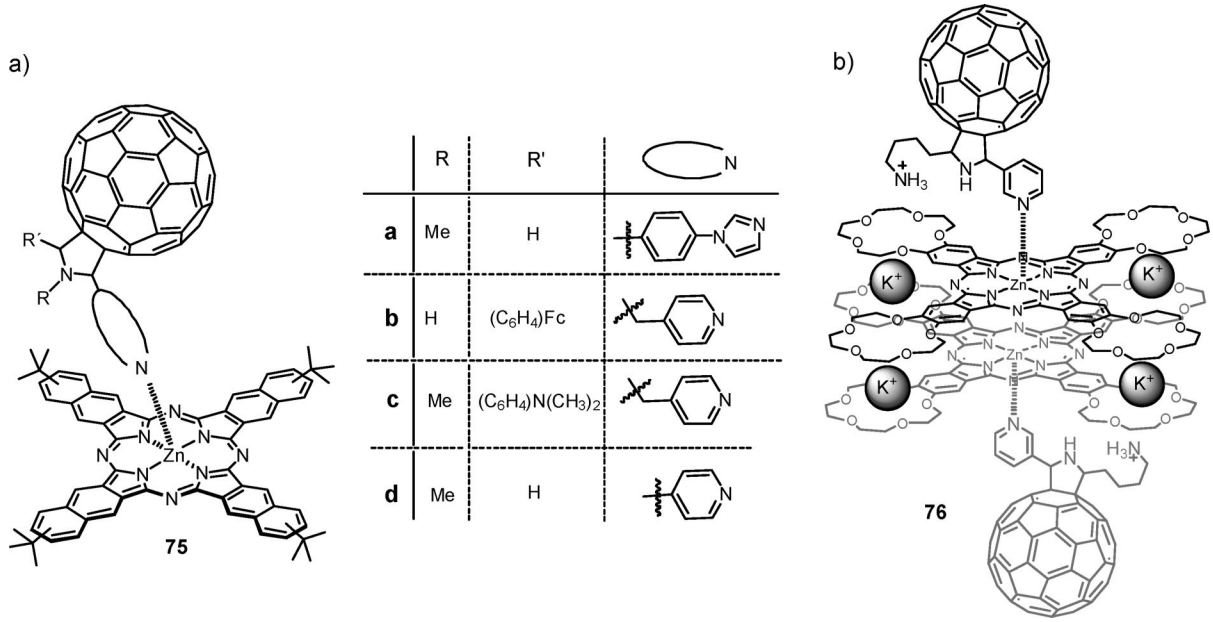

Figure 11. Structures of the supramolecular (a) Zn^{II}Nc−C_{60} dyads **75a**−**d** and (b) crown ether Pc_2−$(C_{60})_2$ ensemble **76**.

the supramolecular complex **72** ($K_a = 2.6 \times 10^6$ M^{-1} in toluene/dichloromethane).[122] The electrochemical behavior of supramolecular complex **72** and its constituents **73** and **74** was also studied, revealing that dyad **72** presents the C_{60}-based reduction potentials negatively shifted with respect to those of **74**. Likewise, the first and second anodic Pc-based potentials are less positive than those of **73**. On this basis, it can be concluded that there are significant ground-state interactions between the Pc donor and the C_{60} fullerene acceptor.

During the past few decades, metal-directed self-assembly has become a major tool used by chemists to prepare large and elaborate complexes from relatively simple components. The resulting metallosupramolecular species present large energies associated with the metal−ligand bond formation.

Fullerenes derivatized with appropriate ligands have been attached via supramolecular interactions to molecules bearing complementary metal centers. In particular, the coordination of a C_{60}-containing ligand to a transition-metal center has been successfully demonstrated for Zn^{II}Pors and C_{60} functionalized with pyridine or imidazole ligands.[123−126] The same approach has also been applied to prepare Zn(II) naphthalocyanine (Zn^{II}Nc)−C_{60} dyad **75a** (Figure 11a).[127] This tetra-*tert*-butyl-substituted Zn^{II}Nc was used since it has a good solubility in many organic solvents and an intense absorption band in the near-IR region. Moreover, the presence of a zinc atom within the Nc system allowed for the axial ligation of a fulleropyrrolidine bearing an imidazole coordinating ligand in noncoordinating solvents such as toluene and *o*-DCB, giving rise to complex **75a**, which shows a moderate stability. Similarly, analogue systems of **75a**, containing either Fc (i.e., triad **75b**) or (*N*,*N*-dimethylamino)phenyl entities (i.e., triad **75c**) as secondary electron donors were constructed using the same supramolecular approach.[128]

More recently, Pc−C_{60} supramolecular tetrad **76** has been reported, which is constituted by two crown ether-containing Zn^{II}Pc units, four potassium ions, and two fullerene derivatives bearing both a pyridine and a terminal ammonium moiety (Figure 11b).[129] Ensemble **76** is held together by a combination of metal−ligand interactions between the pyridine group on the fullerene derivative and the Zn^{II}Pc central atom and cation−crown ether interactions between the four crown ether substituents on the two Pc rings and four potassium ions, leading to the formation of a cofacial Pc−Pc dimer. A further contribution to the stability of complex **76** is obtained via the interaction of the terminal alkylammonium moiety present on the fullerene derivative to one of the crown ether macrocycles. This latter complexation occurs without destroying the $4K^+$/Pc−Pc sandwich dimer.

The same metal−ligand interactions have been used to assemble the supramolecular triad **77** in which a covalently linked, peripherally substituted boron dipyrromethene (Bodipy)−Pc conjugate has been axially coordinated to a

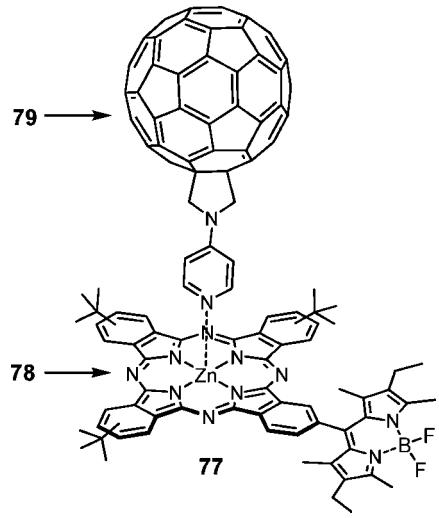

Figure 12. Structure of the supramolecular $Zn^{II}Pc-Bodipy-C_{60}$ triad **77**.

C_{60} fullerene derivative bearing a pyridine moiety (Figure 12).[130] Acid-catalyzed condensation of formyl-Pc **10a** with 3-ethyl-2,4-dimethylpyrrole afforded the dipyrromethane-substituted Pc, which was then oxidized in situ by treatment with *p*-chloranil to give the corresponding dipyrromethene derivative. Finally, this latter compound was subject to deprotonation (treatment with triethylamine) and treated with boron trifluoride etherate to afford the Bodipy−Pc derivative **78** in an overall yield of 28%. Electrochemical and optical measurements provided evidence for strong ground-state electronic interactions between the Bodipy and the $Zn^{II}Pc$ constituents. Ensemble **78** was then reacted with *N*-(4-pyridyl)-3,4-fulleropyrrolidine **79**, thus obtaining the supramolecular complex **77**.

Catechol ligands are well-known building blocks for the construction of metallosupramolecular complexes using Ti(IV). This self-assembly methodology was successfully utilized by the groups of Torres and Ito, who published independently the axial coordination of a catechol-functionalized C_{60} fullerene to a titanium(IV) oxide Pc ($Ti^{IV}OPc$) (Scheme 15). Ito's group followed a synthetic procedure involving the former axial coordination of 4-formylcatechol to tetra-*tert*-butyl-$Ti^{IV}OPc$ to give **80** and subsequent Prato reaction between the axial formyl moiety and C_{60} in the presence of *N*-methyl glycine to yield dyad **81**.[131] The Torres group instead explored a more convergent route, which involved the preparation of a catechol subunit bearing a C_{60} moiety followed by displacement of the oxygen atom of the tetra-*tert*-butyl-$Ti^{IV}OPc$ to give the axially substituted dyad **81**.[132] Photophysical studies demonstrated the occurrence of PET from the photoexcited Pc to the fullerene unit. In addition, the nonlinear absorptive properties of this dyad have also been studied using the open-aperture Z-scan technique.[133]

The presence of Ru(II) in the central cavity of Pcs allows either one or two ligands to be linked to the macrocycle in its axial positions. Such $Ru^{II}Pcs$ in fact form stable and rigid supramolecular architectures through metal coordination of, for example, pyridine derivatives. These features have been exploited to construct a series of $Ru^{II}Pc-C_{60}$ hybrids (**82**−**84**) bearing an orthogonal geometry (Figure 13).[134]

Starting from the tetra-*tert*-butylated phthalocyaninato ruthenium(II) derivative having a strongly ligating axial carbonyl moiety at one of the two axial Ru(II) coordination sites, dyad **82** and triad **84** were prepared by treatment with a monopyridyl-functionalized C_{60} ligand in the former case and, in the latter, with a highly elaborated *trans*-1-bis[*N*-(4-pyridyl)fulleropyrrolidine] ligand, which holds two pyridyl ligands in an antiparallel arrangement. Triad **83** was prepared in a similar manner from the monopyridyl-functionalized C_{60} ligand and the tetra-*tert*-butylated phthalocyaninato ruthenium(II) derivative having two benzonitrile molecules at the axial positions. Arrays **82**−**84** exhibited electronic coupling between the two electroactive components in the ground state, as shown by electrochemical experiments.

The supramolecular functionalization of surfaces by adsorption and self-assembly of Pc macrocycles has also been

Scheme 15. Synthesis of $Ti^{IV}Pc-C_{60}$ 81 Following Two Different Synthetic Routes[a]

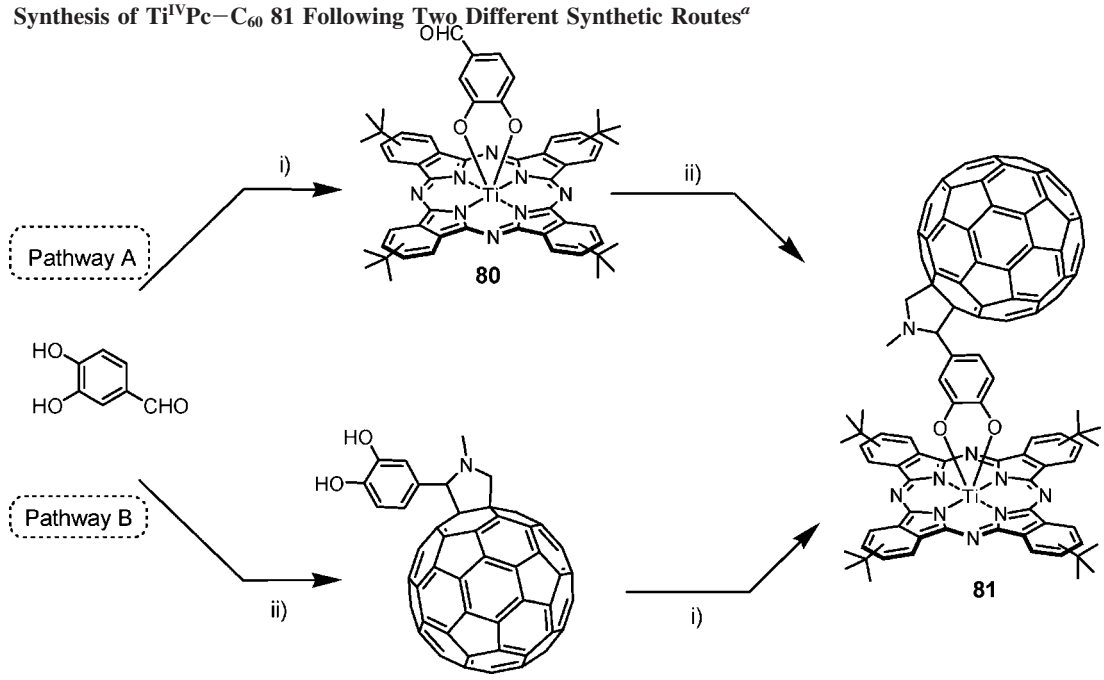

[a] Reagents and conditions: (i) tetra-*tert*-butyl-$Ti^{IV}OPc$, THF, reflux; (ii) C_{60} fullerene, *N*-methylglycine, *o*-DCB, 140 °C.

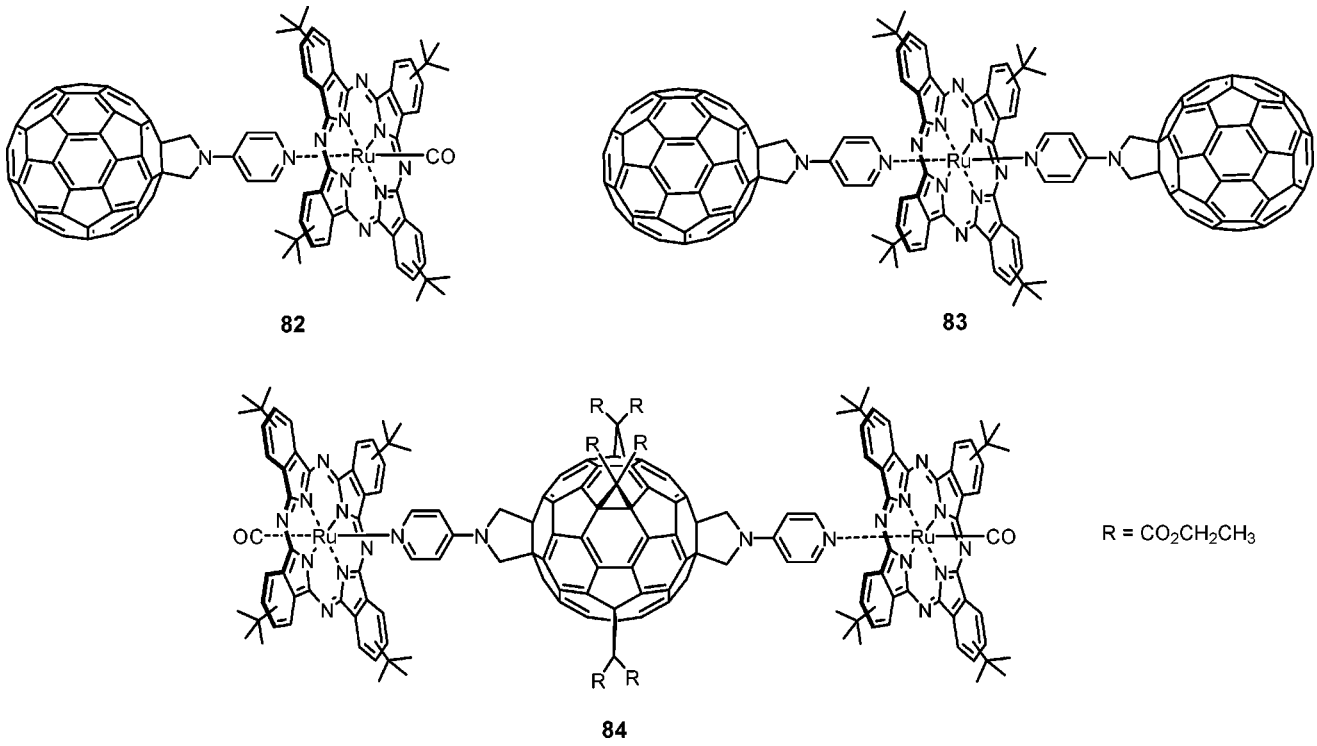

Figure 13. Structures of the supramolecular $Ru^{II}Pc-C_{60}$ dyad **82** and triads **83** and **84**.

achieved, which allows preparation of open, two-dimensional packing motifs that can accommodate complementary guest acceptor molecules such as C_{60} fullerene[135−137] or buckyball-type molecules such as corannulene.[138,139] Recently, a similar approach has been used to prepare a surface-supported, three-component system in which the metastable, two-dimensional, two-component packing motif resulting from Pc and Por macrocycles adsorbed on Ag(111) acts as a bimolecular "chessboard" toward the supramolecular assembly of a third active component (i.e., C_{60} fullerene), which is selectively trapped in the open spaces (Figure 14).[140]

More recently, C_{60} monolayers on Ag(111) have been used to promote the molecular orientation of $Cu^{II}Pcs$ in thin films.[141] In situ near-edge X-ray absorption fine structure measurements and low-temperature scanning tunneling microscopy studies revealed that, on such monolayers, the $Cu^{II}Pc$ is able to form densely packed thin films, in which the macrocycles adopt a standing-up configuration with the molecular plane of the Pc slightly tilting from the surface normal on the C_{60} monolayer.

3. Subphthalocyanine−Fullerene Donor−Acceptor Systems

3.1. Covalently-Linked Subphthalocyanine−Fullerene Systems

SubPcs are 14-π-electron aromatic macrocycles possessing a singular C_3-symmetrical cone-shaped structure.[42] Similar to Pcs, SubPcs possess unique physicochemical properties which make these macrocycles ideal candidates for their incorporation in D−A molecular systems, although the use of SubPcs in D−A systems has been exploited only recently. Up to a few years ago, in fact, the design and preparation of sophisticated SubPc-based systems had to face the severe limitations imposed by the low yields and not full reproducibility of the synthetic methodologies used to prepare these macrocycles. However, the development of milder and more

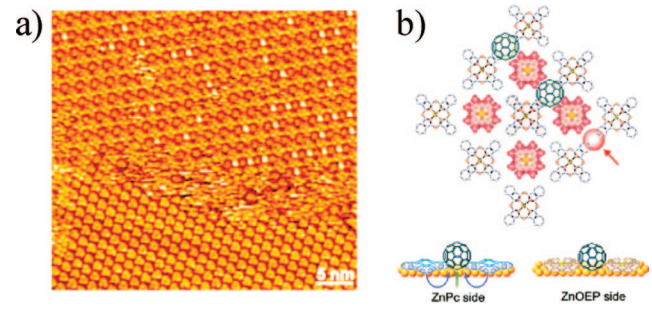

Figure 14. (a) Scanning tunneling microscopy image of a C_{60} array in the bimolecular chessboard consisting of $Zn^{II}Pc$ and $Zn^{II}Por$ on Au(111). (b) Proposed models for the top and side views of the C_{60} array in the bimolecular chessboard. Reprinted from ref 140. Copyright 2008 American Chemical Society.

reliable synthetic procedures, together with the search of novel functionalization approaches, opened the way for the preparation of D−A SubPc-based molecular systems. SubPc''s can be functionalized either at the peripheral or at the axial position. Peripheral functionalization requires the substitution at the isoindole units, and in analogy to the synthesis of Pc- or Por-based D−A systems, it usually involves the preparation, isolation, and subsequent functionalization of unsymmetrically substituted macrocycles. However, and differently from Pcs or Pors, SubPcs can also be easily functionalized covalently at their axial position, typically by exchange of the halogen atom with a nucleophile. This approach bears the twofold advantage that (i) it avoids the preparation and low-yield isolation of unsymmetrically substituted SubPcs and ii) it allows preparation of functionalized SubPc systems in which the macrocycle electronic characteristics are mostly preserved.

Similarly to the case of Pcs, C_{60} fullerene has also been used as a molecular component in D−A SubPc-based architectures.

The first SubPc−C_{60} fullerene conjugate (**85b**) was reported in 2002 (Scheme 16).[142] The synthesis of this dyad

Scheme 16. Synthesis of SubPc−C_{60} Fullerene Dyads 85a−d[a]

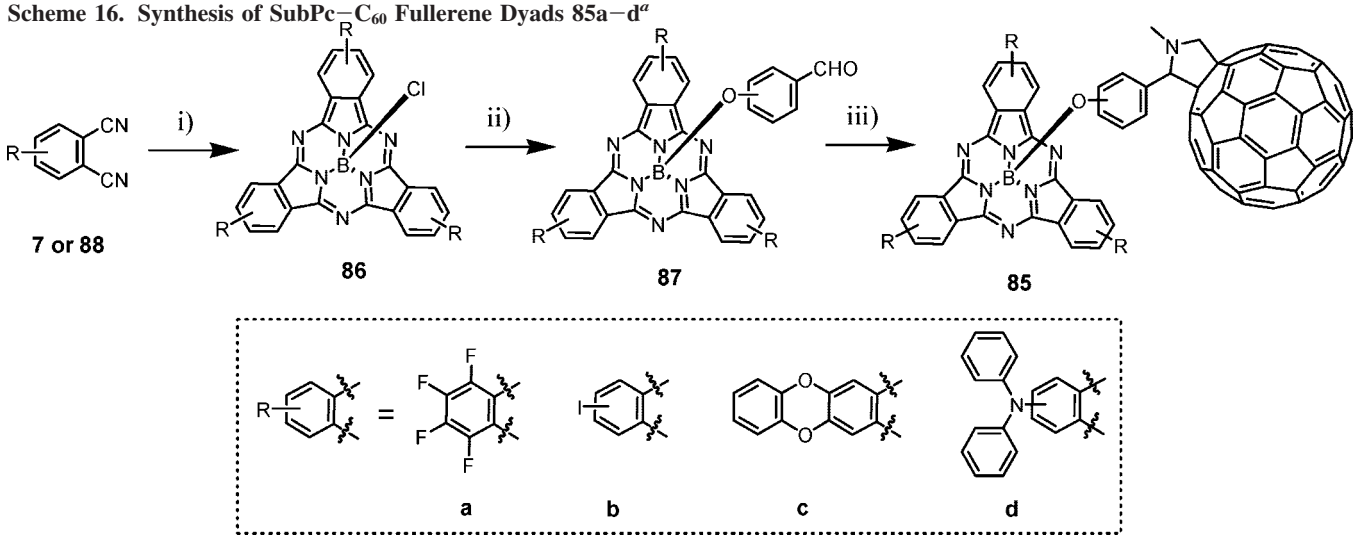

[a] Reagents and conditions: (i) **7** for **86b** or **88a,c,d** for **86a,c,d**, BCl_3, argon, *p*-xylene, reflux; (ii) *o*-, *m*-, and *p*-hydroxybenzaldehyde (for *o*-**87**, *m*-**87**, and *p*-**87**, respectively), toluene, 110 °C [**86b**, diphenylamine, Cs_2CO_3, Pd_2(dibenzylideneacetone)$_3$, 2,2′-bis(diphenylphosphino)-1,1′-binaphthyl, argon, toluene, reflux for **87d**]; (iii) C_{60} fullerene, *N*-methylglycine, toluene, 100 °C.

involves the preparation of SubPc **86b** by condensation reaction of 4-iodophthalonitrile (**7**) in the presence of boron trichloride. Reaction of SubPc **86b** with *o*-, *m*-, or *p*-hydroxybenzaldehyde afforded the aldehyde-containing SubPc *o*-**87b**, *m*-**87b**, or *p*-**87b**, respectively. The latter SubPcs were then reacted with C_{60} fullerene in the presence of *N*-methylglycine, thus obtaining SubPc−C_{60} dyads *o*-, *m*-, and *p*-**85b**, respectively (43−58% yields).

UV/vis studies on these SubPc−C_{60} fullerene dyads revealed a small bathochromic shift in the SubPc Q-band with respect to the Q-band of the corresponding SubPc compounds lacking the fullerene moiety, a sign of a ground-state electronic communication between the SubPc and the C_{60} fullerene units. Electrochemical studies on *o*-, *m*-, and *p*-**85b** revealed that *m*-**85b** is the easiest to reduce and also the easiest to oxidize in the dyads' series, indicating the weakest ground-state interaction between the SubPc and the fullerene subunits. In turn, this finding indicates that, at least in the ground state, the electronic communication between the SubPc and C_{60} fullerene is occurring through-bond and not through-space.

The presence of three peripheral iodo atoms in SubPcs *o*-, *m*-, and *p*-**87b** opens up the possibility to further functionalize this macrocycle via some metal-catalyzed reactions. Palladium-catalyzed amination reaction of SubPcs **87b** with diphenylamine was in fact used to prepare SubPcs **87d**, which, subsequently subjected to Prato reaction conditions, afforded SubPc−C_{60} fullerene dyads **85d**.[143] Cyclic voltammetry experiments carried out on SubPc−C_{60} fullerene dyads *o*-, *m*-, and *p*-**85d** revealed that, as in the case of **85b**, the *meta*-configured spacer induces both easier reduction and oxidation of the two electroactive subunits.

The degree of electronic communication between the SubPc and C_{60} fullerene units could also be adjusted at the level of the peripheral substituents. In this context, a series of four SubPc−C_{60} fullerene dyads (*m*-**85a**−**d**) were prepared and comparatively studied.[144] In such dyads, the nature of the linker between the SubPc and the fullerene was kept unchanged (*meta* substitution), whereas the nature of the peripheral SubPc substituents was varied from the electron-withdrawing fluorine (*m*-**85a**) or iodine (*m*-**85b**) atoms to the electron-donating ether (*m*-**85c**) or amino (*m*-**85d**) groups. Similarly to the preparation of dyads *m*-**85b**,**d**, the synthesis of *m*-**85a,c** also involved the preparation of the respective SubPcs **86a**,**c**, which were obtained by condensation reaction of tetrafluorophthalonitrile **88a** (for **86a**) or phthalonitrile **88c** (for **86c**) in the presence of boron trichloride. Reaction of SubPc **86a**(**c**) with *m*-hydroxybenzaldehyde afforded the aldehyde-containing SubPc *m*-**87a**(**c**), which was subsequently reacted with C_{60} fullerene in the presence of *N*-methylglycine, thus yielding SubPc−C_{60} dyad *m*-**85b**(**c**). Electrochemical studies on these dyads (*m*-**85b**,**c**) revealed that the first SubPc oxidation process could be progressively shifted to lower potentials (by ca. 200 mV) in the series *m*-**85a** > *m*-**85b** > *m*-**85c** > *m*-**85d**, whereas the first C_{60}-based reduction process remained virtually unaffected. The modulation of the electron-donating character of the SubPc due to the nature of the peripheral substituents results, as well, in different deactivation pathways of the photoexcited states of these dyads (i.e., energy transfer (for *m*-**85a**,**b**) versus electron transfer (*m*-**85c**,**d**) dynamics).

More recently, a SubPc−diazobenzene−C_{60} fullerene triad (**89**), in which the SubPc and C_{60} fullerene units are spaced by a diazobenzene molecular bridge, has also been prepared (Figure 15).[145] In such a system, the incorporation of the diazo moiety opens up the possibility to control the relative position of the donor and the acceptor moieties within the triad through the isomerization of the diazo unit by applying a photonic stimulus. Compound **89** was obtained by axial substitution of SubPc−Cl with a diazobenzene molecule bearing a hydroxyl moiety on one of its benzene rings and an aldehyde moiety on the other, followed by Prato reaction of the as-prepared aldehyde-containing, SubPc−diazobenzene system with C_{60} fullerene and *N*-octylglycine.

Recently, tricomponent (**90**) and tetracomponent (**91**) systems composed of one SubPc and one triphenylamine (TPA) unit and either one (i.e., **90**) or two (i.e., **91**) C_{60} fullerene moieties have also been prepared (Scheme 17).[146] The synthesis of compounds **90** and **91** starts with the preparation of (4-methoxyphenyl)diphenylamine (**92**) through the coupling of diphenylamine with 4-iodoanisole under Ullmann conditions, followed by Vilsmeier formylation, thus obtaining both the monoformylated (**93**) and bisformylated (**94**) products. Demethylation of **93** (**94**) affords compound

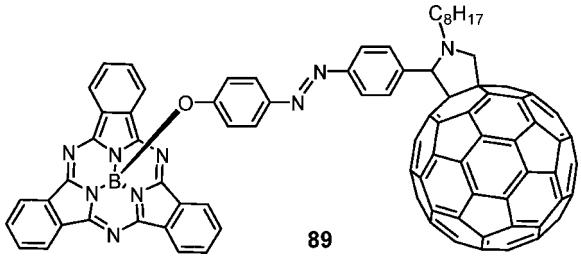

Figure 15. Molecular structure of SubPc−diazobenzene−C_{60} fullerene **89**.

95 (**96**), which is coupled with an unsubstituted SubPc presenting a chlorine atom in its axial position. The resulting aldehyde-containing, SubPc−TPA system **95** (**96**) is reacted with C_{60} fullerene in the presence of *N*-methylglycine, leading to triad **90** (tetrad **91**).

Molecular orbital calculations (B3LYP/3-21G method) on triad **90** showed that the electron distribution of the HOMO was found to be entirely located on the TPA subunit, while the electron distribution of the LUMO + 3 and LUMO was found to be entirely located over the SubPc and C_{60} fullerene moieties, respectively. A similar trend was found for tetrad **91**.

Recently, SubPc−C_{60} fullerene trisadducts **97a**−**c** have also been prepared (Figure 16) and their photophysics studied.[147] These compounds were prepared from appropriately substituted SubPcs bearing three pendent malonate groups, which react with C_{60} fullerene via a triple Bingel−Hirsch reaction, leading to trisadducts **97a**−**c**. Interestingly, it was found that, due to the semirigid nature of the tethers employed, this latter reaction proceeded with high regioselectivity and full diastereoselectivity. UV/vis and electrochemical studies revealed evidence of ground-state communication between the two complementary π-surfaces (i.e., SubPc and C_{60}). This communication is dependent on the nature of the linker (i.e., phenyl, phenoxy, or thiophenoxy), the strongest interaction taking place for compound **97a**, which has the shortest D−A distance.

SubPc systems in which two[148,149] (or three)[150] SubPc units are sharing one (or two) isoindole ring(s) have also been prepared via statistical condensation of a 1,2,4,5-tetracyanobenzene and an appropriately substituted phthalonitrile in the presence of BCl_3. Such fused systems, which can present different topological isomeric forms, possess substantially different electronic properties with respect to pristine SubPcs. In these systems in fact the extended conjugation causes the lowering of the HOMO−LUMO energy gap (e.g., the Q-band absorption of these dimers may reach 700 nm) and, consequently, of their singlet-excited-state energies. The possibility for these SubPc fused systems to promote energy or charge transfer processes in D−A conjugates has also been recently investigated through the preparation of SubPc fused dimer−C_{60} fullerene dyad **98** (Scheme 18).[151]

The synthesis of **98** involves the preparation and isolation of the *syn* topoisomer **99** (this topoisomer is obtained in a 1:1 ratio with the *trans* topoisomer), which is first reacted with 3-hydroxybenzaldehyde. The resulting *syn* isomer **100** is reacted with C_{60} fullerene and *N*-methylglycine, affording the C_{60} bisadduct ensemble **98** in 14% yield. This compound was characterized and its photophysics properties investigated.

3.2. Subphthalocyanine−Fullerene Supramolecular Systems

A pyridyl-containing SubPc has also been used recently for the construction of a D−A supramolecular cage (Figure 17).[152] The rigid concave structure of SubPcs represents in fact a geometrically interesting synthon for the preparation of supramolecular cages[153] since it offers a suitable cavity for the complexation of spherical guest molecule such as C_{60} fullerene. Evidence of the encapsulation of C_{60} fullerene within the SubPc cage was obtained from electrospray mass spectrometry experiments and the ^{1}H NMR technique, the latter technique showing a broadening of the signals corresponding to the protons of the SubPc core and the pyridyl groups.

4. Phthalocyanines and Subphthalocyanines Connected to Related Acceptor Systems

Although the aim of this review is restricted to the preparation and photophysical study of Pc− and SubPc−carbon nanostructure systems, in this section we will briefly report, for the sake of comparison, some other Pc/SubPc systems in which the macrocycle has been connected to related acceptor units such as PDIs or AQs, among others.

Similarly to fullerenes, PDI, an important class of compounds within the larger family of the perylene dyes, are excellent electron acceptor units that have been widely incorporated in D−A hydrids. These chromophores, which share with Pcs some interesting physical properties such as high absorption coefficients, a rich redox chemistry, and high charge-carrier mobilities, have also been covalently connected to Pcs.

In this context, the first report of a Pc−PDI system is represented by pentad **101** (Figure 18).[154] Photophysical investigations on this system revealed that quantitative, ultrafast energy transfer from the PDI to the Pc units occurs

Scheme 17. Molecular Structures of SubPc−TPA−C_{60} Fullerene Triad 90 and Tetrad 91[a]

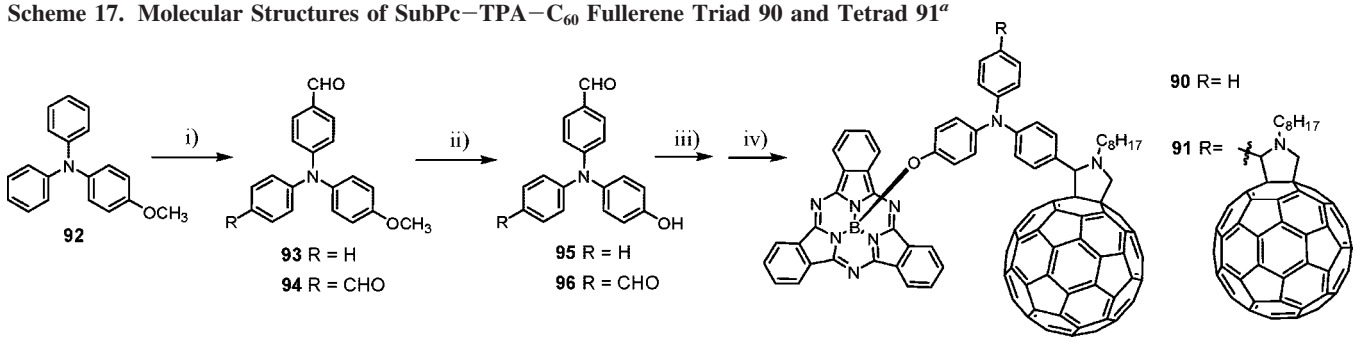

[a] Reagents and conditions: (i) $POCl_3$, DMF, 1,2-dichloroethane, reflux; (ii) boron tribromide (1.0 M solution in CH_2Cl_2), CH_2Cl_2, 0 °C; (iii) SubPcCl, toluene, reflux; (iv) C_{60} fullerene, *N*-methylglycine, toluene, 100 °C.

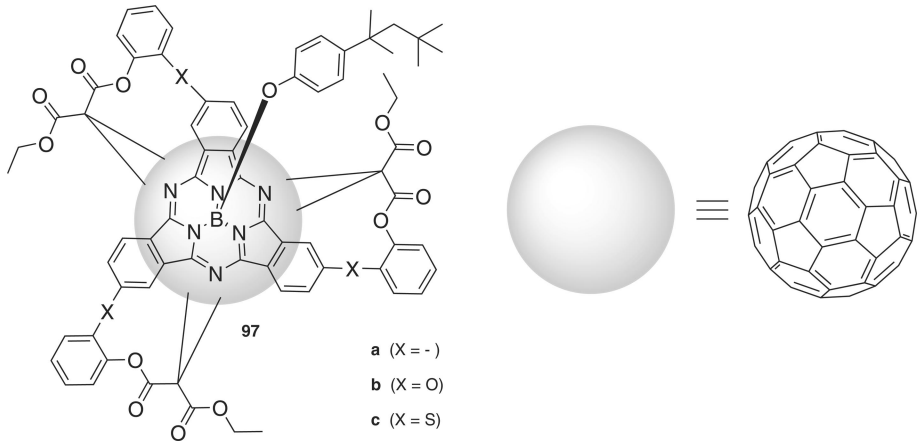

Figure 16. Molecular structure of SubPc−C_{60} fullerene trisadducts **97a−c** (top view).

Scheme 18. Synthesis of SubPc Fused Dimer−C_{60} Fullerene 98[a]

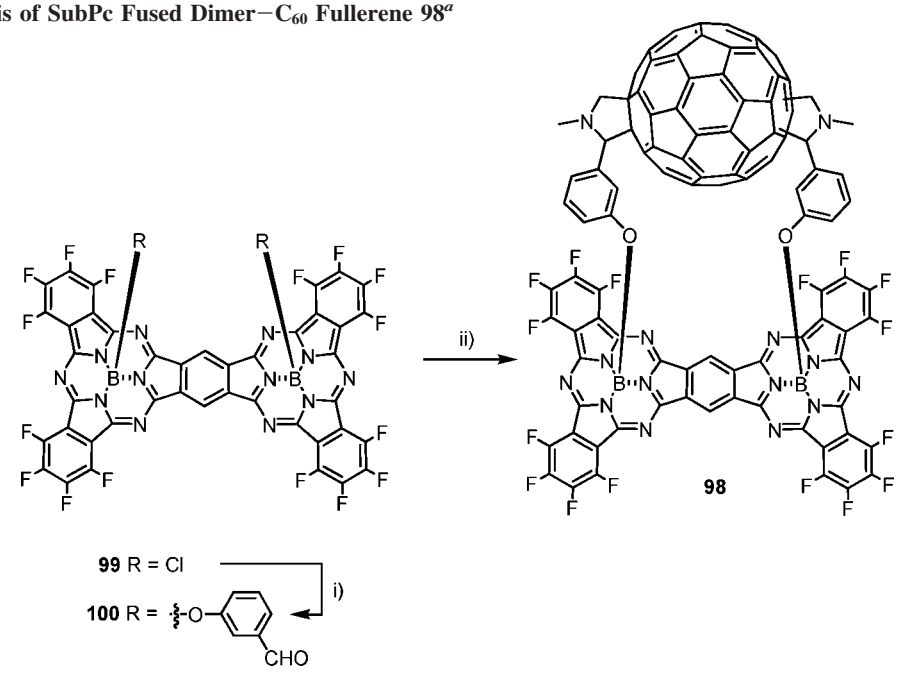

[a] Reagents and conditions: (i) 3-hydroxybenzaldehyde, toluene, reflux; (ii) C_{60} fullerene, *N*-methylglycine, toluene, reflux.

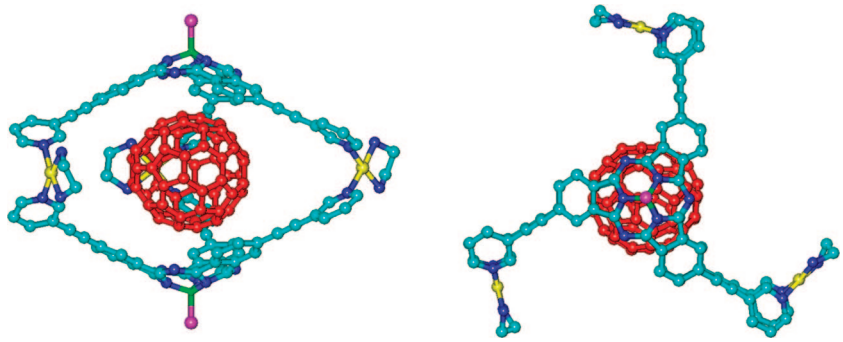

Figure 17. Ball-and-cylinder representation of the top (right) and side (left) views of the ZINDO/1-optimized geometry of the SubPc cage complexing a C_{60} fullerene molecule. 3,5-Di-*tert*-butylphenoxy axial groups and hydrogen atoms have been omitted for clarity.

through the formed large supramolecular nanoaggregates upon photoexcitation of the PDI moiety.

More recently, covalent systems based on PDI covalently linked to one[155,156] or two[157] Pc units have also been reported. Both energy and charge transfer dynamics have been observed in these systems upon photoexcitation of the Pc units.

A series of D−A triads (**102a−c**), in which an excellent acceptor moiety such as AQ has been covalently connected with two Pc units, have also been prepared (Figure 19) and their photophysical and electrochemical properties investigated.[158,159] These studies demonstrate that the substitution pattern at the AQ moiety exerts a profound influence over the aggregation status of the resulting Pc_2−AQ triads,

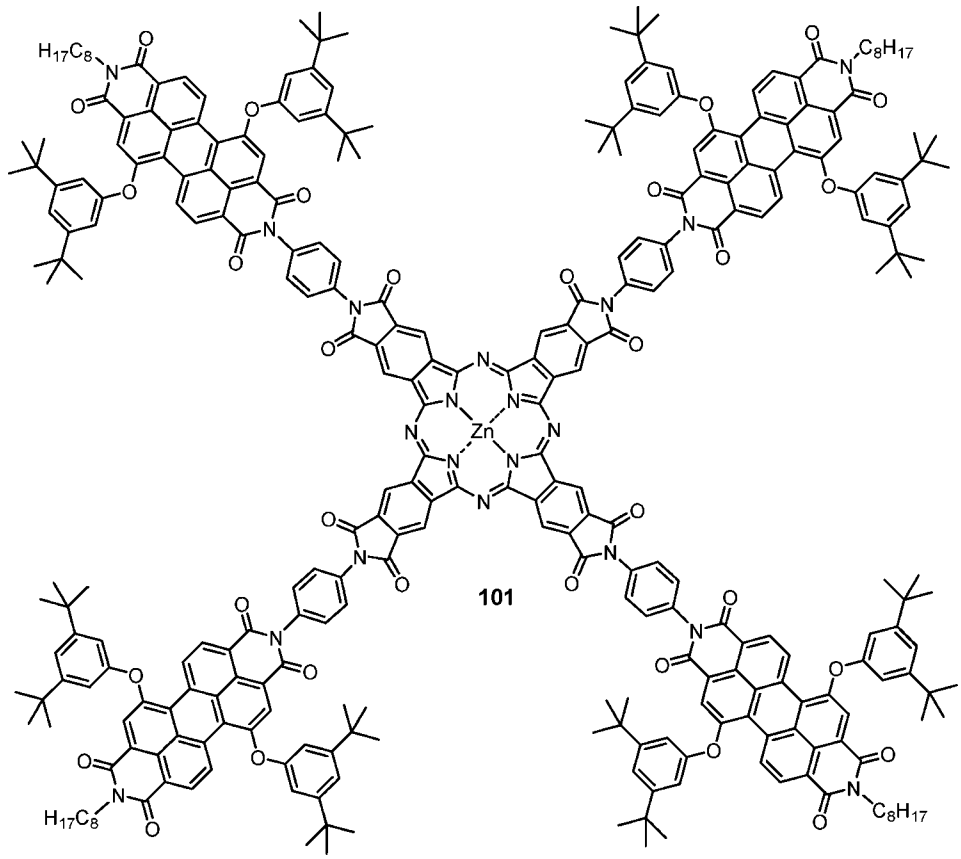

Figure 18. Molecular structure of Pc−PDI_4 pentad **101**.

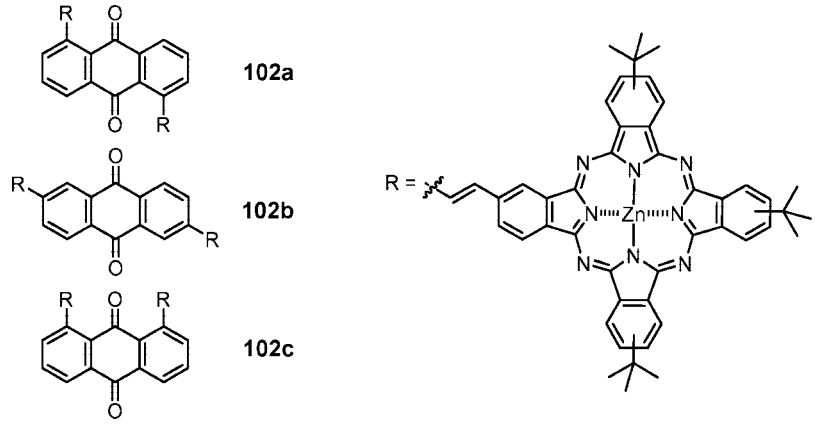

Figure 19. Molecular structures of Pc_2−AQ triads **102a**−**c**.

in a system in which the triad topology (i.e., "packed" in the case of **102c** or "extended" in the case of **102a**,**b**) is able to drastically influence both the inter- and intramolecular interactions between the Pc donor and the AQ acceptor moieties. Flavin moieties have also been covalently linked to Pcs.[160]

Recently, a supramolecular system based on Pc and PDI has been reported.[161] Following a Ru−pyridine coordination motif, a $Ru^{II}Pc_2$−PDI supramolecular complex (**103**) has been synthesized (Figure 20). The photophysical behavior of this array has been investigated, observing the occurrence of a PET process from the Pc to the PDI moiety and a remarkable stabilization of the formed radical ion pair, which has a lifetime of 115 ± 5 ns.

Ionic self-assembly (i.e., self-organization on the basis of electrostatic interactions) between oppositely charged dyes such as a cationic PDI and an anionic $Cu^{II}Pc$ derivative has also been employed for the preparation of a supramolecular polymer.[162]

Pcs can behave also as energy and/or electron acceptors for the preparation of D−A Pc-based architectures when linked to strong donor moieties such as Fc[163−166] or ruthenium polypyridine complexes.[167] Among the molecular "donor" partners that have been incorporated in Pc-based systems, Pors deserve a special mention. Thus, for example, a large number of molecular systems comprising both Pc and Por macrocycles have been prepared, in which the two chromophores have been connected via an amino group[168] or a triple bond[169−171] or directly linked through the β-pyrrolic position of the Por macrocycle.[172,173] Recently, discrete supramolecular Pc−Por−Pc assemblies have also been prepared using saddle distorted components, namely, a

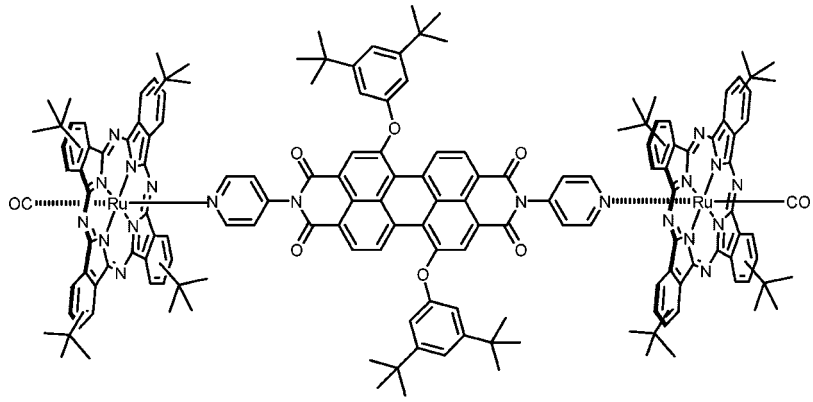

103

Figure 20. $Ru^{II}Pc_2$−PDI triad **103**.

protonated dodecaphenyl-Por and an octaphenyl-Zn^{II}Pc, using 4-pyridinecarboxylate as the supramolecular linking unit. Both metal−ligand and hydrogen-bonding interactions allow the assembly of this multicomponent supramolecular system.[174] Photoexcitation of the assembly gives rise to the generation of an unprecedented intrasupramolecular electron transfer state, involving radical cations of both one-electron-reduced diprotonated Por and one-electron-oxidized Pc, via the singlet excited states of both the Por and the Pc moieties.

Light-harvesting arrays containing four[175] or eight[176] Por macrocycles covalently linked to a central Pc unit, in a star-shaped molecular architecture, have also been synthesized. Photophysical experiments on such systems indicate that very efficient energy transfer occurs from the Por peripheral units to the Pc core and that the excited-state properties of the Pc are not altered in a deleterious manner by the presence of the adjacent Pors.

More recently, Bodipys, a versatile class of functional dyes which present large extinction coefficients (at ca. 500 nm), high fluorescence quantum yields, and reasonably long excited singlet-state lifetimes, have been axially coupled to a Si^{IV}Pc via Si−O axial substitution.[177,178] In such ensembles, the fate of the photoexcited states can be modulated in terms of both energy and electron transfer, depending on the presence of adequate moieties on the axial Bodipy subunits. Very recently, a Zn^{II}Pc−Bodipy conjugate, in which the Bodipy unit is tethered to the peripheral position of a Pc macrocycle, has been synthesized, and its photophysical properties have been studied.[179]

SubPc and Pc represent a formidable couple for the preparation of D−A systems. Both compounds in fact present complementary optical absorptions which cover a very wide section (up to 750 nm) of the UV/vis spectrum. In this context, a series of SubPc−Pc dyads connected by a short and rigid conjugated spacer through the periphery of both macrocycles have been prepared and their electrochemical and photophysical properties investigated.[180] SubPcs having a pyridyl group located at the axial position have also been complexed to a series of Zn^{II}- and Ru^{II}Pors and Zn^{II}- and Ru^{II}Pcs to form the corresponding SubPc−Por and SubPc−Pc heterodyads.[181]

Besides being versatile electron donors, SubPcs can be converted, depending on the peripheral substituents, to excellent electron-accepting molecules, with their first reduction potential reaching values even lower than that of fullerene derivatives. The utilization of SubPcs as electron acceptors has been recently demonstrated in a series of dyads comprising a SubPc peripherally substituted with electron-withdrawing groups (i.e., fluorine, nitro, or sulfonyl) and axially connected to an electron donor moiety such as Fc[182] or TPA.[183] On the other hand, SubPcs substituted axially with a Bodipy or distyryl-containing Bodipy moiety have been synthesized. Both systems exhibit a highly efficient PET process, either from the excited Bodipy to the SubPc core or from the excited SubPc to the distyryl Bodipy unit.[184]

5. Decoration of Carbon Nanotubes with Phthalocyanines

CNTs[58−60] can be considered as key materials in the nanotechnological progress[185] as a consequence of their nanometer-scale size and the extraordinary combination of physical properties (electrical, optical, mechanical, etc.) they exhibit. Important potential applications of CNTs include electronics and sensing,[186,187] energy conversion,[188−192] or biological functions.[193] Even though multiwalled carbon nanotubes (MWCNTs) were the first type of tubular carbon nanotubes discovered,[194] the leading carbon nanotubular structures in terms of scientific relevance are the single-walled carbon nanotubes (SWCNTs), which can be considered as small graphite sheets that have been rolled up to form seamless nanocylinders.

Functionalization of CNTs with molecules having photoactive properties offers the possibility for the development of hybrid systems that can be incorporated in optoelectronic devices. In particular, SWCNTs provide continuous electronic states in their conduction band for collecting electrons from, for instance, a π^*-state of an organic conjugated molecule. In turn, these electrons might be transported under nearly ballistic conditions along the nanotube 1-D axis. Thus, the combination of SWCNTs with a light-harvesting/electron donor molecule is expected to lead to novel nanoconjugate systems that bear great promise for major breakthroughs in converting solar energy into electricity.[65] The covalent or noncovalent attachment of electron donors, including Fc[195,196] and tetrathiafulvalene,[197,198] to the nanotube surface is at the forefront of investigations. In addition, much attention has been paid to the covalent and noncovalent attachment of Pors to SWCNTs to achieve nanoscale systems capable of generating long-lived charge-separated states upon photoexcitation.[199−208] The photoinduced CS in these assemblies has been utilized to generate photocurrent in photoelectrochemical cells for solar energy conversion.[209−211] In this

context, Pc−SWCNT hybrids also emerge as important building blocks in photovoltaics.

Two general approaches for the functionalization of SWCNTs have been reported: the covalent attachment of molecules to the open edges or sidewalls of SWCNTs and the noncovalent interactions of aromatic molecules or macromolecules to the outer nanotube walls. In principle, the noncovalent functionalization is particularly attractive because, following this approach, the electronic structure of the nanotubes remains essentially unaffected. However, the stability of the ensembles resulting from the covalent addition of functional molecules to the nanotube is much higher, which is desirable in terms of preparation and reproducibility of possible devices. Moreover, the covalent approach allows some control in the degree of functionalization and, therefore, in the properties of the hybrid material. However, some aspects of the covalent functionalization of SWCNTs are not satisfactorily controlled. First, the position of the attached molecules along the tube is difficult to determine. Indeed, the reactivity at the tips of the tube is higher, as a consequence of the larger pyramidalization of the carbon atoms, but some reactivity is also expected along the sidewalls as a consequence of the π-orbital misalignment of the bonds at a certain angle to the tube axis. Second, SWNTs are formed by a mixture of tubes with different diameters and helicities and, accordingly, with different electronic character (metallic, semiconducting, ...). In general, metallic SWNTs are more reactive in addition reactions than semiconducting ones, and in both cases, the reactivity is inversely proportional to the diameter of the tubes. This selectivity has been utilized for the separation of carbon nanotubes, with the aim of obtaining SWNTs with a single electronic character, either metallic or semiconducting.[212]

5.1. Covalent Attachment of Phthalocyanines to Carbon Nanotubes

The most classical approach to the covalent functionalization of the surface of the SWCNTs involves the reaction of the nanotubes with strong acids, usually mixtures of concentrated sulfuric and nitric acids.[213] This oxidizing treatment opens the SWCNTs, giving rise to short uncapped CNTs (pipes with an average length of 100−300 nm) bearing oxygen-containing groups, such as carboxylates, at the end of the pipes and at defective sites of the sidewalls. Therefore, the carboxyl groups can be readily derivatized to acid chlorides by treatment with $SOCl_2$ and subsequently coupled to amines or alcohols.

A former work on the preparation of covalent Pc−SWCNT ensembles by the oxidative route was reported by the groups of Torres and Blau.[214] In their study, SWCNTs with carboxylic moieties at the open ends were used to prepare a hybrid Zn^{II}Pc−SWCNT system by means of amide bond formation. This approach involves the preparation of an unsymmetrically substituted Pc in which one isoindole unit bears an amino moiety and the other three units are functionalized with *tert*-butyl groups that will afford solubility to the target hybrid system. Therefore, a suspension of the acyl chloride-functionalized nanotube material was reacted with an excess of the amino-containing Pc, affording the Pc−SWCNT hydrid. The material was characterized using UV/vis and IR spectroscopies, as well as TEM, the latter technique showing that the nanotubes are no longer aggregated into large bundles. Although the Pc moieties bear *tert*-butyl groups, the resulting nanotube material was scarcely soluble in most of the organic solvents, thus avoiding its photophysical characterization.

Similarly, Xu et al. reported another Pc−SWCNT system that was prepared by reaction between acyl chloride SWCNTs and an octaamino-substituted, sandwich-type erbium(III) bisphthalocyaninato ($Er^{III}Pc_2$) complex.[215] The resulting material showed evidence of ground-state charge transfer (CT) from the Pc rings to the SWCNTs. Acyl chloride MWCNTs were also functionalized by reaction with tetraamino-Mn^{II}Pc.[216] The photoconductivity of the resulting tetraamino-Mn^{II}Pc−MWCNT hybrid material in a single-layered device was higher than that of the pristine tetraamino-Mn^{II}Pc and a tetraamino-Mn^{II}Pc/MWCNT blended composite, as a consequence of an optimized CT from the Pcs to the MWCNTs within the covalently linked material. More recently, the same synthetic method (i.e., preparation of acyl chloride MWCNTs which were then reacted with amine-containing Pcs) was used to prepare a hybrid free base Pc/MWCNT system with enhanced optical limiting properties.[217] Photophysical studies on this hybrid system showed a substantial decrease of the Pc fluorescence intensity, suggesting a quenching of the free base Pc singlet excited state by the covalently linked MWCNTs.

Another approach to the preparation of Pc−MWCNT systems through reaction of carboxylic acid-containing MWCNTs consists in the esterification of the acid groups with 1,6-hexanediol and subsequent *ipso* substitution of 4-nitrophthalonitrile by the free hydroxyl group attached to the MWCNTs (Scheme 19).[218] Phthalonitrile-bonded MWCNTs were then further reacted with an appropriately substituted phthalonitrile in the presence of a copper salt to afford the covalently functionalized Cu^{II}Pc−MWCNT hybrid, which happened to be soluble in a variety of organic solvents. Thermogravimetric analysis led to an estimation of a 10% weight content of Cu^{II}Pc within the hybrid material. The Cu^{II}Pc−MWCNT hybrid material showed better photoconductivity than pristine Cu^{II}Pc and the Cu^{II}Pc/MWCNT blended composite.

The covalent attachment of Pcs at the CNT sidewalls has also been undertaken. Covalent approaches for sidewall functionalization of nanotubes generally involve the use of very reactive species,[61,219] such as aryl radicals, aryl cations, nitrenes, carbenes, or 1,3-dipoles. Similarly to the C_{60} fullerene functionalization, one effective methodology for the functionalization and solubilization of CNTs was described by Prato and co-workers,[220] which consists in the 1,3-dipolar cycloaddition of azomethine ylides to the CNTs. This approach usually affords functionalized CNTs that are soluble enough to facilitate manipulation and solution studies.

Torres and co-workers carried out the preparation of Pc−SWCNT ensembles **105** using the 1,3-dipolar cycloaddition of azomethine ylides protocol.[221] In this work, two different approaches were followed for the preparation of the target hybrids (Scheme 20). One approach involved the 1,3-dipolar cycloaddition of an azomethyne ylide generated in situ by reaction of *N*-octylglycine and *p*-formylbenzoic acid to the double bonds of SWCNTs, to yield the acid-derivatized nanotubes **104**, which were then reacted with Pc **106a** (Scheme 20, route A). The other synthetic pathway involved the straightforward 1,3-dipolar cycloaddition reaction of *N*-octylglycine and formyl-containing Pc **106b** (Scheme 20, route B). Thermogravimetric analysis of both

Scheme 19. Synthesis of a Covalently Linked $Cu^{II}Pc$−MWCNT Hybrid

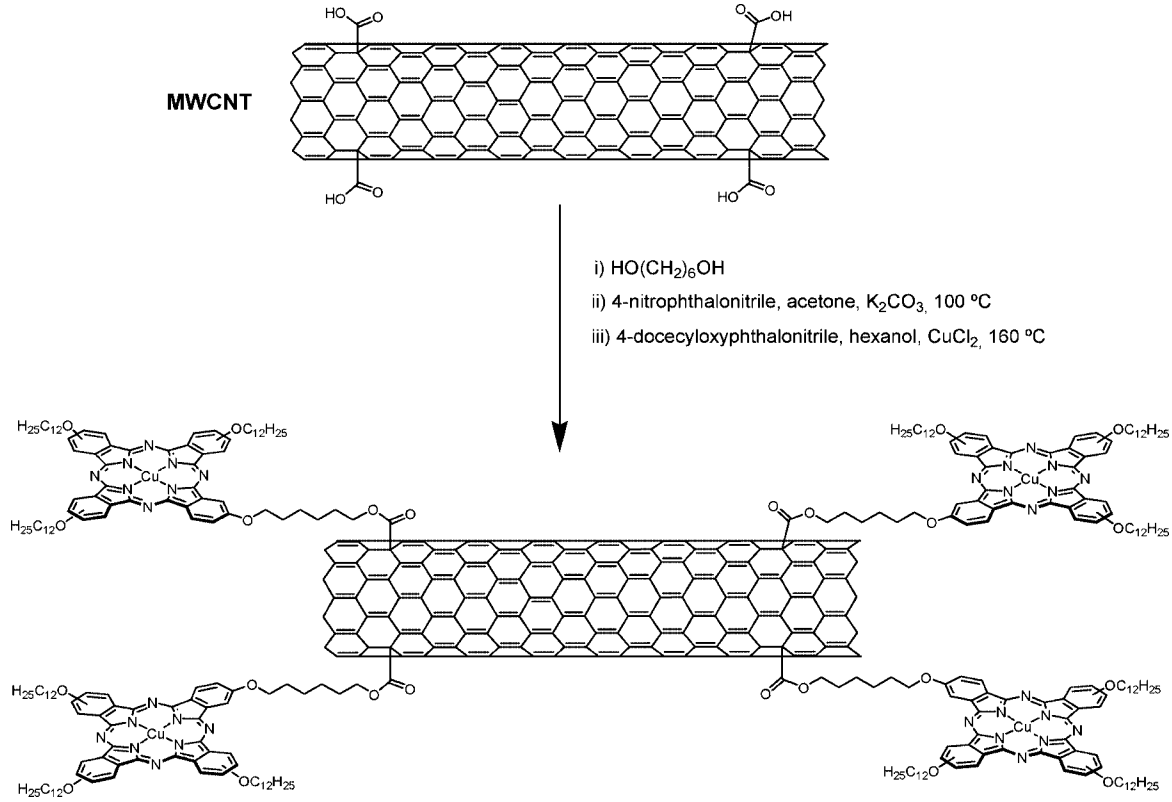

materials showed that the number of Pc units in the Pc−SWCNT ensemble prepared by the stepwise route (**105a**) (1 Pc every 300 carbon atoms) is higher than that of the straightforward approach (**105b**) (1 Pc every 500 carbon atoms). This fact is a result of the large excess of reactants (i.e., *p*-formylbenzoic acid and *N*-octylglycine) used in the former route to force the functionalization of the poorly reactive nanotube sidewalls. However, in the latter approach, a little excess of reactants (i.e., Pc **106b** and *N*-octylglycine) was used since the unsymmetrically substituted Pc **106b** is, indeed, a highly elaborate material. In addition, both materials were characterized using other analytical, spectroscopic, and imaging (i.e., TEM) techniques. All data were consistent with a successful functionalization of the SWCNTs with Pc molecules. The UV/vis spectrum of the ensembles showed the features of both constituents, that is, the Q-band of the Pc core and the typical van Hove singularities of SWCNTs ranging from the visible to the near-IR. The presence of the latter bands confirms that the electronic structure of the SWCNTs is preserved to some extent. In addition, Raman spectroscopy confirms the covalent attachment to the nanotube sidewalls. Photophysical experiments revealed that the nanotubes act as the electron acceptor component within this $Zn^{II}Pc$−SWCNT material, as previously observed in related Por−SWCNT ensembles.[200]

The groups of Torres, Prato, and Guldi also reported the preparation of an analogue of **105**, in which metal-free Pcs and nanotubes were linked through a flexible spacer (i.e., H_2Pc−SWCNT).[95] Photophysical studies on this material revealed a behavior similar to that observed for the ensembles having a rigid bridge (i.e., **105**), where both the Pcs and the nanotube surface are in close proximity. This fact seems to indicate that the nature of the spacer does not have a notable effect on the PET process in these hybrid systems.

The main disadvantage of the stepwise synthetical approaches described above (i.e., route A) is that not all the former functionalities attached to the nanotube react with the Pc molecules and, therefore, the incorporation of Pc units to the nanotube surface is not maximized. An elegant solution to this problem was provided by Campidelli et al., who used the Cu(I)-catalyzed, "click" 1,3-dipolar cycloaddition reaction between azide and acetylene derivatives as a tool to achieve the total derivatization of the reactive groups present in the nanotube with Pc molecules.[222] Specifically, they reported the functionalization of SWCNTs with 4-((trimethylsilyl)ethynyl)aniline following the procedure developed by Tour and co-workers for the addition of aromatic radicals to the CNT sidewalls.[223] In a second step, the click reaction of these ethynyl-functionalized SWCNTs with Pc **107** bearing an azide group yielded **108** (Scheme 21). Thermogravimetric analysis of the intermediate phenylacetylene-funtionalized material **109** indicated the presence of approximately 1 phenylacetylene functional group every 165 carbon atoms. This value fully fits with the estimation of the number of Pc units introduced after the click reaction, thus pointing out the success of this approach. Photophysical characterization of **108** demonstrated, as in previous examples, the electron injection from the photoexcited $Zn^{II}Pc$ to the nanotube.

Scheme 20. Synthesis of Covalent $Zn^{II}Pc-SWCNT$ Hybrids 105[a]

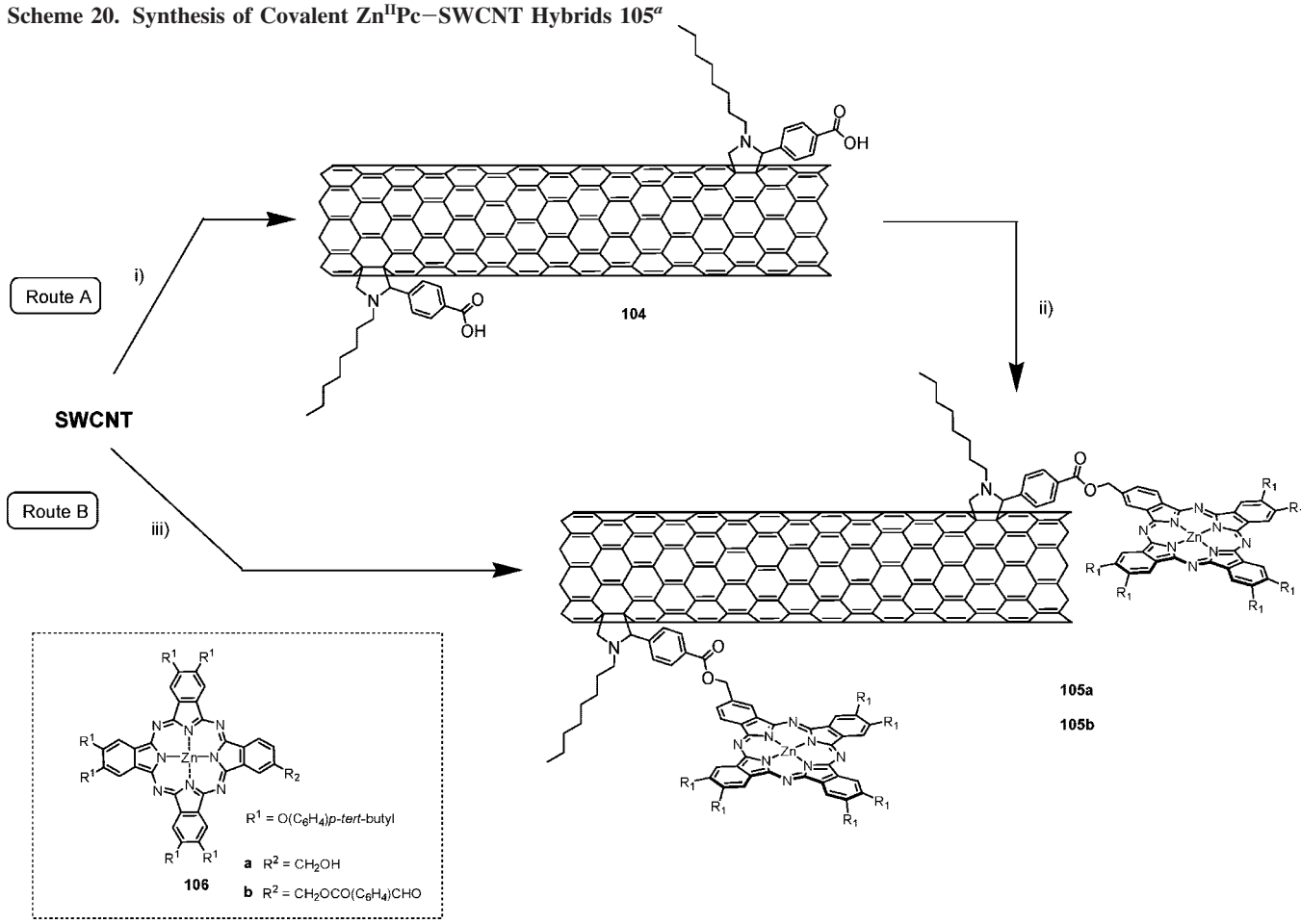

[a] Reagents and conditions: (i) *N*-octylglycine, 4-carboxybenzaldehyde, *o*-DCB, 180 °C; (ii) **106a**, 1-ethyl-3-(3-(dimethylamino)propyl)carbodiimide (EDC), hydroxybenzotriazole (HOBt), THF, rt; (iii) **106b**, *N*-octylglycine, *o*-DCB, 180 °C.

5.2. Noncovalent Interactions between Phthalocyanines and Carbon Nanotubes

The main advantage of the noncovalent functionalization of CNTs is that it fully preserves the electronic network of these tubular structures. For this reason, this approach is also of paramount importance for developing new nanomaterials. Particularly, the immobilization of Pc molecules onto CNTs may give rise to novel nanodevices where the photophysical and conducting properties of the Pcs are coupled to the unspoiled electronic properties of the nanotubes. The immobilization of the Pc cores onto the CNT sidewalls results from the $\pi-\pi$ interaction between the conjugated surface of the CNTs and the aromatic Pc macrocycles.

Wang et al. reported that CNTs can fade the color of chloroform solutions of tetra-*tert*-butyl-Pc as a result of the immobilization of the Pc cores on the nanotube sidewalls.[224] The adsorption of the Pc molecules on the CNT surface was observed by TEM and AFM, which showed the formation of nanoparticles of several to tens of nanometers.

Hydrogen-bonding-based interactions between tetrasulfonate-substituted $Cu^{II}Pc$ and oxidized MWCNTs take place in concentrated dispersions of both components.[225] The affinity between the two materials was shown to result in ground-state charge transfer from the MWCNT scaffold to the Pc molecules, which behaved as electron acceptor components owing to the presence of electron-withdrawing moieties at the periphery of the macrocycles. Upon spin-casting of such a dispersion, uniform, thin films were obtained. Spectroscopic and morphological studies evidenced that the Pc cores stacked in columns along the MWCNT scaffold, in such a way that the plane of the macrocycle was parallel to the nanotube surface (Figure 21).

Another remarkable example reported by D'Souza and co-workers describes the noncovalent functionalization of SWCNTs with $Zn^{II}Nc$ using a pyrene-based derivative as a bridge between the Nc and the nanotube.[205] It is well-known that pyrene strongly binds through $\pi-\pi$ interactions on the SWCNT sidewalls.[226] To assemble Nc molecules on the SWCNT, the pyrene entity was functionalized with a phenylimidazole ligand (i.e., ImPy), since the phenylimidazole can strongly coordinate to the zinc center of the donor macrocycle (Figure 22). Therefore, D−A Nc/ImPy/SWCNT nanohybrids have been constructed and characterized by various physicochemical techniques including TEM, UV/vis, and electrochemical methods. PET from the singlet excited $Zn^{II}Nc$ entity to the SWCNT acceptor unit was probed by steady-state and time-resolved emission studies.

More recently, conjugate **110**/SWCNT has been reported in which a heteroleptic bis(phthalocyaninato)terbium(III) complex (**110**) bearing a pyrenyl group has been grafted to SWCNTs using $\pi-\pi$ interactions, as demonstrated by high-resolution TEM, emission spectroscopy, and AFM (Figure 23).[227] An average load of 1 molecule of **110** per 7−8 nm

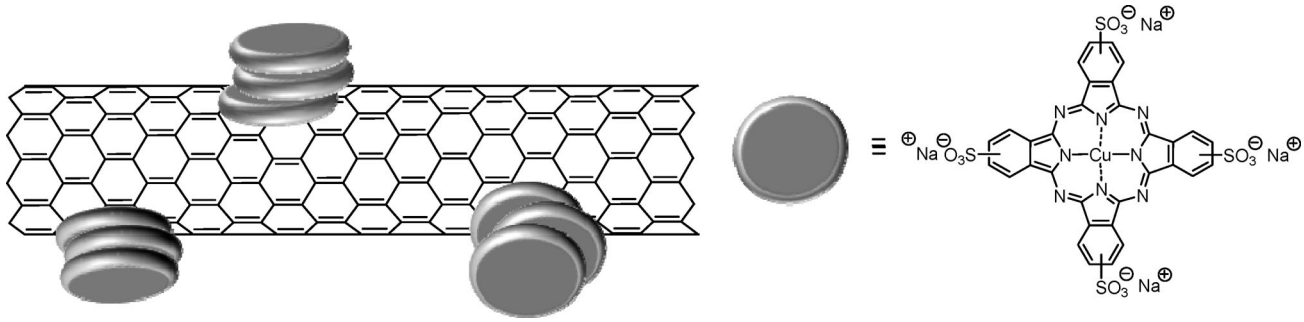

Figure 21. Schematic representation of the columnar stacking of tetrasulfonate-substituted Cu^{II}Pcs on a MWCNT.

Scheme 21. Synthesis of Zn^{II}Pc−SWCNT 108 by a Click Cu(I)-Catalyzed Procedure

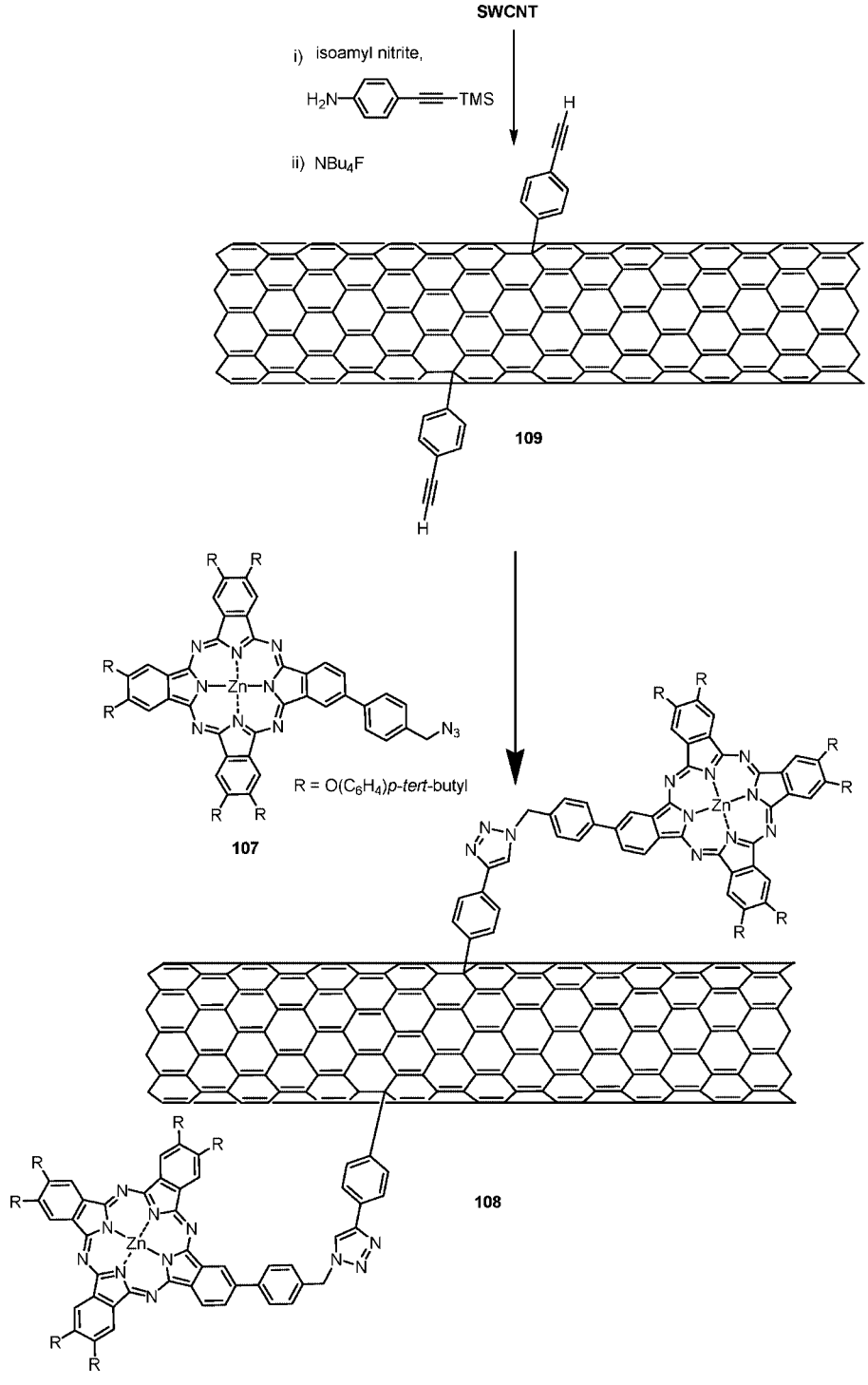

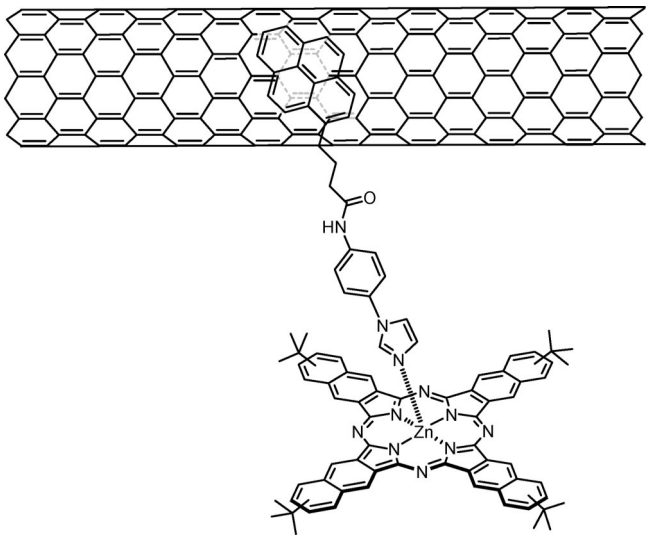

Figure 22. Noncovalent assembly of a SWCNT and a $Zn^{II}Nc$ using an imidazolylpyrene bridge.

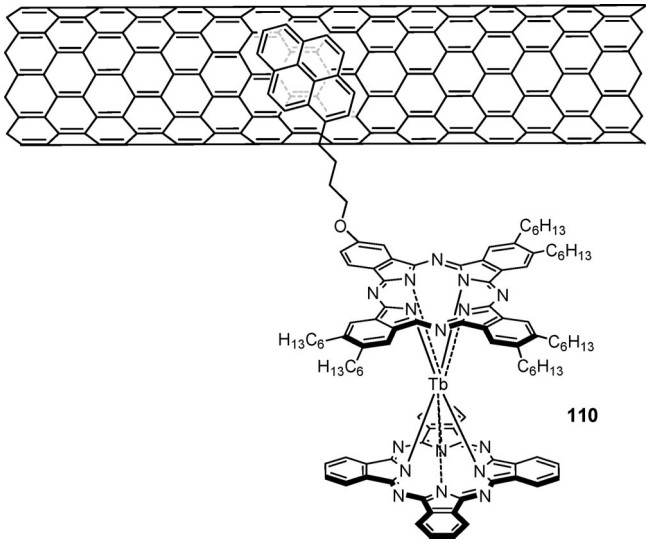

Figure 23. Noncovalent assembly of a SWCNT and conjugate **110** using a pyrene bridge.

of SWCNT length was obtained. The rationale behind the preparation of system **110**/SWCNT lies in the magnetic properties of the heteroleptic complex **110**, which exhibits temperature and frequency dependence of ac magnetic susceptibility, typical of single-molecule magnets (SMMs). Interestingly, magnetization studies revealed that the SMM behavior of heteroleptic complex **110** is retained and even improved in the hybrid **110**/SWCNT system.

From a chemist's perspective, one of the most fascinating properties of CNTs is their ability to encapsulate molecules and confine them to form quasi-1-D arrays.[228] Forming restricted 1-D assemblies of Pcs by encapsulation into carbon-based nanotubular structures may lead to materials with improved photophysical and (opto)electronic properties as a result of excitonic interactions between the dyes, as long as a precise control of internal stacking is achieved. Schulte et al. reported the encapsulation of $Co^{II}Pc$ molecules into MWCNTs.[229] Even though no internal order could be determined by TEM, near-edge X-ray absorption fine structure (NEXAFS) measurements revealed nonrandom stacking of the Pcs inside the nanotubes.

Recently, a system constituted of $Zn^{II}Pcs$ loaded onto chemically oxidized single-walled carbon nanohorns ($SWCNH_{ox}$) functionalized with protein bovine serum albumin (BSA) has been reported.[230] In such a system, the loading of the Pcs onto the nanotubes is made possible by the presence of large pores (1−5 nm) on the tubular nanostructures through which the Pc units can pass, whereas the interaction of the serum albumin with the tubular nanostructure is realized by the presence of carboxylic acid residues at the edges of the $SWCNH_{ox}$ pores.

Some examples can also be found in the literature regarding photoconductivity measurements of composites comprising CNTs and Pc molecules. Thus, for example, chemically modified MWCNTs (i.e., holding dodecylamide chains) have been blended with $Ti^{IV}OPc$, forming $Ti^{IV}OPc$/MWCNT composites that have been used to fabricate photoconductive devices.[231] Enhanced photosensitivity was observed in these $Ti^{IV}OPc$/MWCNT devices, the composite containing 6 wt % CNTs reaching a 5-fold higher value with regard to undoped $Ti^{IV}OPc$ devices. This result was interpreted in terms of photoinduced CT from the $Ti^{IV}OPc$ to the MWCNT component. The same authors have described the MWCNT-templated assembly of the reduced form of a sandwich-type erbium(III) phthalocyaninate ($HEr^{III}Pc_2$).[232] TEM images showed MWCNTs enrobed with Pc nanoparticles and nanowires. The photoconductivity of the MWCNT−$HEr^{III}Pc_2$ hybrid material was also measured, showing enhanced photosensitivity as a result of the formation of a CT complex. UV/vis experiments supported this finding and showed that, when the MWCNT content was increased, a new band centered at 770 nm concomitantly arose, which was related to the oxidation of the $HEr^{III}Pc_2$ component.

On the other hand, coupling CNTs with Pcs having catalytic activity characteristics offers the possibility for the development of hybrid materials with improved catalytic and analyte sensing capabilities. CNTs have been known to promote electron transfer reactions when used as electrode-modifying material. Electrode modification with CNTs is usually carried out by their direct immobilization on the surfaces of carbon electrodes, and the resulting electrodes can be further modified with other chemically and biologically active materials.[233] In particular, transition-metal−Pc complexes are well recognized for their excellent electrocatalytic activity toward the detection of different analytes.[234] For this reason, the attachment of metallic Pc complexes on CNTs and the immobilization of the hybrid material on electrodes has led to systems with excellent electrocatalytic characteristics.[235−240] An interesting example describes the electrochemical properties of self-assembled films of SWCNTs coordinated to tetraamino-$Co^{II}Pc$ by sequential self-assembly onto a preformed aminoethanethiol self-assembled monolayer on a gold electrode.[241] Electrochemical studies show that the presence of SWCNTs greatly improves the electronic communication between the tetraamino-$Co^{II}Pc$ and the Au electrode surface. SWCNT/tetraamino-$Co^{II}Pc$ self-assembled films exhibit good electrocatalytic responses toward the detection of dopamine. A similar example describes the preparation of layer-by-layer films of polyamidoamine−MWCNTs alternated with tetrasulfonated $Ni^{II}Pc$.[242] Also in this case, the incorporation of CNTs enhanced the Pc-mediated redox process and its electrocatalytic properties for detecting dopamine.

Ye et al. have reported the immobilization of Pcs at the surface of CNTs as a tool to obtain electrochemical biosensing platforms.[243] The authors have constructed a highly

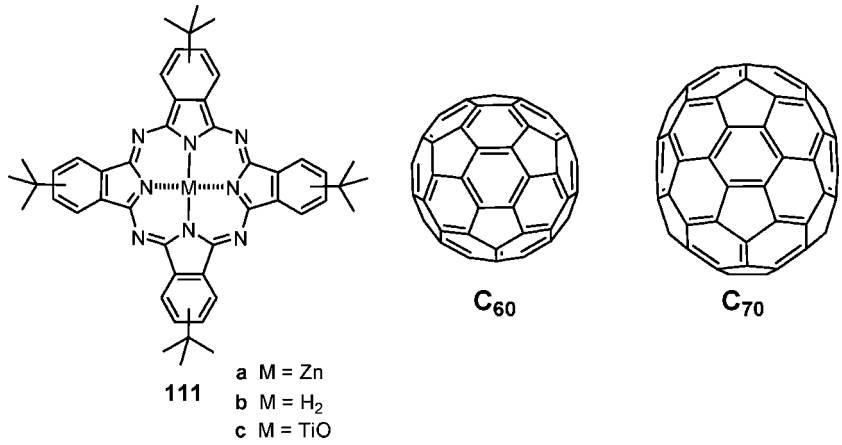

Figure 24. Molecular structures of Pcs **111a−c** and C_{60} and C_{70} fullerene.

sensitive and selective glucose sensor by immobilization of $Fe^{III}Pc$ on well-aligned MWCNTs and subsequent coimmobilization of glucose oxidase biomolecules as model enzymes onto the MWCNT surface.

In addition, the nonlinear optical behavior of noncovalent ensembles of CNTs and Pcs has also been studied. Therefore, mixing $Zn^{II}Pc$ solutions and SWCNT dispersions gives rise to nanocomposite systems with improved optical limiting capabilities in comparison to pure Pc-based materials.[244]

6. Photophysics of Phthalocyanine− and Subphthalocyanine−Carbon Nanostructure Systems

6.1. Nonspecific, Intermolecular Interactions between Phthalocyanines and Fullerenes in Solution

In 1997 Ito and co-workers reported the intermolecular CT between ground-state $Zn^{II}Pc$ **111a** and photoexcited C_{60} or C_{70} fullerene, which exhibited an interesting twist (Figure 24).[245] Excitation of fullerene in a mixture of **111a**/C_{60} (C_{70}) in benzonitrile gives rise to the rapid formation of new photoproducts. Spectroscopically, the photoproducts are identified with relative ease by characteristic absorption changes in the near-IR: Maxima around 840 nm are clear attributes of the $Zn^{II}Pc^{\bullet+}$, while the transient absorbance at 1080 nm (or 1380 nm) resembles the diagnostic marker of the fullerene radical anion $C_{60}^{\bullet-}$ (or $C_{70}^{\bullet-}$). The contribution of ^{3}*C_{60} (or ^{3}*C_{70}) to the observed electron transfer dynamics was confirmed by adding O_2 to a benzonitrile solution containing Pc **111a** and fullerene, which resulted in the almost complete suppression of $C_{60}^{\bullet-}$ (or $C_{70}^{\bullet-}$), thus confirming that intersystem crossing from ^{1}*C_{60} (or ^{1}*C_{70}) to ^{3}*C_{60} (or ^{3}*C_{70}) occurs before ^{1}*C_{60} (or ^{1}*C_{70}) accepts an electron from **111a**.

In nonpolar solvents, the energy levels for the radical ion pair state are, however, significantly raised. As a direct consequence, the electron transfer mechanism is shut off, while the intriguing energy transfer route is activated. The latter was confirmed spectroscopically through the triplet-excited-state markers of $Zn^{II}Pc$ and the absence of the radical ion pair features. Interestingly, the quantum yields for the photoinduced CT were found to be higher for C_{70} than for C_{60} and scaled linearly with increasing $Zn^{II}Pc$ concentration.

It is important to notice that any electronic communication between **111a** and C_{60} is limited to the excited state, although a more recent study describes the occurrence of ground-state electronic interactions between unsubstituted Zn^{II} or H_2Pc and fullerene also in solution.[246]

A few years later, similar photophysical studies were carried out on **111a**/C_{60} (C_{70}), but this time photoexciting exclusively the $Zn^{II}Pc$ by simply selecting 670 nm as the excitation wavelength, where neither C_{60} nor C_{70} absorbs.[247] The growth of the transient absorption bands attributable to $C_{60}^{\bullet-}$ (i.e., 1080 nm) or $C_{70}^{\bullet-}$ (i.e., 1380 nm) and $Zn^{II}Pc^{\bullet+}$ (i.e., 840 nm) and the concomitant decay of the $Zn^{II}Pc$ triplet-excited-state features (i.e., 480 nm) confirm the presence of a CT mechanism. Again, the presence of O_2 favored an energy transfer over a CT deactivation mechanism, thus confirming the participation of the $Zn^{II}Pc$ triplet excited state as an important intermediate in the formation of the charge-separated ion pairs.

Photoexciting H_2Pc **111b** in a **111b**/fullerene mixture revealed that the CT rate constants and CT efficiencies are considerably smaller when compared to those of $Zn^{II}Pc$ **111a** (i.e., CT efficiencies of 0.07 versus 0.77 in benzonitrile). This was rationalized on the basis of the different electron-donating abilities presented by the two Pcs. Nevertheless, it is notable that quantum yields of less than unity imply alternative deactivation mechanisms, including energy transfer and/or collisional quenching. Decreasing the solvent polarity further decreased the CT efficiencies. Excited triplet states of C_{60} and C_{70} showed, in an interplay with $Ti^{IV}OPc$ **111c**, the same electron and energy transfer reactivity.[248]

In summary, in polar solvents, an intermolecular electron transfer takes place in **111a**/C_{60} and **111b**/C_{60} mixtures from the triplet states (i.e., ^{3}*$Zn^{II}Pc$, ^{3}*H_2Pc, or ^{3}*C_{60}) to yield radical ion pair states, the exact pathway depending exclusively on the excitation wavelength used.

6.2. Photophysics of Phthalocyanine−Fullerene Systems

Next, the CT behavior and the thermal CR features of several of the covalently and noncovalently linked Pc−C_{60} fullerene conjugates described above were analyzed, in terms of both the nature of the spacer between the donor and the acceptor units (e.g., Figure 25) and the number of Pc and C_{60} moieties in the multicomponent ensembles.

The first, and structurally simpler, Pc−C_{60} system whose photophysical behavior was studied is represented by the $Zn^{II}Pc$−C_{60} conjugate **8a**. This dyad, in which the two active units are directly linked, reveals a marked redistribution of

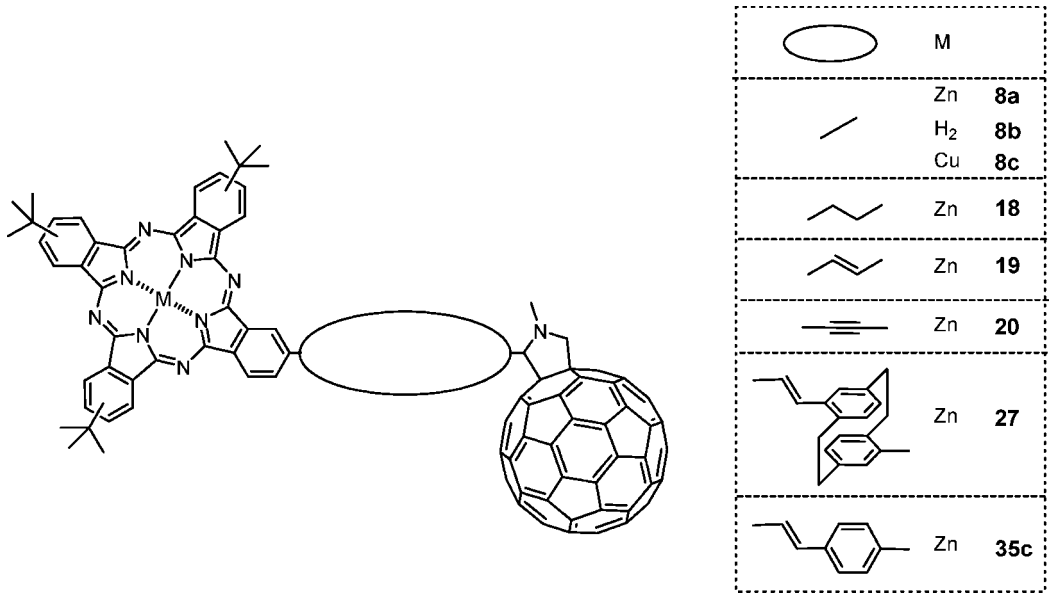

Figure 25. Molecular structures of Pc−C_{60} fullerene dyads **8**, **18**−**20**, **27**, and **35c**.

CT density from the electron-donating Zn^{II}Pc to the electron-accepting C_{60}, as reflected by the CT absorption band at 740 nm observed in the UV/vis.[87,249,250] The same features are observed when the Pc and C_{60} units are in close proximity such as in **42a**, where strong CT occurs.[101,251]

Interestingly, in none of the other reported Zn^{II}Pc−C_{60} conjugates is such a spectroscopic signature discernible to a notable extent, their absorption spectra being described as the linear sums of the individual components (see below). In such dyads, strong Zn^{II}Pc absorption maxima are registered around 350 nm and around 685−690 nm, the latter flanked by a shoulder around 650 nm and a minor maximum at 610 nm. In the visible part of the solar spectrum, meaningfully intense C_{60} transitions are restricted to bands at 330 and 435 nm. Much weaker transitions, with extinction coefficients well below 1000 M^{-1} cm^{-1}, extend, nevertheless, to ca. 700 nm.

Unambiguous evidence for CT in Pc−C_{60} ensembles can be gathered from transient absorption measurements. When the photoexcitation features of a Zn^{II}Pc reference compound that lacks the electron-accepting C_{60} moiety (i.e., **111a**) are probed, the Zn^{II}Pc singlet excited state emerges as an important reference point. The latter, which is formed essentially right after the conclusion of the laser pulse, is seen as a broad transient maximum at 490 nm followed by bleaching between 610 and 685 nm. This bleach is basically a mirror image of the ground-state absorption. The Zn^{II}Pc singlet−singlet transient decays on the 3000 ps time scale via intersystem crossing (i.e., 3.1 ns) to afford the Zn^{II}Pc triplet-excited-state features: a broad transient with a maximum at 500 nm and two minima at 350 and 680 nm. In the absence of molecular oxygen, the Zn^{II}Pc triplet excited state returns to the singlet ground state over the course of several hundred microseconds with a rate constant of 3.5×10^4 s^{-1} in THF.

Distinct is the fate of the photoexcited species when the electron-accepting C_{60} unit is connected to the Pc such as in **8a**. In fact, photoexciting Zn^{II}Pc−C_{60} **8a** at 670 nm generates the Zn^{II}Pc singlet excited characteristics that decay rather quickly, in stark contrast to the intersystem crossing dynamics of the singlet-excited-state features of **111a**. Kinetically, the Zn^{II}Pc singlet-excited-state decay in **8a** is tied to the formation of new transient species. Spectroscopically, the new species reveal distinct maxima at 520, 840, and 1000 nm. The maxima at 520 and 840 nm are attributes of the one-electron-oxidized Zn^{II}Pc radical cation, whereas the maximum at 1000 nm matches the absorption of the one-electron-reduced C_{60} radical anion (Figure 26). The transient absorption measurements show clearly that the lifetime of the radical ion pair state depends strongly on the polarity of the solvent.

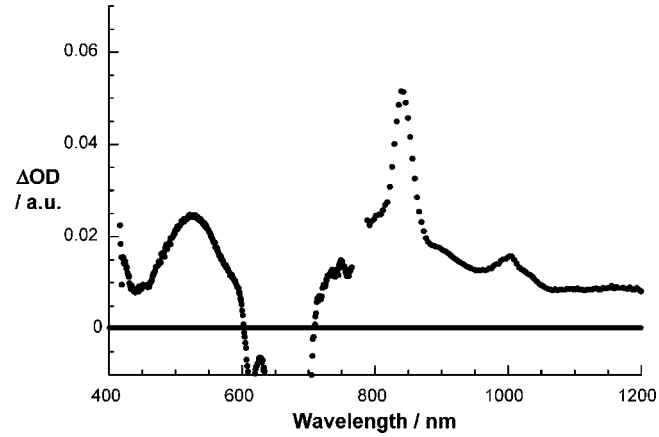

Figure 26. Differential absorption spectrum (visible and near-IR) obtained upon femtosecond flash photolysis (670 nm, 150 nJ) of **8a** in argon-saturated THF with a time delay of 100 ps at rt.

Important is the comparison of Pc−C_{60} conjugates **8a**−**c**[86] with the related Zn^{II}Por−C_{60} or H_2Por−C_{60} conjugates.[53] In particular, a number of key differences should be highlighted. First, significant red shifts of the visible absorption features are observed for the Pc-based derivatives (i.e., ∼700 nm versus ∼600 nm). This favors unquestionably the utilization of light in the range of the maximum solar flux. Second, the absorption cross sections of Pcs in the visible range of the solar spectrum (i.e., $\varepsilon > 200\,000$ M^{-1} cm^{-1} versus $\varepsilon \approx 10\,000$ M^{-1} cm^{-1}) enhance the light-harvesting ability of these systems compared to the Por-based ones. Third, Pc−C_{60} ensembles present larger energy gaps (i.e., $-\Delta G_{CS}° > 0.7$ eV versus $-\Delta G_{CS}° < 0.7$ eV), and faster rates evolve for the CS processes, which, in turn, assist in suppressing alternative deactivation channels for the singlet excited state

Table 1. Charge-Separated Lifetimes of Some Pc−, SubPc−, and Nc−C_{60} Covalent and/or Supramolecular Systems

ref	compd	charge-separated lifetime (ps)	ref	compd	charge-separated lifetime (ps)
87	**8a**[k]	32[a] 49[b] 450[c] 1.1×10^4 [d]	120	**67**[k]	1.5×10^6 [e]
88	**13**[k]	1.4×10^9 [f]	120	**71**[k]	1.3×10^6 [e]
90	**18**[k]	50[a] 131[b] 755[c] 1×10^4 [d]	122	**72**[k]	3×10^3 [d]
90	**19**[k]	30[a] 120[b] 979[c] 1.4×10^4 [d]	127	**75a**[m]	1.9×10^4 [d] 1.1×10^4 [g]
90	**20**[k]	36[a] 154[b] 1.2×10^3[c] 1.3×10^4 [d]	128	**75b**[m]	15×10^3 [g]
92	**27**[k]	330[a] 2.4×10^3 [b] 2.6×10^4 [c] 4.58×10^5 [d]	128	**75c**[m]	10×10^3 [g]
94	**31**[k]	$>3 \times 10^3$ [d]	128	**75d**[j,m]	
96	**34/35a**[k]	475[b]	129	**76**[k]	6.7×10^6 [a]
92	**35c**[k]	3.5×10^4 [d]	130	**77**[k]	40×10^3 [d]
101	**42a**[k]	83[a]	132	**81**[k]	1.74×10^3 [b] 1.23×10^3 [e]
102	**42a**[i,k]	3.3×10^6	134	**82**[k]	1.5×10^5 [c] 1.7×10^5 [d]
104	**45**[k]	360[b] 2.2×10^3 [c] 2.1×10^4 [d]	134	**83**[k]	1.2×10^3 [c] 1.3×10^5 [d]
105	**50**[k]	1×10^3 [a] 650[h]	134	**84**[k]	500[c] 370[d]
106	**54**[k]	180[a] 1.15×10^3 [b] 2.97×10^3 [c]	143	*o*-**85d**[l]	73[a] 133[b] 4.055×10^3 [d]
109	**58**[k]	2.0×10^5 [a] 1.6×10^5 [d]	143	*m*-**85d**[l]	111[a] 192[b] 4.35×10^3 [d]
110	**59**[k]	5.0×10^3 [a]	143	*p*-**85d**[l]	235[a] 319[b] $>5 \times 10^3$ [d]
112	**60**[k]	1.0×10^3 [a]	146	**90**[l]	6.7×10^5 [a] $<7 \times 10^3$ [d] 4×10^5 [h]
113	**61a**[k]	12.6×10^6 [g]	146	**91**[l]	1.052×10^6 [a] 4.7×10^4 [d]
			147	**97a**[l]	97×10^3 [b]

[a] Benzonitrile. [b] THF. [c] Anisole. [d] Toluene. [e] Dichloromethane. [f] Water. [g] *o*-DCB. [h] DMF. [i] Langmuir−Blodgett film. [j] Too fast to record. [k] Refers to Pc−C_{60} systems. [l] Refers to SubPc−C_{60} systems. [m] Refers to Nc−C_{60} systems.

such as radiative and nonradiative decays. Finally, smaller energy gaps for the CR step (i.e., $-\Delta G_{CR}°$) are observed for Pc−C_{60} systems, which pull these processes closer to the top of the Marcus parabola and, therefore, destabilize the radical ion pair states. Replacing Zn^{II}Pc with Cu^{II}Pc (i.e., **8c**) assists in raising the radical ion pair state due to an anodically shifted oxidation potential and, in turn, in elongating its lifetime (Table 1).

Similarly, the nature of the linker in **18**−**20** has an influence on the lifetime of the radical ion pair states as a consequence of the differently hybridized carbon atoms.[90] In general, the lifetimes of these excited states tend to be shortest in the system that lacks any spacer at all (i.e., **8**), while the longest lifetimes are found in the system that carries the triple bond spacer (i.e., **20**). Interestingly, the difference between the double-bonded (i.e., **19**) and triple-bonded (i.e., **20**) systems resembles the trend seen in *p*-phenylenevinylene- and *p*-phenyleneethynylene-containing D−A systems.[252,253]

Implementing *p*-cyclophanevinylene or *p*-phenylenevinylene bridges in **27** or **35c**, respectively, exerts an appreciable stabilization of the radical ion pair state, relative to **8a** and **18**−**20** (Table 1).[92] This trend is likely due to the larger D−A distances in **27** and **35c**. As a general rule, the increase of the distance between the donor and the acceptor units leads to a stabilization of the radical ion pair lifetimes as has been observed in several Por−C_{60} systems in which a systematic variation of the spatial distance and relative orientation between the two active units has been done.[53]

Pronounced effects on the charge-separated lifetimes are actually seen when a *p*-cyclophanevinylene bridge is employed (Table 1). *p*-Cyclophane is regarded as a pseudoconjugated spacer that per se weakens the electronic coupling between Zn^{II}Pc and C_{60}, when compared to the *p*-phenylenevinylene building block. Please note that the latter is one of the most proficient building blocks for the design of molecular wires with β values as low as 0.01 $Å^{-1}$.[253]

The photoinduced communication between a double-decker lanthanide(III) bis(phthalocyaninato) and a C_{60} moiety in a series of $[Ln^{III}(Pc)(Pc')]-C_{60}$ dyads (Ln = Sm, Eu, Lu) (**31a**−**c**) has also been studied.[94] In the dyads **31a**−**c**, excitation at 665 nm, which photoexcites exclusively the $[Ln^{III}(Pc)(Pc')]$ moiety, leads to a rapid excited-state deactivation, that is, doublet-to-quartet intersystem crossing (i.e., 3.5 ps) and ground-state recovery (i.e., 16 ps), similarly to what has been observed for the sandwich complexes **33a**−**c**. This is probably due to the short lifetimes of the excited states of the $[Ln^{III}(Pc)(Pc')]$ double-decker components that bring about alternative deactivation mechanisms. On the contrary, when dyads **31a**−**c** are photoexcited at 387 nm, which excites both the C_{60} and the $[Ln^{III}(Pc)(Pc')]$ components, the charge-separated-state features started to evolve, namely, the fingerprint absorption of one-electron-reduced C_{60} at 1010 nm and the one-electron-oxidized $[Ln^{III}(Pc)(Pc')]$ component at 515 and 760 nm, as confirmed by electrochemical and radiolytical assays. No notable decay is seen for the newly formed charge-separated state on the time scale of the femtosecond experiments, that is, 3 ns, which suggests an upper limit for the lifetime of >3 ns in toluene (Table 1).

More recently, temperature-dependent photophysical studies have also been carried out on $Pc-C_{60}$ dyad **42a**. These studies revealed that in this dyad the formation of the charge separation state is preceded by the formation of an intramolecular exciplex as a transient state.[254] It was observed for such a system that the formation rates of the exciplex and the charge-separated states, as well as the charge recombination rate, were independent of the temperature, and thus, these processes were activationless. This finding seems to be a general rule and suggests that aromatic $\pi-\pi$ interactions between closely spaced donor and acceptor moieties could be an important factor for exciplex formation as transient states in PET reactions.

Photophysical studies on a flexible, azacrown-containing linker connecting the Pc and the C_{60} units in dyad **39** were also carried out.[99] These studies did not show any sign of charge transfer dynamics for the dyad either alone or upon addition of potassium salts. This is in accordance with the UV/vis experiments, which suggest that no significant changes upon complexation or aggregation take place despite the presence of the ionophilic bridge (vide supra). The photolysis data suggest that the presence of the fullerene group can modify the excited-state lifetime of the Pc by energy transfer or some other nonradiative process, but evidence for charge transfer in **39** could not be inferred.

The photophysical behavior of multicomponent $Pc-C_{60}$ ensembles other than dyads (i.e., triads, tetrads, etc.) has also been studied.

The tripodal motif **50**, in which three-electron-donor Pc units and a fulleropyrrolidine moiety are covalently connected to a central tetraphenylmethane unit, deserves a special mention.[105] In such a system, CS is only realized in polar solvents such as benzonitrile and DMF, whereas less polar solvents such as toluene, anisole, or THF are ineffective to trigger a CT event. Compound **50** seems just to decay with kinetics similar to those found in a reference system lacking the electron-accepting C_{60} moiety. Accordingly, any measurable radical ion pair state lifetimes are limited to polar solvents with values of 1000 and 650 ps in benzonitrile and DMF, respectively (Table 1).

Compound **54**, which holds two Pcs and two fullerenes connected through triple bond containing bridges, presents lifetimes that are essentially on the order of those seen for **8a** and **18**−**20** (Table 1).[106] A probable rationale implies the close proximities that the $Zn^{II}Pc$ and the C_{60} moieties might adopt in **54**. The minimized structure of the tetrad, based on MM+ calculations, illustrates that through-space deactivations are plausible, which prohibit the feasibility of forming long-lived radical ion pair states. Linking instead two C_{60} moieties to one $Zn^{II}Pc$ (i.e., **45**) proved to be more successful in terms of increasing the lifetime of the charge-separated state.[104] In fact, a lifetime of 21 ns was derived for the radical ion pair state in toluene. This value is 1 order of magnitude larger than those measured for $Zn^{II}Pc-C_{60}$ **8a** (Table 1).

The quantum yields of the CS process of the above-mentioned systems depend on several factors such as solvent polarity and D−A separation. They certainly maximize at short D−A separation (i.e., **8a**) and in solvents of medium polarity (i.e., anisole or THF). On the contrary, lower quantum yields are typically found in polar solvents (i.e., benzonitrile) and $Pc-C_{60}$ systems with large D−A separations (i.e., **27** or **35c**).

Solid-state photophysical studies on $Pc-C_{60}$ dyad **8a** were also carried out, revealing the occurrence of a long-lived, photoinduced CS state with a lifetime several orders of magnitude higher than that in solution. The observed stabilization of the CS state within the photoexcited $Pc-C_{60}$ **8a** in the solid has prompted the utilization of this dyad as active material in photovoltaic devices, either alone[249,255] or blended with a conjugated polymer mixture,[250] although in both cases the power conversion efficiencies under simulated solar illumination were found to be low.

The effect of the molecular organization on the photoperformances of a $Pc-C_{60}$ fullerene molecular system were also studied in Langmuir−Blodgett films of **42a** using femtosecond pump−probe and microsecond flash photolysis methods as well as nanosecond time-resolved Maxwell displacement charge.[102] A detailed analysis of these data revealed the occurrence, upon photoexcitation, of a short-lived (i.e., picosecond time scale), intramolecular and a longer lived (i.e., microsecond time scale), intermolecular radical ion pair state. The noted stabilization in the Langmuir−Blodgett films with respect to the solution[101] is probably due to migration of the photogenerated $Zn^{II}Pc^{\bullet+}$ radical cations/$C_{60}^{\bullet-}$ radical anions to spatially close, homologue units. These findings demonstrate that the molecular organization in Pc-based molecular ensembles often leads to significant changes in the CT features of these compounds.

More recently, alternate bilayer structures of PDI and either $Pc-C_{60}$ dyad **42a** or free base Pc were prepared by the Langmuir−Schäfer method and studied using a range of optical spectroscopy methods including femtosecond pump−probe and up-conversion. An efficient quenching of the PDI fluorescence by the free base Pc or $Pc-C_{60}$ dyad **42a** was observed in both steady-state and time-resolved fluorescence measurements. The quenching is due to energy transfer from the PDI to the Pc chromophore in both the PDI|Pc and PDI|**42a** films. In addition, in the PDI|$Pc-C_{60}$ dyad **42a** bilayer structure, the energy transfer mechanism is followed by a charge separation deactivation pathway within the $Pc-C_{60}$ dyad layer, yielding a long-lived (a few microseconds) intermolecular charge-separated state.[103]

Polymeric systems incorporating $Zn^{II}Pc$ and C_{60} as pendent groups in a polynorbornene framework have also been prepared through a ring-opening metathesis reaction, obtaining random $Pc-C_{60}$ copolymers (i.e., **61a**,**b**).[113] Fluorescence

studies, which were carried out with copolymers **61a** and **61b**, revealed distinct excited-state interactions. In particular, fluorescence quenching seems to depend on the relative Pc:C_{60} fullerene ratio, and therefore, increasing the relative content of Pc versus C_{60} (from 60:40 in **61a** to 80:20 in **61b**) led to an amplification of the quenching. In **61**, there is no doubt about the formation of long-lived radical ion pair states upon PET from $Zn^{II}Pc$ to C_{60} in the copolymers, which was confirmed by detecting the spectroscopic signatures of the one-electron-oxidized $Zn^{II}Pc^{\bullet+}$ and one-electron-reduced $C_{60}^{\bullet-}$. The lifetime, as determined at various wavelengths, is 12.6 μs (Table 1). A likely rationale implies delocalizing effects on the photophysical properties of the $Zn^{II}Pc-C_{60}$ ensembles, which evolve from the incorporation of the photoactive units within the polymeric frameworks.

The photophysical behavior of $Pc-C_{60}$ systems presenting the C_{60} acceptor unit axially connected to the Pc macrocycle has been also investigated.

In this context, photoexcitation ($\lambda_{exc} = 400$ nm) of a triad comprising a $Si^{IV}Pc$ bearing two axially coordinated C_{60} units (i.e., **59**) results in the formation of a charge-separated state by PET from the singlet excited state of the $Si^{IV}Pc$ to the C_{60} moiety. The charge-separated state has a lifetime of 5 ns in benzonitrile at 298 K (Table 1).[110]

A $Pc-C_{60}$ fullerene covalent system (**60**) comprising two different electron acceptor entities, namely, NDI and C_{60}, axially coordinated to a central $Si^{IV}Pc$ has also been reported.[112] NDI was chosen as an electron acceptor moiety because of its low reduction potential and the location of its singlet excited state, which is higher in energy than those of $Si^{IV}Pc$ and C_{60}, thus providing a large driving force for the CS process. Photoirradiation of **60** at 380 nm leads to the exclusive formation of the NDI singlet-excited-state species (at this wavelength the extinction coefficients of both Pc and C_{60} are quite low), which evolves into a $Si^{IV}Pc^{\bullet+}(NDI)_2^{\bullet-}(C_{60})_2$ radical ion pair state that outlasts that seen in a related $Si^{IV}Pc-NDI_2$ system lacking the two C_{60} moieties (1000 vs 250 ps) (Table 1). This stabilization of the charge-separated state could be explained considering that electron shifts from the $NDI^{\bullet-}$ to the adjoining C_{60} moiety to generate $Si^{IV}Pc^{\bullet+}(NDI)_2(C_{60})_2^{\bullet-}$ can occur, as demonstrated by the fullerene radical anion fingerprint at around 1000 nm. These results clearly demonstrate that, from a photophysical standpoint, the presence of the two adjacent electron-accepting moieties (i.e., NDI and C_{60}) in pentad **60** leads to a significant stabilization of the photoinduced charge-separated states.

The preparation of $Si^{IV}Pc$-based dendrimeric systems through the axial coordination of fullerodendrimers, carrying up to eight C_{60} units, to a $Si^{IV}Pc$ (i.e., **58**) was also pursued as a means to stabilize the radical ion pair state. A proof of concept is the fact that increasing the dendron generation, that is, increasing the number of C_{60} units from 2 to 8 (i.e., **58**), helps to enhance the radical ion pair state lifetime probably due to electron migration among the C_{60} subunits (Table 1).[109]

D−A $Pc-C_{60}$ fullerene systems based on supramolecular interactions have also been reported and their photophysics studied. For example, the presence of titanium as the metal center in the Pc macrocycle allows for the axial coordination of appropriately substituted C_{60} fullerene derivatives such as in the axially substituted $Ti^{IV}Pc-C_{60}$ **81**.[132] This system undergoes PET upon irradiation with visible light to produce a long-lived radical ion pair state. In fact, analysis of the metastable radical ion pair features revealed CS lifetimes in deoxygenated THF and dichloromethane of 1740 and 1230 ns, respectively (Table 1).

The photophysical properties of $Pc-C_{60}$ fullerene supramolecular systems based on metal−ligand axial coordination between a $Zn^{II}Nc$ and C_{60} derivatives bearing an imidazole functionality (i.e., dyad **75a**)[127] have been studied. Again, photoinduced energy/electron transfer reactions are the inception for creating a radical ion pair state.[39] The calculated rates of CS and CR for dyad **75a** were 1.4×10^{10} and 5.3×10^7 s^{-1} in toluene and 8.9×10^9 and 9.2×10^7 s^{-1} in *o*-DCB, respectively (Table 1).

Metal−ligand interactions have also been used to assemble Pc−Bodipy−C_{60} triad **77**.[130] Photophysical studies on this supramolecular system showed a drastic quenching of the Pc fluorescence when fullerene derivative **79** was added to a solution of Pc−Bodipy **78** in toluene, suggesting an efficient interaction taking place between the photoexcited Pc and C_{60}. The charge transfer mechanism as the major deactivation pathway for the photoexcited Pc moiety in **77** was inferred by transient absorption spectroscopy. In fact, irradiation of the supramolecular ensemble **77** within the visible range leads to a charge-separated Bodipy−$Pc^{\bullet+}-C_{60}^{\bullet-}$ radical ion pair state, through a sequence of excited-state and charge transfers, characterized by a remarkably long lifetime of 39.9 ns in toluene. Comparative photophysical experiments using fullerene derivative **79** and a Pc unit lacking the Bodipy moiety gave charge separation lifetimes of less than 5 ns. These results suggest that, in the supramolecular complex **77**, the Bodipy subunit not only plays a useful role in light harvesting, but also stabilizes the radical ion pair state produced after photoexcitation of the Pc moiety.

Other metallosupramolecular systems were built up through $Zn^{II}Nc$/pyridine axial coordination having the Nc as the primary electron donor and C_{60} as the primary electron acceptor (i.e., dyad **75d**) and either Fc (triad **75b**) or (*N*,*N*-dimethylamino)phenyl (triad **75c**) as secondary electron donors.[128] Important is the fact that the secondary electron donor unit assists in prolonging the radical ion pair state lifetime. Likewise, endowing C_{60} with two pyridines allows binding of a $Zn^{II}Nc$ and leads to an efficient intramolecular CT.[256]

$Ru^{II}Pc-C_{60}$ supramolecular systems **82**−**84** have also been prepared through metal coordination of linear C_{60} monopyridyl (i.e., **82** and **83**) and bispyridyl (i.e., **84**) ligands to $Ru^{II}Pc$.[134] With respect to the excited-state features, it is found that $Ru^{II}Pc-C_{60}$ D−A hybrids are a versatile platform to fine-tune the outcome and dynamics of CT processes. A real asset is, in this context, the use of $Ru^{II}Pcs$ rather than $Zn^{II}Pcs$, which present a high-lying triplet excited state. In other words, the energy-wasting and unwanted CR has been successfully suppressed in these systems, with radical ion pair state lifetimes on the order of hundreds of nanoseconds for the monosubstituted C_{60} adducts (i.e., **82** and **83**), by pushing it far into the Marcus inverted region (Table 1). In triad **84**, which presents a unique hexakis-C_{60} functionalization, a cathodic shift of the reduction potential is observed, which in turn raises the radical ion pair state energy. Nevertheless, the energy of the triplet excited state localized on the $Ru^{II}Pc$ is not high enough, thus offering a rapid deactivation of the radical ion pair state. Thermodynamic considerations suggest that the dynamics of this process is

nearly activationless, a hypothesis that is well corroborated by experimental results.

Simple biomimetic organization principles also provide the means for the facile preparation of D−A hybrids such as **67** and **71**.[120] Threading a dibenzylammonium unit through a dibenzo-24-crown-8 macrocycle, for example, affords pseudorotaxane-like complexes **67** and **71** with binding constants of 1.4×10^4 and 1.9×10^4 M^{-1}, respectively, as implied from a progressive, nonlinear quenching of the $Zn^{II}Pc$ fluorescence. The rationale behind the preparation of supramolecular triad **71** was to enforce the proximity of the fullerene moiety of **68**·PF_6 to the Pc moieties, in stark contrast with assembly **67** in which a coconformer having the fullerene moiety far from the Pc macrocyle could also be possible. Photophysical studies on **67** and **71** systems revealed the formation, in both cases, of microsecond-lifetime radical ion pair states (1.5 and 1.3 μs, respectively) as a result of efficient intracomplex electron transfer events (Table 1). The similar magnitude of these two lifetimes suggests a comparable relative arrangement of the two active units (i.e., Pc and C_{60}) in both dyad **67** and triad **71**. On the other hand, it is worth mentioning that these supramolecular ensembles present a stabilization of more than 2 orders of magnitude of their radical ion pair state lifetimes with respect to covalently linked $Zn^{II}Pc-C_{60}$ conjugates.

Less effective, in terms of achieving long-lived charge-separated states, is the Watson−Crick hydrogen-bonding recognition motif used to assemble the D−A system **72**.[121,122] Spectroscopic and kinetic data supported excited-state interactions. Time-resolved transient absorption experiments documented, for example, the successful formation of the radical ion pair state. Significantly short lifetimes of 3 ns reflect pronounced coupling between the $Zn^{II}Pc$ and C_{60} moieties (Table 1). This is corroborated by a surprisingly large association constant (i.e., $(1.7 \pm 0.7) \times 10^7$ M^{-1}), especially when compared with that of an analogue $Zn^{II}Por-C_{60}$ system (i.e., $(5.1 \pm 0.5) \times 10^4$ M^{-1}).[257]

Finally, self-organization should be considered as an effective means to stabilize the photogenerated radical ion pair state. As a first example, heteroassociation between complementary Pcs **35a** and **34**, with different peripheral functionalities, such as electron-donating alkoxy (i.e., **35a**) or electron-deficient alkylsulfonyl (i.e., **34**) groups, was assessed by different techniques.[96] These experiments provided unambiguous evidence for the formation of a 1:1 complex with a stability constant of ca. 10^5 M^{-1} in $CHCl_3$. Interestingly, hetereoassociation of $Zn^{II}Pc-C_{60}$ **35a** with the electron-deficient $Pd^{II}Pc$ **34** allowed the construction of D−A sandwich stacks **35a/34**, with a radical ion pair lifetime of 475 ns in THF, a value considerably higher than that observed for $Zn^{II}Pc-C_{60}$ **35a** (i.e., 130 ns) (Table 1).

More recently, a $Pc-C_{60}$ supramolecular tetrad (**76**) exhibiting superior electron transfer properties has been reported.[129] In such a system, the formation of a long-lived charge-separated state occurs from the triplet, rather than the singlet, excited state of the $Zn^{II}Pc$ to the C_{60} moiety. The importance of the cofacial Pc−Pc stacking in stabilizing the charge-separated state is evident when the lifetime of the radical ion pair of **76** (i.e., 6.7 μs) is compared with that of a related crown ether $Pc-C_{60}$ supramolecular dyad (i.e., 4.8 μs) (Table 1).

The self-organization of the amphiphilic $Zn^{II}Pc-C_{60}$ salt **13** in water, which gives rise to the formation of uniformly nanostructured 1-D nanotubules, also leads to considerable changes in the photophysics of this dyad with respect to the molecularly dispersed compound.[88] The photoreactivity of these tubular nanostructures, in terms of ultrafast CS (i.e., $\sim 10^{12}$ s^{-1}) and ultraslow CR (i.e., $\sim 10^3$ s^{-1}), is remarkable. In addition, the $Zn^{II}Pc^{\bullet+}-C_{60}^{\bullet-}$ lifetime of 1.4 ms observed for compound **13** implies an impressive stabilization of 6 orders of magnitude relative to dyad **17** (Table 1). It is worth noting that the CS lifetime found in such $Zn^{II}Pc-C_{60}$ nanotubules reaches into a time domain typically found in thin films of D−A composites, and it is due exclusively to the supramolecular organization of the $Pc-C_{60}$ dyad within the 1-D nanoobjects.

6.3. Photophysics of Subphthalocyanine−Fullerene Systems

In contrast to the majority of the $Pc-C_{60}$ ensembles seen above where the photoexcited species lead to the formation of charge-separated states, in the case of the $SubPc-C_{60}$ series **85b**, in which the relative distance between the two active components was varied by *ortho*, *meta*, and *para* substitution at the bridging phenyl spacer, the energy transfer dominates over the intramolecular electron transfer dynamics.[142,143] This observation is in good agreement with the thermodynamics of the investigated systems, which predict a highly exergonic energy transfer, but a less exergonic CT process. A closer look at the photophysics of these systems reveals, nevertheless, that the initial singlet−singlet energy transfer to C_{60} is followed by intersystem crossing and, finally, a triplet−triplet energy transfer back to the SubPc. Importantly, distance matters when dipole−dipole interactions are operative. These govern, for instance, the transduction of singlet-excited-state energy. As a consequence, the *ortho* isomer *o*-**85b** reacts much faster than the other two isomers (i.e., *m*-**85b** and *p*-**85b**). Triplet−triplet energy transfer, on the other hand, follows a double electron transfer mechanism, where through-bond electronic effects exert a strong impact. Noticeable is the outcome that the change in distance and electronic coupling exerts on the SubPc deactivation rates: *ortho* substitution in *o*-**85b**, which imposes unequivocally the shortest distance between the SubPc and C_{60} subunits, leads to the strongest fluorescence quenching within the **85b** series, whereas the weakest SubPc fluorescence quenching was observed for the *para* isomer ***p*-85b**. This conclusion finds independent support in the electrochemical experiments, where the SubPc oxidation potentials reveal isomer-dependent shifts that suggest the occurrence of through-bond electronic effects.

Increasing the relative $SubPc-C_{60}$ distance by placing a diazobenzene spacer (i.e., **89**) still leads to a strong fluorescence quenching of the SubPc moiety of about 90%.[145] Nevertheless, it is mainly a transduction of singlet-excited-state energy that governs the deactivation of the SubPc singlet excited state. Experimental verification for this hypothesis comes from time-resolved fluorescence measurements. At approximately 100 ps, the SubPc-centered features evolve, while the fluorescence features of C_{60} dominate the fluorescence spectrum at around 1 ns.

Interestingly, a fused SubPc dimer, $(SubPc)_2$, linked to C_{60} (i.e., **98**) gives rise to small perturbations of the π-electronic structure in the ground state, whereas photoexcitation of the $(SubPc)_2$ leads to a complex cascade of energy transfer events. For instance, femtosecond transient absorption experiments corroborate the formation of the SubPc dimer singlet excited state. This transient species converts rapidly

to the fullerene singlet−singlet features above 800 nm, which finally give rise to the population of the SubPc dimer triplet excited state at 1080 nm via intersystem crossing.[151]

Considering the ease of preparing peripherally functionalized SubPcs, control over their electron-donating properties was achieved by attaching substituents of different electronic character, namely, fluorine or iodine atoms and ether or electron-rich diphenylamino groups (i.e., *m*-**85a**−**d**).[144] The differences in the oxidation potentials are as large as 200 mV for the fluorine atom versus the amino group. Excitation of dyads *m*-**85a**−**c**, where the level of the radical ion pair lies high in energy, triggers a sequence of exergonic photophysical events that comprise (i) nearly quantitative singlet−singlet energy transfer to the C_{60} moiety, (ii) fullerene intersystem crossing, and (iii) triplet−triplet energy transfer. A powerful tool to favor the CT dynamics over the energy transfer dynamics is either to increase the polarity of the medium or to lower the D−A redox gap. Only in the case of the amino-functionalized SubPc *m*-**85d** is the energy of the $SubPc^{\bullet+}-C_{60}^{\bullet-}$ radical pair state below those of both triplets (i.e., ^{3}*SubPc and ^{3}*C_{60}).

The effect of the D−A distance in the CT dynamics within the series of the amino-functionalized SubPcs **85d** was also established. Photophysical measurements revealed that the *meta* isomer *m*-**85d** undergoes faster CT than the *ortho* and *para* isomers *o*-**85d** and *p*-**85d** (Table 1). Instead, in the case of the strongly exothermic CR process the rate constants exhibit the trend *ortho* > *meta* > *para* due to a "through-space" mechanism.

Placing the redox-active TPA moiety between SubPc and C_{60} triggers an efficient fluorescence quenching of the SubPc moiety in **90**, a sign of a rapid intramolecular deactivation process.[146] In fact, nanosecond transient absorption measurements in DMF provided spectroscopic proof for the $SubPc-TPA^{\bullet+}-C_{60}^{\bullet-}$ radical ion pair state formation. Considering, however, that the initial excitation of the SubPc is likely to be followed by CS to yield $SubPc^{\bullet-}-TPA^{\bullet+}-C_{60}$, migration of electrons to form $SubPc-TPA^{\bullet+}-C_{60}^{\bullet-}$ competes with CR. Alternatively, a long-range energy transfer might populate the C_{60} singlet excited state. From here, CS would involve the vicinal TPA to afford directly $SubPc-TPA^{\bullet+}-C_{60}^{\bullet-}$ (Table 1). Essentially the same reactivity pattern evolves in the presence of two C_{60} moieties (**91**) rather than in the presence of just one C_{60} moiety. Interestingly, a significant broadening of the radical ion pair state signatures has been interpreted in terms of a mutually interacting C_{60} radical anion (Table 1).

More recently, the photophysics of closely spaced SubPc−C_{60} dyads **97a**,**b** have been investigated.[147] These studies showed a different photophysical behavior for the two compounds. Dyad **97a**, which presents the shortest D−A distance (i.e., 3.30 Å) exhibited, upon photoexcitation at 550 nm, a PET process from the SubPc to the fullerene, whereas for dyad **97b** (D−A distance 3.6 Å) a singlet−singlet energy transfer mechanism occurs, despite the similar HOMO−LUMO gap. A possible rationale implies a partial shift of electron transfer density in **97a** as a consequence of the strong orbital overlap, this situation favoring electron over energy transfer (Table 1).

6.4. Photophysics of Phthalocyanine−Carbon Nanotube Assemblies

Pc−SWCNT hybrid systems have emerged as promising candidates to be incorporated in photosynthetic systems, owing to the well-recognized electron acceptor ability of SWCNTs together with the light-harvesting and electron donor features of Pcs. As mentioned in a previous section, the formation of Pc−CNT composites has been shown to improve the inherent photoconductive properties of the Pc component as a result of CT interactions between the electroactive subunits.[231] Particularly, the understanding of the primary PET processes that occur in covalent Pc−SWCNT nanoconjugates is of superior relevance.

In this context, a series of photophysical experiments have been performed on hybrids **105**,[221] which reveal that, as previously observed in other donor−SWCNT ensembles, SWCNTs serve as the electron acceptor component. Fluorescence experiments in DMF solutions of **105** show a strong quenching of the Zn^{II}Pc fluorescence in the ensemble. Transient absorption studies on the femtosecond time scale show that, upon photoexciting Zn^{II}Pc in **105b**, the singlet fingerprints of the Zn^{II}Pc core appear. At the end of the fast decay, differential absorption changes in the near-IR indicate both the formation of the Zn^{II}Pc radical cation (transient maximum at 840 nm) and the bleaching of the van Hove singularities seen in the ground-state spectrum (minima at 820, 890, 980, 1090, 1150, 1200, and 1310 nm). This behavior is in agreement with the injection of photoexcited electrons from the Zn^{II}Pcs to the nanotubes. CS (i.e., 2.0×10^{10} s^{-1}) and CR (i.e., $(7 \pm 0.5) \times 10^{-5}$ s^{-1}) dynamics reveal a notable stabilization of the radical ion pair product in DMF, the lifetime of the charge-separated state having a major component of ca. 700 ns.

On the other hand, photophysical studies of a related H_2Pc−SWCNT material,[95] where the metal-free Pc macrocycles and the nanotubes are linked through a flexible spacer, reveal a behavior similar to that of the ensemble having a rigid bridge (i.e., **105**), where the Zn^{II}Pcs are close to the nanotube surface. This fact seems to indicate that the nature of the spacer does not have a notable effect on the PET process in such Pc−SWCNT hybrid systems.

Nanoconjugate **108** prepared by click chemistry,[222] which has a higher Zn^{II}Pc content than **105**, has also been investigated with a series of steady-state and time-resolved spectroscopy experiments. A photoinduced communication between the two photoactive components (i.e., SWCNT and Zn^{II}Pc) takes place also in this case. In addition, the photovoltaic potential of this material has been tested by measurement of the photocurrent generated in a photoelectrochemical cell. The cell was built by deposition of a thick film of **108** over an indium tin oxide (ITO) electrode, which was afterward immersed in the electrolyte solution (0.1 M Na_3PO_4). The experiments reveal stable and reproducible photocurrents with monochromatic incident photon-to-current efficiency (IPCE) values as large as 17.3%.

The occurrence of PET has also been demonstrated in D−A self-assembled nanohybrids composed of Zn^{II}Nc and SWCNTs.[205] The nanohybrids were constructed by $\pi-\pi$ stacking of pyrene moieties functionalized with imidazole (i.e., ImPy) ligands, which axially coordinate to Zn^{II}Nc molecules to yield the Zn^{II}Nc−ImPy−SWCNT ensembles. Nanosecond transient absorption experiments show that the photoexcitation of the Zn^{II}Ncs results in the one-electron oxidation of these units, confirmed by the development of a transient broad band around 900−1000 nm corresponding to the $Zn^{II}Nc^{\bullet+}$, with the simultaneous reduction of the SWCNT component. The CR process in these nanohybrids

takes place in a few hundred nanoseconds, which corresponds to a lifetime for the charge-separated state of around 100 ns.

More recently, photophysical studies were carried out on the $Zn^{II}Pc/SWCNH_{ox}$/BSA system.[258] These studies revealed significant electronic communication within the $Zn^{II}Pc/SWCNH_{ox}$ nanoensembles in both the ground and excited states. Moreover, under light illumination of $Zn^{II}Pc/SWCNH_{ox}$/BSA in the presence of an electron mediator such as a methyl viologen dication (MV^{2+}) and a sacrificial hole trap, the formation of the $MV^{\bullet+}$ was observed in an aqueous solvent, whereas in the presence of O^2 biologically active $O^{2\bullet-}$ was generated. The accumulated $MV^{\bullet+}$ or $O^{2\bullet-}$ species are furthermore able to make their excess electrons available to other substrates.

7. Phthalocyanines and Fullerene as Active Components in Organic Solar Cells

Organic solar cells present a planar structure where one or more semiconducting organic layers are inserted between an anode and a cathode. In these photovoltaic devices, the active layer performs also as the light-absorbing material, thus generating an exciton through promotion of an electron from the HOMO to the LUMO level. In a second step, the exciton has to dissociate to generate charge carriers that will move toward the corresponding electrodes, usually an ITO anode and a metallic cathode (i.e., Al, Au, etc.).

The first investigations on organic photovoltaic systems were performed at the end of the 1950s with Por and Pc chromophores as components of the active layer. From these two types of molecules, Pcs have emerged as optimal dyes for solar energy conversion mainly due to the good overlap of their absorption spectrum with the terrestrial solar emission spectrum, their high extinction coefficients (higher than those of Pors), and their good p-type semiconducting behavior. Additional advantages of Pcs are their high thermal stability and the quality of the crystalline films prepared by sublimation of these molecules. Nevertheless, the solar cells prepared exclusively by sublimation of Pcs showed very low conversion efficiencies (i.e., around 0.1%). These values were exceeded in 1986 when Tang[259] put into operation a device comprising two layers of different materials, one of them performing as an electron donor, i.e., a metallo-Pc, and the other one as an electron acceptor. In these devices, the exciton dissociation is facilitated by the electron transfer from the LUMO of the excited donor material to the LUMO of the acceptor component. Efficiency values up to 1% were achieved with this planar p/n heterojunction architecture (Figure 27a).

The main disadvantage of the latter device architecture is the fact that only a very thin layer at the interface of the donor and the acceptor material is effective in promoting the exciton dissociation. To optimize the CT process in the active layer, the bulk heterojuction (BHJ) architecture was introduced (Figure 27b), which is composed of an intermixing of the donor and the acceptor components all along the active layer, thus increasing the contact area between the two materials. In such devices, upon controlling the morphology of the material into an interpenetrating, bicontinuous network of the donor and the acceptor, one can achieve, first, a high interfacial area within the BHJ active layer for efficient exciton dissociation and, second, efficient collection of charges. This concept has been mainly applied to devices containing semiconducting polymers as hole-transport materials in combination with appropriate acceptor molecules, leading to the so-called polymeric solar cells.[260] Particularly successful has been the combination of poly(*p*-phenylenevinylene)- and polythiophene-type polymers with PCBM, a soluble derivative of C_{60}.[261]

Figure 27. Different architectures for organic solar cells: (a) planar p/n heterojunction, (b) BHJ.

The polymeric (or plastic) solar cells hold as a major advantage the ease of processing by spin-casting of organic solutions containing an appropriate mixture of both donor and acceptor components. However, one serious drawback of solution-processed polymeric solar cells is their morphological disorder: A limited miscibility of the components often gives rise to a large segregation into big domains of the donor and acceptor components, which in turn affects the overall device's efficiency. Moreover, the mechanisms of charge generation, transport, and recombination are still to be fully clarified. On the contrary, small organic molecules such as Pcs can be evaporated on substrates, forming films with high macroscopic order. This type of processing is disadvantageous for large-scale device fabrication, but the preparation of such evaporated photovoltaic cells may allow the scientist to study the elementary physical processes that control the performance of the devices.[262] For this reason, Pcs are still objects of considerable scientific interest in the field of organic solar cells.

In this section, we will describe the different architectures reported for Pc/C_{60}-based photovoltaic devices. Many are the examples that can be found in the literature, which make use of either coevaporated $Pc:C_{60}$ active layers or planar heterojunction Pc/C_{60} architectures. However, numerous examples are also reported where both structural designs are simultaneously employed. With the aim of establishing a connection between the different examples that allows a comparison, and also for the sake of clarity, we have divided this section into three different parts. The first one includes examples where a blended $Pc:C_{60}$ active layer has been employed at some position of the device, whereas the second part only compiles examples where the separation of charges occurs exclusively at the interface of the planar Pc donor and C_{60} acceptor layers. A final part is dedicated to the use of covalently linked $Pc-C_{60}$ systems as a component of the active layer.

7.1. Phthalocyanine/Fullerene Blends as Active Layers

As mentioned above, Pcs have been long utilized as active components in solar cells owing to their strong absorption in the visible region of the solar spectrum and good hole-conducting properties. The use of C_{60} as a suitable doping component for enhancing the photoconductivity of Pc films was triggered by the experimental observation of the occurrence of PET processes taking place in $Pc:C_{60}$ mixed solutions from the Pc to the C_{60} units.[245] In this regard, former investigations were carried out on evaporated layers of metal-free Pc, which were doped with different amounts of C_{60} to investigate the effect of the presence of the acceptor molecule

Table 2. Performance Characteristics of Devices Containing Coevaporated Pc:C_{60} as Active Layers

structure and composition of the device	I_o (mW cm^{-2})	V_{OC} (V)	J_{SC} (mA cm^{-2})	FF	η (%)	ref
ITO/MPCI (500 Å)/30 mol % C_{60}:Ti^{IV}OPc (300 Å)/Ti^{IV}OPc (200 Å)/Au	94	0.53	3.4	0.32	0.63	265
ITO/Cu^{II}Pc (35 Å)/ Cu^{II}Pc:C_{60} (1:1) (500 Å)/C_{60} (50 Å)/BCP (120 Å)/Al	100	0.50	5.6	0.41	1.15	270
ITO/Cu^{II}Pc (35 Å)/ Cu^{II}Pc:C_{60} (3:1)/Cu^{II}Pc:C_{60} (1:1)/Cu^{II}Pc:C_{60} (1:3)/C_{60} (50 Å)/BCP (120 Å)/Al	100				1.36	270
ITO/Cu^{II}Pc:C_{60} (60 nm)[a]/TPBI[b] (6 nm)/Al (80 nm)	100	0.52	9.17	0.45	2.15	271
ITO/PEDOT:PSS/p-*m*-MTDATA (50 nm)/Zn^{II}Pc:C_{60} (1:2) (50 nm)/n-MPP (50 nm)/LiF (1 nm)/Al (70 nm)	10	0.45	1.5	0.5	3.37	275
ITO/PEDOT:PSS/*m*-MTDATA (50 nm)/Zn^{II}Pc:C_{60} (1:2) (50 nm)/n-MPP (50 nm)/LiF (1 nm)/Al (70 nm)	100	0.5	6.3	0.33	1.04	275
ITO/p-MeO-TPD (50 nm)/Zn^{II}Pc:C_{60} (1:2) (50 nm)/PTCBI (10 nm)/n-C_{60} (50 nm)/Al (100 nm)	100	0.5	8.3	0.45	1.9	276
ITO/p-MeO-TPD (30 nm)/Zn^{II}Pc:C_{60} (1:2) (60 nm)/n-C_{60} (20 nm)/Al (55 nm)	125	0.45	13.9	0.39	1.95	278
ITO/p-MeO-TPD (30 nm)/Zn^{II}Pc:C_{60} (1:2) (60 nm)/n-C_{60} (20 nm)/Au (8 Å)/p-MeO-TPD (30 nm)/Zn^{II}Pc:C_{60} (1:2) (48 nm)/n-C_{60} (30 nm)/Al (55 nm)	125	0.85	6.6	0.53	2.4	278
ITO/n-C_{60} (10 nm)/C_{60} (15 nm)/Zn^{II}Pc:C_{60} (1:1) (35 nm)/p-DiNPD[c] (20 nm)/Al (1 nm)/Ag (14 nm)/n-C_{60} (10 nm)	100	0.54	7.25	0.58	2.3	280
ITO/C_{70} (5 nm)/Zn^{II}Pc:C_{70} (1:2) (30 nm)/DiNPD[c] (5 nm)/p-PVTPD[d] (40 nm)/p-Zn^{II}Pc (10 nm)/Au	100	0.56	9.88	0.52	2.87	282
ITO/Cu^{II}Pc:C_{60} (1:1) (330 nm)/C_{60} (100 nm)/BCP (75 nm)/Ag	100	0.50	15.4	0.46	3.5	285
ITO/Cu^{II}Pc:C_{60} (1:1) (330 nm)/C_{60} (100 nm)/BCP (75 nm)/Ag	30	0.47	4.2	0.49	3.6	285
ITO/Cu^{II}Pc (150 Å)/Cu^{II}Pc:C_{60} (1:1) (100 Å)/C_{60} (350 Å)/BCP (100 Å)/Ag (1000 Å)	120	0.54	15	0.61	5.0	287
ITO/Cu^{II}Pc (150 Å)/Cu^{II}Pc:C_{60} (1:1) (100 Å)/C_{60} (350 Å)/BCP (100 Å)/Ag (1000 Å)[e]	100	0.53	14	0.63	4.6	300
ITO/Cu^{II}Pc (75 Å)/Cu^{II}Pc:C_{60} (1:1) (125 Å)/C_{60} (80 Å)/PTCBI (500 Å)/Ag (5 Å)/p-*m*-MTDATA (50 Å)/Cu^{II}Pc (60 Å)/Cu^{II}Pc:C_{60} (1:1) (130 Å)/C_{60} (160 Å)/BCP (100 Å)/Ag (1000 Å)	100	1.03	9.07	0.59	5.7	288
ITO/PEDOT:PSS/BP2T (8 nm)/Zn^{II}Pc (10 nm)/Zn^{II}Pc:C_{60} (1:1) (30 nm)/C_{60} (25 nm)/Alq3[f] (5 nm)/Al (100 nm)	100	0.56	9.97	0.55	3.07	303
ITO/PEDOT:PSS/P3HT:PCBM (1:1.1) (200 nm)/LiF (0.5 nm)/Al (1 nm)/WO_3 (3 nm)/Cu^{II}Pc:C_{60} (60 nm)/BPhen (5 nm)/Al (80 nm)	16				4.6	304
ITO/PEDOT:PSS (50 nm)/Cu^{II}Pc (8 nm)/P3HT:PCBM (1:0.8) (80 nm)/Al (100 nm)	100	0.60	8.63	0.54	2.79	305
ITO/Zn^{II}Pc (10 nm)/Zn^{II}Pc:C_{60} (10 nm)/C_{60} (20 nm)/$Sn^{IV}Cl_2$Pc (3 nm)/$F_{16}Cu^{II}$Pc/Zn^{II}Pc (10 nm)/Zn^{II}Pc:C_{60} (10 nm)/C_{60} (10 nm)/Alq3[f] (5 nm)/Al	100	1.04	3.64	0.48	1.81	306

[a] Gradient of donor Cu^{II}Pc and acceptor C_{60} along the active layer. [b] 2,2,2-(1,3,5-Benzenetriyl)tris[1-phenyl-1*H*-benzimidazole]. [c] *N*,*N*′-Diphenyl-*N*,*N*′-bis(4′-[*N*,*N*-bis(naphth-1-yl)amino]biphenyl-4-yl)benzidine. [d] *N*,*N*′-Bis(4-(2,2-diphenylethen-1-yl)phenyl)-*N*,*N*′-bis((4-methylphenyl)phenyl-)benzidine. [e] The active layer was grown by organic vapor-phase deposition. [f] Tris(8-hydroxyquinolinato)aluminum.

on the photoconductivity performances.[263] Electric measurements showed that photoconductivity of the doped films increased by more than 1 order of magnitude compared to that of the undoped films. The ratio between photoconductivity and dark conductivity was also greatly enhanced by the presence of C_{60}.

Ti^{IV}OPc has also been used as a photoactive material in photovoltaic devices, because Ti^{IV}OPc functions as an excellent material for charge-carrier photogeneration. Thus, p/n heterojunction devices using Ti^{IV}OPc as a p-type organic semiconductor in combination with suitable n-type organic materials, i.e., *N*,*N*′-dimethyl-3,4:9,10-perylenebis(dicarboximide) (MPCI), had been described by Shirota and coworkers in 1996.[264] In 2000, the same group tested the effect of C_{60} doping in a three-layer architecture device, namely, ITO/MPCI/C_{60}-doped Ti^{IV}OPc/Ti^{IV}OPc/Au.[265] The performances were compared with those of the two-layer cell ITO/MPCI/Ti^{IV}OPc/Au, the experiments showing that doping the Ti^{IV}OPc-based solar cell with C_{60} improved the quantum yields for the charge-carrier photogeneration and doubled the conversion efficiencies of the device, from 0.34% to 0.63%, under 1 sun (100 mW cm^{-2}) of AM 1.5G white-light illumination (Table 2).

Further on, photoelectrochemical investigations on uniform Langmuir−Schäfer films obtained from mixed solutions of C_{60} and Cu^{II}Pc revealed that this composite system was a candidate for photovoltaic applications.[266] The experiments showed that the open circuit voltage and short circuit current increased when the doping level of C_{60} in the composite films was increased. In the same year, Pannemman et al. prepared both double-layer and coevaporated devices of Zn^{II}Pc and C_{60} with different electrode contacts.[267] Photocurrent measurements showed that the external quantum efficiency of the coevaporated device (i.e., 7%) was higher than that of the double-layer architecture (i.e., 3%). Recent studies have focused on the electronic structures of intermixed Cu^{II}Pc:C_{60} layers, indicating that the $HOMO_{Cu^{II}Pc}-LUMO_{C_{60}}$ gap is significantly enhanced in the mixed layer with regard to that of discrete Cu^{II}Pc/C_{60} junctions.[268] The effects of composition were examined for a series of devices incorporating mixed layers of Pc and C_{60} in different ratios.[269] AFM and electronic absorption spectroscopy studies showed that the mixed layer films of Cu^{II}Pc and C_{60} are smooth and amorphous and undergo intermolecular intermixing.

Further improvements have been achieved using multiple mixed layers, which create a gradient of D−A compositions (Figure 28) and reach power conversion efficiencies up to 1.36% at 1 sun of AM 1.5G illumination (Table 2).[270] Other authors have described the preparation of devices with a concentration gradient of donor Cu^{II}Pc and acceptor C_{60} in

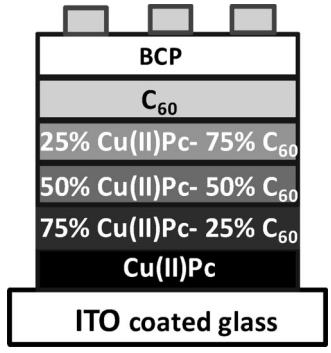

Figure 28. Schematic representation of a multiple mixed layer device.

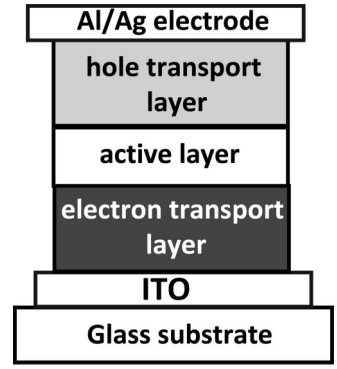

Figure 29. Schematic representation of a p−i−n architecture.

the active layer, prepared by varying the deposition rate of each component, which show efficiencies up to 2.15% (Table 2).[271]

The annealing effect on the morphology, performance, and photophysical properties of these photovoltaic devices has also been studied.[272] Power conversion efficiencies of solar cells subjected to heat treatments were found to be less than those of discrete cells containing no annealed films, probably due to the creation of defects in the annealed films and to morphological templating of C_{60} on top of the $Cu^{II}Pc$ layer, thus reducing the interfacial area for exciton separation. This result had been previously reported by Forrest in low molecular weight solar cells based on $Cu^{II}Pc$.[273] Increasing the temperature inevitably leads to a significant roughening of the mixed layer film surface and to short-circuited devices. Oxygen is also known to harm Pc/C_{60} devices because it affects the photoelectrical properties of C_{60} and the interface between Pc and C_{60} domains.[274]

A major problem of using small-molecule blends is their poor transport properties when they are also used as charge transport layers in the device. Moreover, excitons or charge carriers created close to the metal electrode undergo a quenching process and, therefore, cannot contribute to the photocurrent. The introduction of wide-gap transport layers between the photoactive layer and the electrodes can overcome this problem (Figure 29). A systematic study on these so-called p−i−n photovoltaic devices, combining $Zn^{II}Pc$ as the donor and C_{60} as the electron acceptor in the active layer, was reported by Gebeyehu et al.[275] The mixed layer was prepared using high-vacuum coevaporation of $Zn^{II}Pc$ and C_{60}, and then it was sandwiched between p- and n-doped charge-carrier transport layers, namely, p-doped 4,4′,4″-tris(((3-methylphenyl)phenyl)amino)triphenylamine (*m*-MTDATA) and n-doped perylene-3,4,9,10-tetracarboxylic *N*,*N*′-9-dimethyldiimide (MPP). The authors investigated how differences in the photoactive donor−acceptor layer thickness and donor:acceptor ratio affect the performance of the devices. The performance of these devices happened to be critically dependent on both the transport properties of the interpenetrating network of donors and acceptors and the doped charge transport layers. The insertion of a 3,4-poly((ethylenedioxy)thiophene):poly(styrenesulfonate) (PEDOT:PSS) layer between ITO and the hole transport layer notably improved the performance. At very low incident intensities (0.1 sun of white-light illumination), a 3.37% power conversion efficiency was found for the optimized device, but only a 1.04% conversion under 1 sun intensity, as a consequence of the increase of the cell series resistance due to significant ohmic losses in the transport layers (Table 2). Further improvements were reported by the same authors in similar devices. An optimized device was prepared using p-doped tetrakis(4-methoxyphenyl)benzidine (MeO-TPD) as the hole transport layer, a neat layer of coevaporated 3,4,9,10-perylenetetracarboxylic bisbenzimidazole (PTCBI) added to extend the absorption of the active $Zn^{II}Pc$:C_{60} layer, and n-doped C_{60} as the electron transporting layer. The device with a layer sequence ITO/p-MeO-TPD/$Zn^{II}Pc$:C_{60}(1:2)/PTCBI/n-C_{60}/Al showed an energy conversion efficiency of 1.9% under 1 sun of standard AM 1.5G illumination (Table 2).[276] Other device architectures, such as the metal-intrinsic p-doped type have been also developed.[277]

Sariciftci and co-workers have deeply investigated the use of p−i−n heterostructures for organic solar cells.[278] For an active layer of $Zn^{II}Pc$:C_{60}, p-doped MeO-TPD and n-doped C_{60} turned out to be the best choices for the wide-gap hole and electron transport material, respectively. They demonstrated that, when the active region is separated from the top metal electrode, the photocurrent is nearly doubled. Similar to the Gebeyehu architecture,[275] the optimized single-cell device reached a power conversion efficiency of 1.95% at 125 mW cm^{-2} white-light illumination (Table 2). A tandem cell, namely, a device based on two stacked solar cells, was also constructed. The tandem approach permits the problem of the low total absorption of single cells to be overcome. In this case, the tandem cell showed a power efficiency of 2.4% at 125 mW cm^{-2} white-light illumination (Table 2). This value was lower than predicted (around 3%),[279] because of the fact that the photocurrent is decreased for tandem cells as compared to the single cells.

Leo and co-workers have also investigated the p−i−n architecture. One of their major achievements is the preparation of semitransparent p−i−n organic solar cells using ultrathin metal multilayers composed of Al and Ag as semitransparent top electrodes and additional capping, antireflection layers of n-doped C_{60}. The devices exhibit power conversion efficiencies of 2.1−2.2% with transmissions exceeding 30−50% in the visible part of the spectrum (Table 2).[280] The performance of these semitransparent solar cells has been shown to depend on the interface and morphology of the ultrathin cathode, which can be influenced by varying the composition and layer structure of the metal contact.[281] Another interesting variation developed by these authors is the introduction of high-order C_{70} fullerene owing to its larger absorption of the solar spectrum. By optimizing the energy level alignment to hole transport layers, and the ratio of $Zn^{II}Pc$ to C_{70}, an efficiency of 2.87% is achieved (Table 2), which means a 20% increase with regard to a related device containing C_{60}.[282]

Inverted solar cells are also an object of study.[283] The challenge to reversing the layer sequence of organic PV

devices is to prepare a selective contact bottom cathode for electron collection in the inverted structure, for example, a ZnO interfacial layer between the active layer and the ITO bottom electrode.[284]

The highest efficiency values for solar cells containing Pc:C_{60} blends have been reported by Forrest and co-workers, as a result of a careful purification of the organic materials and a precise design of the devices' structure.[285] First, they reported a device using a 1:1 $Cu^{II}Pc:C_{60}$ ratio, since the absorption spectra of different $Cu^{II}Pc:C_{60}$ films indicated that a higher C_{60} concentration inhibits $Cu^{II}Pc$ aggregation, thereby reducing hole transport in the mixed film. They further realized that the introduction of a C_{60} layer together with an exciton-blocking layer[286] of bathocuproine (BCP) between the $Cu^{II}Pc:C_{60}$ blend and the Ag cathode considerably improved the efficiency. Therefore, a low series resistance photovoltaic cell was constructed, with peak power efficiencies of 3.6% at 0.3 sun and 3.5% under 1 sun of irradiation (Table 2).[285] When an additional layer of $Cu^{II}Pc$ was inserted between the ITO anode and the 1:1 $Cu^{II}Pc:C_{60}$ blend, maximum efficiencies of 5% under 1−4 suns of simulated AM 1.5G solar illumination were achieved (Table 2).[287] This architecture was called a hybrid planar-mixed molecular heterojunction. In a tandem geometry consisting of two hybrid planar-mixed molecular heterojunction cells stacked in series, the authors demonstrated a further increase in power conversion efficiency up to 5.7% (Table 2).[288] Further studies on the relationships among film microstructure, mixing ratio, and charge conduction in mixtures of two organic molecular species were carried out.[289] The results showed that mixed layers of a 1:1 $Cu^{II}Pc:C_{60}$ ratio exhibit mobilities that are reduced by more than 1 order of magnitude when compared to the corresponding films of pure composition, and for that, the performance of organic hybrid planar-mixed molecular heterojunction photovoltaic cells is higher than that of classical blended systems.[290] The role of exciton-blocking layers in improving the efficiency of this type of device has also been explored.[291]

The control of the nanostructure of the active layers is a key point for the development of efficient organic solid-state solar cells,[292] because it strongly influences the photocurrent generation process. Usually, the random distribution of donor and acceptor materials in small-molecule blended solar cells can lead to charge-carrier trapping at bottlenecks and cul-de-sacs in the conducting pathways to the electrodes. For this reason, some efforts have been made to control the nanostructure of codeposited films of Pc and C_{60}.[293−296] In this direction, organic vapor-phase deposition[297] and oblique angle vacuum deposition[298,299] arise as very precise ways to control the morphology of crystalline organic films because they allow, in some cases, the fine control of the positions and orientations of the donor and acceptor materials, thus eliminating resistive conducting pathways while maximizing the interface area. $Cu^{II}Pc$ has been grown on different substrates, giving rise to well-controlled $Cu^{II}Pc$ rods that are aligned vertically between the two electrodes.[300] This highly folded surface (Figure 30) showed a 4-fold increase in area compared to a flat interface. Photovoltaic cells with (1:1) $Cu^{II}Pc:C_{60}$ mixed active layers grown by organic vapor-phase deposition showed power conversion efficiencies similar to those obtained by thermal evaporation (Table 2), but some optimization in the device preparation is still required to reach higher values. The flexible self-assembly behavior of $Cu^{II}Pc$ on a diverse range of substrates with different surface

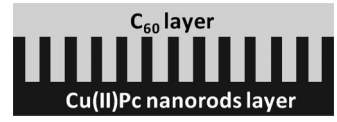

Figure 30. Ideal BHJ of $Cu^{II}Pc$ nanorods and C_{60} obtained by organic vapor-phase deposition.

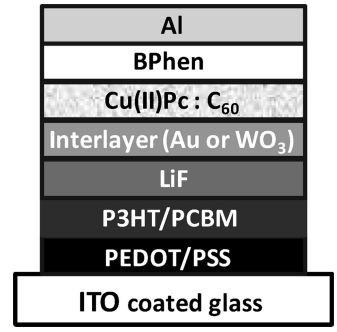

Figure 31. Schematic representation of a tandem solar cell from ref 304.

energies has been also explored as a way to control the morphology of the interface.[301] Another approach for improving the morphology and reducing transport losses is the controlled heating of the substrate during film deposition. It has been shown that heating the substrate during coevaporation of C_{60} and $Zn^{II}Pc$ leads to a significant improvement in the solar cell performance as a consequence of the incidence of better charge-carrier percolation pathways within the $Zn^{II}Pc:C_{60}$ blend.[302]

With the aim of reducing the bulk traps and therefore increasing the carrier mobility in $Zn^{II}Pc$ films of planar mixed molecular heterojunctions, Yan and co-workers have applied a technique called "weak epitaxy growth", which had been previously utilized to prepare high-performance organic thin-film transistors with single-crystal-like carrier mobility. This method involves the deposition of an inducing layer between the $Zn^{II}Pc$ layer and the substrate, this layer determining the quality of the $Zn^{II}Pc$ thin film and the device performances. Using 2,5-bis(4-biphenylyl)bithiophene (BP2T) as the inducing layer, the efficiency reaches values up to 3.07% in planar mixed heterojunction devices with C_{60} (Table 2).[303]

Another exciting approach toward the achievement of maximum practical efficiencies is the preparation of tandem solar cells based on the combination of a poly(3-hexylthiophene) (P3HT):PCBM blend as the active layer of the subcell and a $Cu^{II}Pc:C_{60}$ blend, processed by a gradient coevaporation, as the active layer in the top cell (Figure 31).[304] A highly transparent, high-work-function WO_3 layer has been used as a component of the interconnecting system for the two subcells. The efficiency of the stacked devices was as high as 4.6%, which is close to the sum of the efficiencies of the individual subcells (Table 2). In similarly "tandemlike" cells, PCBM was employed simultaneously to form a bilayer heterojunction subcell with the underlying $Cu^{II}Pc$ and a BHJ subcell with blended P3HT.[305] In comparison with the conventional tandem structure, the device does not have an intercellular connection layer, thus reducing the complexity of the device and the light loss. The power conversion efficiency of the tandem structure (2.79%) is nearly the sum of those of the stand-alone cells of $Cu^{II}Pc$/PCBM (0.43%) and P3HT:PCBM (2.50%) (Table 2).

The use of all organic connecting units to fabricate tandem photovoltaic cells has also been explored. In a recent

Table 3. Performance Characteristics in Vacuum-Evaporated p/n Pc/C_{60} Heterojunction Devices

structure and composition of the device	I_o (mW cm^{-2})	V_{OC} (V)	J_{SC} (mA cm^{-2})	FF	η (%)	ref
ITO/C_{60} (500 Å)/H_2Pc (500 Å)/Au (200 Å)	12.5	0.18	0.089	0.25	0.03	308
ITO/PEDOT:PSS/Cu^{II}Pc (200 Å)/C_{60} (400 Å)/BCP (120 Å)/Al (1000 Å)	150	0.58	18.8	0.52	3.6	286
ITO/PEDOT:PSS/Cu^{II}Pc (200 Å)/C_{60} (400 Å)/BCP (120 Å)/Al (1000 Å)[a]	440				4.2	309
F-doped SnO_2/Cu^{II}Pc (240 Å)/C_{60} (490 Å)/BCP (120 Å)/Al (1000 Å)	100				1.3	316
ITO/Pd^{II}Pc (20 nm)/C_{60} (20 nm)/BCP (15 nm)/Ag (100 nm)	100	0.57	6.8	0.57	2.2	320
ITO/Ti^{IV}OPc (20 nm)[b]/C_{60} (40 nm)/BCP/Al	100	0.57	15.1	0.53	4.2	322
ITO/SubPc (20 Å)/Sn^{II}Pc (100 Å)/C_{60} (400 Å)/BCP (100 Å)/Al (1000 Å)	100	0.4	8.4	0.62	2.1	323
ITO/4 mol % pentacene-doped Cu^{II}Pc (20 nm)/C_{60} (60 nm)/BCP (8 nm)/Al (80 nm).	100	0.52	12.93	0.46	3.06	325
ITO/F4-TCNQ[c] (1 nm) /pentacene (50 nm)/Zn^{II}Pc (6 nm)/C_{60} (40 nm)/BPhen (8 nm)/Al (60 nm)	100	0.49	9.10	0.50	2.1	327
ITO/SubPc (130 Å)/C_{60} (325 Å)/BCP (100 Å)/Al (1000 Å)	100	0.97	3.36	0.57	2.1	330
ITO/SubPc (130 Å)/C_{60} (325 Å)/BCP (100 Å)/Al (1000 Å)	100	0.92	5.42	0.61	3.03	331
ITO/PEDOT:PSS/SubNc (320 Å)/C_{60} (325 Å)/BCP (100 Å)/Ag (1000 Å)[d]	100	0.55	5.6	0.49	1.5	332
ITO/PEDOT:PSS/Cu^{II}Pc (200 Å)/PCBM (300 Å)/BCP (100 Å)/Al (1000 Å)[e]	100	0.64	4.51	0.53	1.18	334
ITO/PEDOT:PSS/Zn^{II}Pc (45 nm)/4%**112**-doped PCBM:MDMO-PPV (4:1)/LiF (0.6 nm)/Al (100 nm)[f]	100	0.57	5.75	0.50	1.6	337

[a] The device area (A) is 0.0075 cm^2. [b] Near-infrared polymorph. [c] 2,3,5,6-Tetrafluoro-7,7,8,8-tetracyanoquinodimethane. [d] The layer of SubNc was deposited by spin-coating of a chlorobenzene solution. [e] The layer of PCBM was deposited by spin-coating of a chlorobenzene solution. [f] The **112**-doped PCBM:MDMO-PPV layer was prepared by spin-coating of a chlorobenzene solution.

example, a $Sn^{IV}PcCl_2$/$Cu^{II}F_{16}$Pc heterojunction is used as the connecting layer of two Zn^{II}Pc:C_{60} hybrid planar-mixed molecular heterojunction single cells, providing the tandem device with transparency and effective recombination for electrons and holes at the interlayer.[306] In the optimized device, the efficiency is increased by 60% with respect to that of the subcell (Table 2).

7.2. Two-Layer Phthalocyanine/Fullerene Heterojunction Devices

All the above-mentioned studies bring out the efficiency of the coevaporation of Pc and C_{60} to form mixed active layers for photoinduced CS. However, it is compulsory to mention that good efficiencies have also been obtained with solar cells where the CS process between the donor Pc and the acceptor C_{60} takes place in a planar p/n heterojunction arrangement.[307]

The longer exciton diffusion length of C_{60} with regard to other acceptor materials makes fullerene a molecule of choice for the optimization of p/n cells. After a former report on the photovoltaic properties of ITO/C_{60}/H_2Pc/Au sandwich solar cells, showing an energy conversion yield of 0.03% when illuminated by white light (Table 3),[308] Forrest and co-workers demonstrated an external power conversion efficiency of 3.6% under AM 1.5G spectral illumination with vacuum-deposited Cu^{II}Pc/C_{60} double-heterostructure photovoltaic cells incorporating an exciton-blocking layer (Table 3).[286] Therefore, this outstanding double-heterostructure cell was fabricated on an ITO anode modified with a thick film of PEDOT:PSS to planarize the ITO, whose rough surface would otherwise result in shorts through the thin film of the active layer. A 200 Å film of Cu^{II}Pc was grown at rt in a vacuum, followed by a 400 Å film of C_{60}. Next, a thick film of BCP as the exciton-blocking layer was deposited, followed by the thermal evaporation of the Al cathode. Further on, a similar double-heterostructure device based on Cu^{II}Pc and C_{60} thin films but with a series resistance as low as 0.1 V cm^2, as a consequence of the low device area (0.0075 cm^2), was reported by the same authors.[309] In this device, the power conversion efficiency reached a maximum of 4.2% under 4.4 suns intensity simulated AM 1.5G (Table 3).

The effect of the organic layer thickness on the photovoltaic efficiency was also investigated in planar heterojunction photovoltaic cells with Cu^{II}Pc as the electron donor layer and C_{60} as the electron acceptor layer,[310,311] as well as the effect of the temperature on the photovoltaic parameters.[312] ITO surface treatments also show an influence on the photoperformance of two-layer Cu^{II}Pc/C_{60} heterojunction solar cells.[313] For example, surface modification of ITO substrates through the use of self-assembled monolayers of molecules with permanent dipole moments, such as 4-chlorobenzoyl chloride, has been used to control the anode work function and the device performance in molecular solar cells comprising a stacked Cu^{II}Pc/C_{60} heterojunction.[314] Use of self-assembled monolayers of dipolar molecules increased the power conversion efficiency by up to an order of magnitude with respect to that of untreated ITO. This improvement was attributed primarily to an enhanced interfacial CT rate at the anode, due to both a decrease in the interfacial energy step between the anode work function and the HOMO level of the organic layer and a better compatibility of the self-assembled monolayer-modified electrodes with the initial Cu^{II}Pc layers. Replacement of the ITO anode by a more available material, such as ZnO, has also been investigated. In particular, a ZnO:Al anode coated with an ultrathin film of Au gives results similar to those obtained with ITO anodes.[315] F-doped SnO_2-coated glass has also been used as the transparent anode for heterojunction Cu^{II}Pc/C_{60} photovoltaic cells.[316] The organic layers were grown by organic vapor-phase deposition, which enabled complete coverage of the rough oxide surface. The power conversion efficiency of the planar heterojunction device happened to be 1.3% at 1 sun of simulated AM 1.5G (Table 3).

Due to its medium energy levels and bipolar characteristics, Cu^{II}Pc has been used in a three-layer device, i.e., a

m-MTDATA/$Cu^{II}Pc/C_{60}$ cell where *m*-MTDATA and C_{60} behave, respectively, as the donor and the acceptor layers and $Cu^{II}Pc$ behaves as an acceptor and a donor, respectively, at its interfaces with *m*-MTDATA and C_{60}. In comparison with a standard $Cu^{II}Pc/C_{60}$ bilayer cell, an efficiency enhancement of over 30% was achieved in the three-layer device.[317]

Other authors have investigated the photovoltaic properties of a stacked bilayer structure using ruthenium(II) phthalocyaninate derivatives instead of other classical metallic complexes.[318] The resulting device showed high series resistance and strong recombination at the interface, which limited the cell performance. In fact, a correlation of hole mobility, exciton diffusion length, and solar cell performances for different metallo-Pcs in stacked metallo-Pc/C_{60} organic solar cells has been recently established,[319] the best performances being obtained for $Zn^{II}Pc$, $Cu^{II}Pc$, and metal-free Pc derivatives. Recent studies have shown that $Pd^{II}Pc$ is a promising donor material with a long exciton diffusion length which leads to highly efficient $Pd^{II}Pc/C_{60}$ solar cells (Table 3).[320] $Ti^{IV}OPc/C_{60}$ planar heterojunction devices have also been studied to determine interfacial dipoles and charge redistribution.[321] The open circuit voltage (V_{OC}) values for $Ti^{IV}OPc$-based photovoltaic devices were found to be ca. 0.2 V higher than those for related $Cu^{II}Pc$-based devices. Another advantage of vacuum-deposited $Ti^{IV}OPc$-based heterojunction devices is that the $Ti^{IV}OPc$ films are easily converted to a near-IR-absorbing polymorph using postdeposition solvent annealing, this transition broadening the absorbance spectrum of the $Ti^{IV}OPc$ film up to 900 nm, along with a substantial texturing of the layer. A recent study shows efficiencies up to 4.2% in solvent-annealed $Ti^{IV}OPc/C_{60}$ planar heterojunction devices (Table 3).[322] $Sn^{II}Pc$ has also demonstrated significant absorption at wavelengths from 600 to 900 nm. An optimized device with the structure ITO/electron blocker (SubPc)/$Sn^{II}Pc/C_{60}$/BCP/Al shows a power conversion efficiency of 2.1% at 1 sun (Table 3).[323] The introduction of an electron blocker layer between ITO and $Sn^{II}Pc$ reduces the dark current, resulting in a doubling of the V_{OC}.

An interesting correlation has been recently found between the performance of C_{60}-based organic photovoltaic cells and the molecular structure and the degree of intermolecular interaction of several Pc-type (i.e., Pcs, Pors, tetrabenzoporphyrazines, and tetranaphthoporphyrazines) donor materials.[324] Generally speaking, materials that show weak intermolecular interactions in thin films often result in low dark currents, but also in poor carrier and exciton transport. Fortunately, this correlation between low dark current and low J_{SC} and FF is not universally observed.

As the carrier mobility of $Cu^{II}Pc$ is lower than that of C_{60}, $Cu^{II}Pc/C_{60}$ devices suffer from an imbalance between hole and electron mobilities, which can seriously affect the global carrier collection efficiency. Doping $Cu^{II}Pc$ with pentacene has been used as a means to improve the hole mobility, and therefore the performance, of stacked $Cu^{II}Pc/C_{60}$ heterojunction cells. Pentacene is one of the few organic semiconductors with charge-carrier mobility in a thin film comparable to that of amorphous silicon. An optimized ITO/pentacene (4%):$Cu^{II}Pc/C_{60}$/BCP/Al solar cell has shown a conversion efficiency of 3.06%, which means a significant improvement with respect to the standard $Cu^{II}Pc/C_{60}$ cell (Table 3).[325] The power conversion efficiency of $Cu^{II}Pc/C_{60}$ heterojunction cells can also be enhanced by n-doping the electron acceptor layer with decamethylcobaltocene.[326] A three-layer heterojunction pentacene/$Zn^{II}Pc/C_{60}$ device has also been constructed,[327] where the $Zn^{II}Pc/C_{60}$ flat heterojunction acts as the photoactive interface for exciton separation. Additionally, excitons from the pentacene layer diffuse to the $ZnPc/C_{60}$ interface and are dissociated into free charge carriers. Efficiencies up to 2.1% were achieved with this architecture (Table 3).

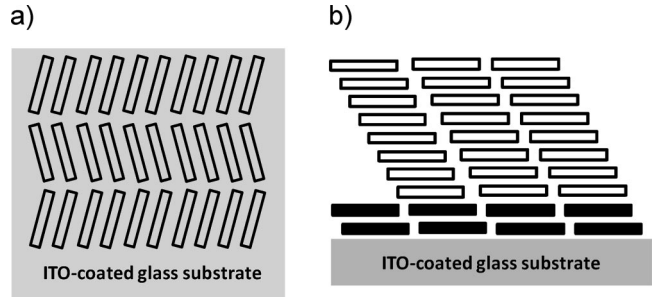

Figure 32. Arrangement of Pcs in (a) an evaporated film over ITO substrate (top view) and (b) an evaporated film over ITO substrate pretreated with 3,4,9,10-perylenetetracarboxylic acid (side view).

The principal reason for the low charge mobility of thin films of evaporated $Cu^{II}Pc$ is the anisotropy of the α-polymorph formed when films are grown on noninteracting substrates. This polymorph is composed of 1-D stacks of Pc molecules, which are aligned with their molecular planes parallel to each other, but with the stacking axis parallel to the substrate surface (Figure 32a). The peak charge mobility in such Pc films occurs along the stacking axis, due to the strong π-coupling between neighboring molecules, which in the case of evaporated solar cells is perpendicular to the optimal direction of charge transport. Hence, mobility in the evaporated $Cu^{II}Pc$ devices takes place by hopping of charges between neighboring stacks, and as a result, the mobility values are low. To achieve 1-D Pc columns with the stacking direction lying parallel to the surface normal, Sullivan and co-workers have deposited 3,4,9,10-perylenetetracarboxylic acid (PTCDA) on the ITO surface before the vacuum deposition of $Cu^{II}Pc$,[328] since it is known that PTCDA molecules behave as structural templates of Pcs. As PCTDA molecules are deposited with their molecular planes parallel to the ITO surface, it is expected that Pcs stack following the underlying structure.[329] Powder X-ray diffraction and electronic absorption experiments on $Cu^{II}Pc$ layers grown on top of PTCDA interlayers on ITO substrates confirmed the columnar stacking of Pc molecules in a nearly perpendicular arrangement with regard to the normal of the surface (Figure 32b). The photovoltaic experiments over the ITO/PTCDA/$Cu^{II}Pc/C_{60}$ device showed an improvement of charge collection owing to the alignment of the $Cu^{II}Pc$ columns with the optimal direction of charge transport, even though the selected PTCDA is clearly not the ideal surface modification in terms of energy level alignment for hole injection. Other templating layers with more appropriate energy levels must be utilized to obtain significant improvements in the device performances.

An interesting replacement of the donor $Cu^{II}Pc$ layer was carried out by Forrest and co-workers, who used SubPc as the donor material.[330] They reported a double-heterostructure SubPc/C_{60} device, which showed an increased V_{OC} with regard to the $Cu^{II}Pc$-based counterpart. The increase in V_{OC} (Table 3) was approximately of the same magnitude as the change in the gap between the LUMO level of C_{60} and the

HOMO level of the corresponding donor, namely, SubPc or $Cu^{II}Pc$, thus confirming that V_{OC} is indeed a function of this band gap. A subsequent study developed by Gommans et al. established SubPc as an extraordinarily efficient donor material when compared to the metallo-Pcs more commonly used in photovoltaic cells.[331] The devices containing SubPc as the donor material showed a maximum power conversion efficiency of 3.03% for an optimized structure of ITO/SubPc/C_{60}/BCP/Al (Table 3). The usefulness of solution-deposited subnaphthalocyanine (SubNc) films as donor layers in planar heterojunction devices has also been evaluated.[332] The use of solution-processed small molecules is promising in the search for low-cost efficient organic photovoltaic devices. A device with an ITO/PEDOT:PSS/spin-coated SubNc/C_{60}/BCP/Ag arrangement has been constructed, showing a much higher current density (5.6 mA cm^{-2}) than the previously reported evaporated SubPc/C_{60} cell (3.36 mA cm^{-2}),[330] as a consequence of the extended conjugation and absorption of the SubNc. The optimized device showed a power conversion efficiency of 1.5%, which represents one of the highest efficiencies to date for planar heterojunction organic solar cells based on solution-processed small molecules. Planar bilayer heterojunctions with C_{60} on top of SubNc have been also prepared, leading to a power conversion efficiency of 2.5%.[333]

Other investigations are devoted to tune the energy levels of the fullerene-type acceptor to optimize charge collection in $Cu^{II}Pc$-based organic solar cells. The device with an ITO/PEDOT:PPS/$Cu^{II}Pc$/spin-coated PCBM/BCP/Al architecture showed improved conversion efficiency (1.18%) under AM 1.5G solar illumination (Table 3) compared to the classical C_{60} counterpart (0.77%).[334] This result was justified in terms of improved interface properties, optimal energy level matching, and more balanced charge transport. The results also show that the upper limit of V_{OC} is mainly determined by the difference between the LUMO of PCBM and the HOMO of $Cu^{II}Pc$.

$Cu^{II}Pc$ has also been utilized as the electron transport layer in ITO/$Cu^{II}Pc$/C_{60}/$Cu^{II}Pc$ devices by Huang and co-workers,[335] playing the role of efficient electron collection from the acceptor layer to the cathode. The experiments indicated that $Cu^{II}Pc$ was superior as the buffer layer compared to the classical BCP in terms of device stability and other performance indicators. The findings suggest that $Cu^{II}Pc$ could be a promising candidate as the electron transporting material in $Cu^{II}Pc$/C_{60}-based photovoltaic cells.

Bilayer organic solar cells have been prepared using $Zn^{II}Pc$ and a novel, highly soluble pyrrolidinofullerene derivative bearing three chelating pyridyl groups (**112**) (Figure 33).[336] Previous solution studies demonstrated the formation of supramolecular complexes between the two compounds by axial coordination of the pyridine moieties to the central zinc atom of the Pc core. Spin-coating a film of **112** on a vacuum-evaporated layer of $Zn^{II}Pc$ resulted in a solar cell showing better performance than the cell obtained by spin-coating PCBM over the $Zn^{II}Pc$ evaporated layer. This result was rationalized by formation of a supramolecular complex between **112** and $Zn^{II}Pc$ at the bilayer interface, which enhances the CT between components and, indeed, increases the photovoltaic performance of the device. This concept has also been applied to a multicomponent organic solar cell architecture. To achieve efficient photocurrent generation in the full range from 350 to 820 nm, a polymer BHJ cell based on poly((2-methoxy-5-((3,7-dimethyloctyl)oxy)-*p*-phenylene)vinylene) (MDMO-PPV) and PCBM and a bilayer $Zn^{II}Pc$/**112** cell have been merged (Table 3).[337] Thus, a blend of fullerene derivatives, namely, PCBM and **112**, mixed in different ratios with MDMO-PPV has been spin-coated on the $Zn^{II}Pc$ film sublimed on an ITO substrate. Evaporation of the top aluminum electrode yields photovoltaic devices that demonstrate power conversion efficiencies of up to 2% and efficient photocurrent generation.

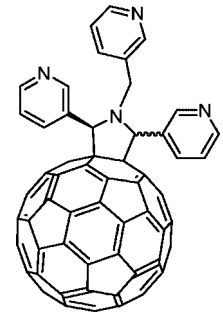

112

Figure 33. Molecular structure of pyrrolidinofullerene derivative **112**.

7.3. Covalent Phthalocyanine−Fullerene Systems as Components of Photoactive Layers

The covalent linkage between the donor and acceptor components can be used as a tool to optimize the CS process in the photoactive layer. Moreover, in a dyad system where the donor and acceptor parts are covalently linked, problems with phase separation are, indeed, avoided. Nevertheless, for the effective use of such covalent systems in photovoltaic applications, a long charge-separated-state lifetime is necessary in the solid state to avoid recombination and increase the chances of positive and negative charges reaching the electrodes. PET from the donor to the acceptor component can easily take place in covalent Pc−C_{60} dyads, as demonstrated by solution experiments. Particularly, dyad **8a** exhibits a long-lived charge-separated state in polar solvents.[85,86] To evaluate the potential of covalent Pc−C_{60} systems as photoactive components in organic solar cells, Loi et al. have prepared spin-coated films of dyad **8a** and performed a photophysical characterization of the material in the solid state.[249,255] The found lifetime of about 0.2 ms is several orders of magnitude longer than that reported for the dyad in solution, which is a clear indication of the stabilization of the charge transfer state in the solid. Solar cells using thin films of Pc−C_{60} **8a** as the active material were fabricated by spin-coating from a toluene solution onto a PEDOT:PSS-modified ITO electrode. The device showed a V_{OC} of 0.32 V and a short circuit photocurrent of 0.2 mA cm^{-2}, this resulting in low power conversion efficiency (i.e., 0.02%) under simulated solar illumination of 80 mW cm^{-2}.[249,255] A Pc with two covalently attached C_{60} spheres (i.e., **45**) has also been evaluated as a candidate for the construction of photovoltaic devices.[104] The solution-processed device showed an open circuit voltage of 320 mV and a short circuit photocurrent of 0.3 mA cm^{-2} under white-light illumination at 100 mW cm^{-2}.

As mentioned at the beginning of this section, the combination of poly(*p*-phenylenvinylene)- and polythiophene-type polymers (for example, MDMO-PPV and P3HT) with PCBM has been particularly successful for the development of highly efficient organic solar cells.[261] The utilization of

these polymer materials in solution-processed BHJ solar cells has led to power conversion efficiencies beyond 5%.[338] However, in recent years, some research groups have proposed new polymer structures as alternatives to P3HT and MDMO-PPV, since the performances of these two polymers are somehow limited by their relatively large band gap. To overcome this problem, the incorporation of smaller band gap semiconducting polymeric materials and/or organic molecules absorbing in the near-IR region has become an important task.[339] The addition of dyes such as Pcs with a good match to the maximal photon flux (i.e., between 600 and 800 nm) to polymer:PCBM blends has been envisioned as a promising strategy to achive high conversion efficiencies.[340,341] In fact, photocurrent enhancement and an increase of the V_{OC} have been found to be induced by metal-free Pc sensitization of poly[2-methoxy-5-(2′-(ethylhexyl)oxy)-1,4-phenylenevinylene] (MEH-PPV):C_{60} blends. In addition, enhancement of the light-harvesting efficiency in a P3HT/PCBM bulk heterojunction solar cell has been demonstrated by the introduction of $Si^{IV}Pc$, which increased the short circuit current density and hence improved the overall power conversion efficiency by 20% compared to those of the P3HT:PCBM control device.[342] Following the same motivation, Negebauer et al. have prepared devices composed of a solution-processed blend of MDMO-PPV and dyad **8a**,[250] where the $Zn^{II}Pc$ component can improve the light absorption of the device and also contribute to the CS process. In this case, an energy transfer process was found to take place from MDMO-PPV to the $Zn^{II}Pc$ component of the dyad. Thus, in addition to the absorptions around 400 and 700 nm from $Zn^{II}Pc-C_{60}$ dyad **8a**, the absorption of MDMO-PPV around 500 nm is expected to contribute also to the photocurrent. The V_{OC} of the solution-processed device was 0.5 V, which is significantly larger compared with the 0.32 V value obtained with pure $Pc-C_{60}$ devices.[249,255] However, the short circuit current in the mixture is lower, thereby indicating charge transport problems within the device. Better results have been obtained using a multilayered organic solar cell architecture, by spin-coating a H_2Pc-C_{60} dyad between a donor layer of P3HT and an acceptor C_{60} layer. The device exhibited 1.5 times higher efficiency than the reference lacking the intermediate dyad layer.[343]

One of the main problems of polymer-containing solution-processed BHJ active layers is the phase separation between the conjugated polymer and the acceptor component, usually a fullerene derivative. Both species tend to undergo uncontrolled macrophase separation, which influences negatively the PET and the charge transport in the blend and, thus, reduces the efficiency of the devices. In this regard, the "double-cable" approach,[344] where fullerenes are grafted onto the conjugated polymer backbone, has emerged as a plausible solution to solve this problem. In addition, the use of intrinsically bipolar materials, in which both small-molecule donor and acceptor photoactive units are covalently linked within the same macromolecular structure, is also beneficial, because it allows control of the morphology within the photoactive layer and thus the gain of an intimate contact between the donor and the acceptor counterparts. However, the double-cable approach has not been as successful as expected, since the enforced proximity of the donor and acceptor components leads to a rapid recombination of the carriers.

In this regard, Pc- and C_{60}-containing copoly(norbornenes) **61**[113] were explored as active components of solution-processed solar cells. The spatial proximity of the donor and the acceptor moieties within the polymer induces photoinduced electronic communication between the Pc and C_{60} fullerene in solution. However, solution-processed devices using copolymer **61a** as the active layer give rise to low power conversion efficiencies (ca. 0.07%) under simulated solar illumination.

8. Conclusions and Outlook

During the past few decades, significant efforts have been directed toward the preparation of synthetic model compounds that mimic the multifacet functions of the natural photosynthetic systems, ranging from light harvesting to CT. In this context, the tunable absorption features of Pcs and related compounds such as SubPcs render them ideal antenna systems that harvest light over a broad range of the solar spectrum. At the same time, they exhibit an excellent electron-donating character, which makes them perfect candidates for their incorporation into D−A architectures. In this context, carbon nanostructures such as fullerenes and CNTs offer a myriad of incentives for their incorporation into D−A systems due to their extraordinary electron acceptor features.

In this connection, molecular materials based on the combination of Pcs and SubPcs with carbon nanostructures are currently under active investigation, as they lead to innovative materials and composites with unique optoelectronic properties that originate at the molecular level. Particularly, photoinduced unidirectional electron transfer processes occur in such Pc−carbon nanostructure systems as widely demonstrated by photophysical investigations.

One of the most outstanding applications of these materials is their incorporation in photovoltaic devices in which generation of electrical current from solar energy takes place. To accomplish this function, specific requirements must be met: collection of light energy, separation of charges, an appropriate active layer morphology that ensures charge migration, stability, etc.

Some opportunities can already be envisioned in this regard. The preparation, for example, of stable near-IR-absorbing Pcs could improve the light-harvesting capabilities, whereas the use of novel carbon-based materials such as higher fullerenes, endohedral metallofullerenes, or new allotropes of CNTs with improved electron-accepting features allows the gain of some control over the separation of charges within the material.

Insight into the supramolecular self-assembly of donors and acceptors, at surfaces or interfaces, by means of AFM and scanning tunneling microscopy is a real asset, since it provides valuable guidelines about the organization of these systems and the morphology of the material in films. This information is of paramount importance for the optimization of devices in terms of improved charge mobility.

Notable is the progress in the field of electron transfer in covalent and noncovalent Pc/carbon nanostructure conjugates and hybrids. However, much more remains to be done, especially when considering the application of these systems in molecular photovoltaics. The challenges and opportunities that rest on these targets should attract the efforts of many researchers in this fast-emerging and important area.

9. Abbreviations

AFM	atomic force microscopy
AQ	anthraquinone

BCP	bathocuproine
BHJ	bulk heterojuction
Bodipy	boron dipyrromethene
CR	charge recombination
CS	charge separation
CT	charge transfer
1-D	one-dimensional
D−A	donor−acceptor
DBU	1,8-diazabicyclo[5.4.0]undec-7-ene
o-DCB	*o*-dichlorobenzene
DMF	dimethylformamide
Fc	ferrocene
HOMO	highest occupied molecular orbital
IR	infrared
ITO	indium tin oxide
LUMO	lowest unoccupied molecular orbital
MDMO-PPV	poly((2-methoxy-5-((3,7-dimethyloctyl)oxy)-*p*-phenylene)vinylene)
MeO-TPD	tetrakis(4-methoxyphenyl)benzidine
MPCI	*N*,*N*′-dimethyl-3,4:9,10-perylenebis(dicarboximide)
MPP	perylene-3,4,9,10-tetracarboxyl-*N*,*N*′-9-dimethyldiimide
m-MTDATA	4,4′,4″-tris(((3-methylphenyl)phenyl)amino)-triphenylamine
MWCNT	multiwalled carbon nanotube
Nc	naphthalocyanine
Pc	phthalocyanine
PCBM	1-(3-carboxypropyl)-1-phenyl-[6,6]-C_{61}
PDI	perylenediimide
PEDOT:PSS	poly(3,4-(ethylenedioxy)thiophene):poly-(styrenesulfonate)
PET	photoinduced electron transfer
P3HT	poly(3-hexylthiophene)
Por	porphyrin
PTCBI	3,4,9,10-perylenetetracarboxylic bisbenzimidazole
PTCDA	3,4,9,10-perylenetetracarboxylic acid
rt	room temperature
SubNc	subnaphthalocyanine
SubPc	subphthalocyanine
SWCNT	single-walled carbon nanotube
TEM	transmission electron microscopy
THF	tetrahydrofuran
TPA	triphenylamine
V_{OC}	open circuit voltage

10. Acknowledgments

Funding via grants from MEC and MICINN (CTQ2008-00418/BQU, CONSOLIDER-INGENIO 2010 CDS2007-00010 Nanociencia Molecular, FOTOMOL, PSE-120000-2008-3), ESF-MEC (MAT2006-28180-E, SOHYDS), EU (Solar-N-type, MRTN-CT-2006-035533, ROBUST DSC, FP7-Energy-2007-1-RTD, No. 212792), COST Action D35, and CAM (MADRISOLAR, S-0505/PPQ/000225) is gratefully acknowledged (T.T.). The Deutsche Forschungsgemeinschaft (Grant SFB 583), Cluster of Excellence "Engineering of Advanced Materials", FCI, and Office of Basic Energy Sciences of the U.S. Department of Energy are gratefully acknowledged (D.M.G.). G.B. thanks the Spanish MEC for a "Ramón y Cajal" contract. We also thank the Universidad Autónoma de Madrid for providing excellent research conditions and infrastructure. We also thank all students, co-workers, and senior researchers who perform exciting research in our groups and contribute to the progress in the field of molecular materials based on phthalocyanines.

11. Note Added after ASAP Publication

Errors were found in the author affiliations, the caption for Figure 14, and Figure 7 in the version that posted on April 5, 2010. The errors were corrected in the version that posted on April 12, 2010.

12. References

(1) Wasielewski, M. R. *Chem. Rev.* **1992**, *92*, 435.
(2) Gust, D.; Moore, T. A.; Moore, A. L. *Acc. Chem. Res.* **1993**, *26*, 198.
(3) *The Photosynthetic Reaction Center*; Deisenhoifer, J., Norris, J. R., Eds.; Academic Press: New York, 1993.
(4) Gust, D.; Moore, T. A. In *The Porphyrin Handbook*; Kadish, K. M., Smith, K. M., Guilard, G., Eds.; Academic Press: New York, 2000; Vol. 8, p 153.
(5) Gust, D.; Moore, T. A.; Moore, A. L. *Acc. Chem. Res.* **2001**, *34*, 40.
(6) *Molecular Mechanisms of Photosynthesis*; Blankenship, R. E., Ed.; Blackwell: Malden, MA, 2002.
(7) Balzani, V.; Credi, A.; Venturi, M. *ChemSusChem* **2008**, *1*, 26.
(8) Benniston, A. C.; Harriman, A. *Mater. Today* **2008**, *11*, 26.
(9) *Acc. Chem. Res.* **2009**, *42*, 1859 (special issue).
(10) *Photoinduced Electron Transfer*; Fox, M. A., Chanon, M., Eds.; Elsevier: Amsterdam, 1988.
(11) Gust, D. *Nature* **1997**, *386*, 21.
(12) *Electron Transfer in Chemistry*; Balzani, V., Ed.; Wiley-VCH: Weinheim, Germany, 2001; Vols. *1*−*4*.
(13) Li, F.; Yang, S. I.; Ciringh, Y.; Seth, J.; Martín, C. H.; Singh, D. L.; Kim, D.; Birge, R. R.; Bocian, D. F.; Holten, D.; Lindsey, J. S. *J. Am. Chem. Soc.* **1998**, *120*, 10001.
(14) D'Souza, F.; Deviprasad, G. R.; Zandler, M. E.; El-Khouly, M. E.; Fujitsuka, M.; Ito, O. *J. Phys. Chem. B* **2002**, *106*, 4952.
(15) Fukuzumi, S.; Ohkubo, K.; Wenbo, O.; Ou, Z.; Shao, J.; Kadish, K. M.; Jutchison, J. A.; Ghiggino, K. P.; Sintic, P. J.; Crossley, M. J. *J. Am. Chem. Soc.* **2003**, *125*, 14984.
(16) Sutton, L. R.; Scheloske, M.; Pirner, K. S.; Hirsch, A.; Guldi, D. M.; Gisselbrecht, J. P. *J. Am. Chem. Soc.* **2004**, *126*, 10370.
(17) Choi, M.-S.; Yamazaki, T.; Yamazaki, I.; Aida, T. *Angew. Chem., Int. Ed.* **2004**, *43*, 150.
(18) Guldi, D. M.; Giacalone, F.; de la Torre, G.; Segura, J. L.; Martin, N. *Chem.—Eur. J.* **2005**, *11*, 7199.
(19) de la Torre, G.; Giacalone, F.; Segura, J. L.; Martin, N.; Guldi, D. M. *Chem.—Eur. J.* **2005**, *11*, 1267.
(20) Guldi, D. M.; Rahman, G. M. A.; Sgobba, V.; Ehli, C. *Chem. Soc. Rev.* **2006**, *35*, 471, and references therein.
(21) *Phthalocyanines. Properties and Applications*; Leznoff, C. C., Lever, A. B. P., Eds.; VCH Publishers (LSK) Ltd.: Cambridge, U.K., 1989, 1993, 1996; Vols. *1*−*4*.
(22) *Phthalocyanine Materials: Structure, Synthesis and Function*; McKeown, N. B., Ed.; Cambridge University Press: Cambridge, U.K., 1998.
(23) de la Torre, G.; Vazquez, P.; Agullo-Lopez, F.; Torres, T. *J. Mater. Chem.* **1998**, *8*, 1671.
(24) Hanack, M.; Heckmann, H.; Polley R. In *Methods of Organic Chemistry (Houben-Weyl)*; Schaumann, E., Ed.; Georg Thieme Verlag: Stuttgart, Germany, 1998; Vol. E 9d, p 717.
(25) Kobayashi, N. *Curr. Opin. Solid State Mater. Sci.* **1999**, *4*, 345.
(26) de la Torre, G., Nicolau, M., Torres, T. In *Supramolecular Photosensitive and Electroactive Materials*; Nalwa, H. S., Ed.; Academic Press: New York, 2001; p 1.
(27) Kobayashi, N. *Coord. Chem. Rev.* **2002**, *227*, 129.
(28) *The Porphyrin Handbook*; Kadish, K. M., Smith, K. M., Guilard, R., Eds.; Academic Press: San Diego, 2003; Vols. *15*−*20*.
(29) de la Torre, G.; Vazquez, P.; Agullo-Lopez, F.; Torres, T. *Chem. Rev.* **2004**, *104*, 3723.
(30) de la Torre, G.; Claessens, C. G.; Torres, T. *Chem. Commun.* **2007**, 2000.
(31) Claessens, C. G.; Hahn, U.; Torres, T. *Chem. Rec.* **2008**, *8*, 75.
(32) Rio, Y.; Rodriguez-Morgade, M. S.; Torres, T. *Org. Biomol. Chem.* **2008**, *6*, 1877.
(33) Bottari, G.; Diaz, D. D.; Torres, T. *J. Porphyrins Phthalocyanines* **2006**, *10*, 1083.
(34) Martinez-Diaz, M. V.; Quintiliani, M.; Torres, T. *Synlett* **2008**, 1.
(35) de la Torre, G.; Bottari, G.; Hahn, U.; Torres, T. *Struct. Bonding* **2010**, *135*, 1.
(36) de la Torre, G.; Claessens, C. G.; Torres, T. *Eur. J. Org. Chem.* **2000**, 2821.
(37) de la Torre, G.; Torres, T. *J. Porphyrins Phthalocyanines* **2002**, *6*, 274.
(38) El-Khouly, M. E.; Ito, O.; Smith, P. M.; D'Souza, F. *J. Photochem. Photobiol., C* **2004**, *5*, 79.
(39) D'Souza, F.; Ito, O. *Coord. Chem. Rev.* **2005**, *249*, 1410.

(40) Gonzalez-Rodriguez, D.; Bottari, G. *J. Porphyrins Phthalocyanines* **2009**, *13*, 624.
(41) D'Souza, F.; Ito, O. *Chem. Commun.* **2009**, 4913.
(42) Claessens, C. G.; Gonzalez-Rodriguez, D.; Torres, T. *Chem. Rev.* **2002**, *102*, 835.
(43) Torres, T. *Angew. Chem., Int. Ed.* **2006**, *45*, 2834.
(44) Geyer, M.; Plenzig, F.; Rauschnabel, J; Hanack, M.; del Rey, B.; Sastre, A.; Torres, T. *Synthesis* **1996**, 1139.
(45) Imahori, H.; Sakata, Y. *Adv. Mater.* **1997**, *9*, 537.
(46) Martin, N.; Sanchez, L.; Illescas, B.; Perez, I. *Chem. Rev.* **1998**, *98*, 2527.
(47) Echegoyen, L.; Echegoyen, L. E. *Acc. Chem. Res.* **1998**, *31*, 593.
(48) Diederich, F.; Gomez-Lopez, M. *Chem. Soc. Rev.* **1999**, *28*, 263.
(49) Guldi, D. M. *Chem. Commun.* **2000**, 321.
(50) Guldi, D. M.; Prato, M. *Acc. Chem. Res.* **2000**, *33*, 695.
(51) Fukuzumi, S.; Guldi, D. M. In *Electron Transfer in Chemistry*; Balzani, V., Ed.; Wiley-VCH: New York, 2001; Vol. 2, p 270.
(52) *Fullerenes: From Synthesis to Optoelectronic Properties*; Guldi, D. M., Martin, N., Eds.; Kluwer Academic Publishers: Dodrecht, The Netherlands, 2002.
(53) Guldi, D. M. *Chem. Soc. Rev.* **2002**, *31*, 22.
(54) Giacalone, F.; Martin, N. *Chem. Rev.* **2006**, *106*, 5136.
(55) *Fullerenes: Principles and Applications*; Langa, F., Nierengarten, J.-F.; Eds.; Nanoscience and Nanotechnology Series; The Royal Society of Chemistry: Cambridge, U.K., 2007.
(56) Delgado, J. L.; Herranz, M. A.; Martin, N. *J. Mater. Chem.* **2008**, *18*, 1417.
(57) Guldi, D. M.; Illescas, B. M.; Atienza, C. M.; Wielopolski, M.; Martin, N. *Chem. Soc. Rev.* **2009**, *38*, 1587.
(58) *Carbon Nanotubes and Related Structures: New Materials for the Twenty-First Century*; Harris, P., Ed.; Cambridge University Press: Cambridge, U.K., 2001.
(59) Dresselhaus, M. S., Dresselhaus, G., Avouris, P. *Carbon Nanotubes: Synthesis, Structure, Properties and Applications*; Springer-Verlag: Berlin, 2001.
(60) Reich, S., Thomsen, C., Maultzsh, J. *Carbon Nanotubes: Basic Concepts and Physical Properties*; VCH: Weinheim, Germany, 2004.
(61) Tasis, D.; Tagmatarchis, N.; Bianco, A.; Prato, M. *Chem. Rev.* **2006**, *106*, 1105.
(62) Kostarelos, K.; Lacerda, L.; Pastorin, G.; Wu, W.; Wieckowski, S.; Luangsivilay, J.; Godefroy, S.; Pantarotto, D.; Briand, J.-P.; Muller, S.; Prato, M.; Bianco, A. *Nat. Nanotechnol.* **2007**, *2*, 108.
(63) Sgobba, V.; Guldi, D. M. *J. Mater. Chem.* **2008**, *18*, 153.
(64) Prato, M.; Kostarelos, K.; Bianco, A. *Acc. Chem. Res.* **2008**, *41*, 60.
(65) Sgobba, V.; Guldi, D. M. *Chem. Soc. Rev.* **2009**, *38*, 165.
(66) Araki, Y.; Ito, O. *J. Photochem. Photobiol., C* **2008**, *9*, 93.
(67) Palomares, E.; Martinez-Diaz, M. V.; Haque, S. A.; Torres, T.; Durrant, J. R. *Chem. Commun.* **2004**, 2112.
(68) Reddy, P. Y.; Giribabu, L.; Lyness, C.; Snaith, H. J.; Vijaykumar, C.; Chandrasekharam, M.; Lakshmikantam, M.; Yum, J.-H.; Kalyanasundaram, K.; Grätzel, M.; Nazeeruddin, M. K. *Angew. Chem., Int. Ed.* **2007**, *46*, 373.
(69) Cid, J.-J.; Yum, J.-H.; Jang, S.-R.; Nazeeruddin, M. K.; Martinez-Ferrero, E.; Palomares, E.; Ko, J.; Grätzel, M.; Torres, T. *Angew. Chem., Int. Ed.* **2007**, *46*, 8358.
(70) Morandeira, A.; Lopez-Duarte, I.; Martinez-Diaz, M. V.; O'Regan, B.; Shuttle, C.; Haji-Zainulabidin, N. A.; Torres, T.; Palomares, E.; Durrant, J. R. *J. Am. Chem. Soc.* **2007**, *129*, 9250.
(71) Imahori, H.; Umeyama, T.; Ito, S. *Acc. Chem. Res.* **2009**, *42*, 1809.
(72) *Organic Photovoltaics: Concepts and Realization*; Brabec, C., Dyakonov, V., Parisi, J., Sariciftci, N. S., Eds.; Springer-Verlag: Berlin, 2003.
(73) Imahori, H.; Fukuzumi, S. *Adv. Funct. Mater.* **2004**, *14*, 525.
(74) Segura, J. L.; Martin, N.; Guldi, D. M. *Chem. Soc. Rev.* **2005**, *34*, 31.
(75) *Organic Photovoltaics: Mechanisms, Materials, and Devices*; Sun, S.-S., Sariciftci, N. S., Eds.; CRC Press: Boca Raton, FL, 2005.
(76) Guenes, S.; Neugebauer, H.; Sariciftci, N. S. *Chem. Rev.* **2007**, *107*, 1324.
(77) Thompson, B. C.; Frechet, J. M. J. *Angew. Chem., Int. Ed.* **2008**, *47*, 58.
(78) *Organic Photovoltaics: Materials, Device Physics, and Manufacturing Technologies*; Brabec, C., Ed.; Wiley-VCH: Weinheim, Germany, 2008.
(79) *Acc. Chem. Res.* **2009**, *42*, 1689 (special issue).
(80) Linssen, T. G.; Duerr, K.; Hanack, M.; Hirsch, A. *J. Chem. Soc., Chem. Commun.* **1995**, 103.
(81) Durr, K.; Fiedler, S.; Linssen, T.; Hirsch, A.; Hanack, M. *Chem. Ber.* **1997**, *130*, 1375.
(82) Huang, W.; Wang, S.; Liang, R.; Gong, Q.; Qiu, W.; Liu, Y.; Zhu, D. *Chem. Phys. Lett.* **2000**, *324*, 354.
(83) Zhu, P.; Wang, P.; Qiu, W.; Liu, Y.; Ye, C.; Fang, G.; Song, Y. *Appl. Phys. Lett.* **2001**, *78*, 1319.
(84) Tian, Z.; He, C.; Liu, C.; Yang, W.; Yao, J.; Nie, Y.; Gong, Q.; Liu, Y. *Mater. Chem. Phys.* **2005**, *94*, 444.
(85) Gouloumis, A.; Liu, S. G.; Sastre, A.; Vazquez, P.; Echegoyen, L.; Torres, T. *Chem.−Eur. J.* **2000**, *6*, 3600.
(86) Guldi, D. M.; Zilbermann, I.; Gouloumis, A.; Vazquez, P.; Torres, T. *J. Phys. Chem. B* **2004**, *108*, 18485.
(87) Guldi, D. M.; Gouloumis, A.; Vazquez, P.; Torres, T. *Chem. Commun.* **2002**, 2056.
(88) Guldi, D. M.; Gouloumis, A.; Vazquez, P.; Torres, T.; Georgakilas, V.; Prato, M. *J. Am. Chem. Soc.* **2005**, *127*, 5811.
(89) Guldi, D. M.; Rahman, G. M. A.; Zerbetto, F.; Prato, M. *Acc. Chem. Res.* **2005**, *38*, 871.
(90) Quintiliani, M.; Kahnt, A.; Wolfle, T.; Hieringer, W.; Vazquez, P.; Gorling, A.; Guldi, D. M.; Torres, T. *Chem.−Eur. J.* **2008**, *14*, 3765.
(91) Bottari, G.; Olea, D.; Gomez-Navarro, C.; Zamora, F.; Gomez-Herrero, J.; Torres, T. *Angew. Chem., Int. Ed.* **2008**, *47*, 2026.
(92) Kahnt, A.; Guldi, D. M.; de la Escosura, A.; Martinez-Diaz, M. V.; Torres, T. *J. Mater. Chem.* **2008**, *18*, 77.
(93) Sukeguchi, D.; Yoshiyama, H.; Shibata, N.; Nakamura, S.; Toru, T.; Hayashi, Y.; Soga, T. *J. Fluorine Chem.* **2009**, *130*, 361.
(94) Ballesteros, B.; de la Torre, G.; Shearer, A.; Hausmann, A.; Herranz, M. Á.; Guldi, D. M.; Torres, T. *Chem.−Eur. J.* **2010**, *16*, 114.
(95) Ballesteros, B.; Campidelli, S.; de la Torre, G.; Ehli, C.; Guldi, D. M.; Prato, M.; Torres, T. *Chem. Commun.* **2007**, 2950.
(96) de la Escosura, A.; Martinez-Diaz, M. V.; Guldi, D. M.; Torres, T. *J. Am. Chem. Soc.* **2006**, *128*, 4112.
(97) Geerts, Y. H.; Debever, O.; Amato, C.; Sergeyev, S. *Beilstein J. Org. Chem.* [Online] **2009**, *5*, Article 49, http://www.beilstein-journals.org/bjoc/single/articleFullText.htm?publicId=1860-5397-5-49.
(98) de la Escosura, A.; Martinez-Diaz, M. V.; Barbera, J.; Torres, T. *J. Org. Chem.* **2008**, *73*, 1475.
(99) Sastre, A.; Gouloumis, A.; Vazquez, P.; Torres, T.; Doan, V.; Schwartz, B. J.; Wudl, F.; Echegoyen, L.; Rivera, J. *Org. Lett.* **1999**, *1*, 1807.
(100) Bingel, C. *Chem. Ber.* **1993**, *126*, 1957.
(101) Isosomppi, M.; Tkachenko, N. V.; Efimov, A.; Vahasalo, H.; Jukola, J.; Vainiotalo, P.; Lemmetyinen, H. *Chem. Phys. Lett.* **2006**, *430*, 36.
(102) Lehtivuori, H.; Kumpulainen, T.; Efimov, A.; Lemmetyinen, H.; Kira, A.; Imahori, H.; Tkachenko, N. V. *J. Phys. Chem. C* **2008**, *112*, 9896.
(103) Lehtivuori, H.; Kumpulainen, T.; Hietala, M.; Efimov, A.; Lemmetyinen, H.; Kira, A.; Imahori, H.; Tkachenko, N. V. *J. Phys. Chem. B* **2009**, *113*, 1984.
(104) Gouloumis, A.; de la Escosura, A.; Vazquez, P.; Torres, T.; Kahnt, A.; Guldi, D. M.; Neugebauer, H.; Winder, C.; Drees, M.; Sariciftci, N. S. *Org. Lett.* **2006**, *8*, 5187.
(105) Quintiliani, M.; Kahnt, A.; Vazquez, P.; Guldi, D. M.; Torres, T. *J. Mater. Chem.* **2008**, *18*, 1542.
(106) Kahnt, A.; Quintiliani, M.; Vazquez, P.; Guldi, D. M.; Torres, T. *ChemSusChem* **2008**, *1*, 97.
(107) Quintiliani, M.; Garcia-Frutos, E. M.; Vazquez, P.; Torres, T. *J. Inorg. Biochem.* **2008**, *102*, 388.
(108) Kim, K. N.; Choi, C. S.; Kay, K.-Y. *Tetrahedron Lett.* **2005**, *46*, 6791.
(109) El-Khouly, M. E.; Kang, E. S.; Kay, K.-Y.; Choi, C. S.; Araki, Y.; Ito, O. *Chem.−Eur. J.* **2007**, *13*, 2854.
(110) Martin-Gomis, L.; Ohkubo, K.; Fernandez-Lazaro, F.; Fukuzumi, S.; Sastre-Santos, A. *Org. Lett.* **2007**, *9*, 3441.
(111) Martin-Gomis, L.; Ohkubo, K.; Fernandez-Lazaro, F.; Fukuzumi, S.; Sastre-Santos, A. *J. Phys. Chem. C* **2008**, *112*, 17694.
(112) El-Khouly, M. E.; Kim, J. H.; Kay, K.-Y.; Choi, C. S.; Ito, O.; Fukuzumi, S. *Chem.−Eur. J.* **2009**, *15*, 5301.
(113) de la Escosura, A.; Martinez-Diaz, M. V.; Torres, T.; Grubbs, R. H.; Guldi, D. M.; Neugebauer, H.; Winder, C.; Drees, M.; Sariciftci, N. S. *Chem. Asian J.* **2006**, *1*, 148.
(114) Fukuda, T.; Masuda, S.; Kobayashi, N. *J. Am. Chem. Soc.* **2007**, *129*, 5472.
(115) Fukuda, T.; Sugita, I.; Kobayashi, N. *Chem. Commun.* **2009**, 3449.
(116) Fukuda, T.; Hashimoto, N.; Araki, Y.; El-Khouly, M. E.; Ito, O.; Kobayashi, N. *Chem. Asian J.* **2009**, *4*, 1678.
(117) Pinzon, J. R.; Cardona, C. M.; Herranz, M. A.; Plonska-Brzezinska, M. E.; Palkar, A.; Athans, A. J.; Martin, N.; Rodriguez-Fortea, A.; Poblet, J. M.; Bottari, G.; Torres, T.; Gayathri, S. S.; Guldi, D. M.; Echegoyen, L. *Chem.−Eur. J.* **2009**, *15*, 864.
(118) Stevenson, S.; Rice, G.; Glass, T.; Harlch, K.; Cromer, F.; Jordan, M. R.; Craft, J.; Hadju, E.; Bible, R.; Olmstead, M. M.; Maltra, K.; Fisher, A. J.; Balch, A. L.; Dorn, H. C. *Nature* **1999**, *401*, 55.
(119) Martinez-Diaz, M. V.; Fender, N. S.; Rodriguez-Morgade, M. S.; Gomez-Lopez, M.; Diederich, F.; Echegoyen, L.; Stoddart, J. F.; Torres, T. *J. Mater. Chem.* **2002**, *12*, 2095.
(120) Guldi, D. M.; Ramey, J.; Martinez-Diaz, M. V.; de la Escosura, A.; Torres, T.; Da Ros, T.; Prato, M. *Chem. Commun.* **2002**, 2774.

(121) Sessler, J. L.; Jayawickramarajah, J.; Gouloumis, A.; Pantos, G. D.; Torres, T.; Guldi, D. M. *Tetrahedron* **2006**, *62*, 2123.
(122) Torres, T.; Gouloumis, A.; Sanchez-Garcia, D.; Jayawickramarajah, J.; Seitz, W.; Guldi, D. M.; Sessler, J. L. *Chem. Commun.* **2007**, 292.
(123) Armaroli, N.; Diederich, F.; Echegoyen, L.; Habicher, T.; Flamigni, L.; Marconi, G.; Nierengarten, J.-F. *New J. Chem.* **1999**, 77.
(124) Da Ros, T.; Prato, M.; Guldi, D. M.; Alessio, E.; Ruzzi, M.; Pasimeni, L. *Chem. Commun.* **1999**, 635.
(125) D'Souza, F.; Rath, N. P.; Deviprasad, G. R.; Zandler, M. E. *Chem. Commun.* **2001**, 267.
(126) Hauke, F.; Swartz, A.; Guldi, D. M.; Hirsch, A. *J. Mater. Chem.* **2002**, *12*, 2088.
(127) El-Khouly, M. E.; Rogers, L. M.; Zandler, M. E.; Suresh, G.; Fujitsuka, M.; Ito, O.; D'Souza, F. *ChemPhysChem* **2003**, *4*, 474.
(128) El-Khouly, M. E.; Araki, Y.; Ito, O.; Gadde, S.; Zandler, M. E.; D'Souza, F. *J. Porphyrins Phthalocyanines* **2006**, *10*, 1156.
(129) D'Souza, F.; Maligaspe, E.; Ohkubo, K.; Zandler, M. E.; Subbaiyan, N. K.; Fukuzumi, S. *J. Am. Chem. Soc.* **2009**, *131*, 8787.
(130) Rio, Y.; Seitz, W.; Gouloumis, A.; Vázquez, P.; Sessler, J. L.; Guldi, D. M.; Torres, T. *Chem.—Eur. J.* **2010**, *16*, 1929.
(131) Chen, Y.; El-Khouly, M. E.; Sasaki, M.; Araki, Y.; Ito, O. *Org. Lett.* **2005**, *7*, 1613.
(132) Ballesteros, B.; de la Torre, G.; Torres, T.; Hug, G. L.; Rahman, G. M. A.; Guldi, D. M. *Tetrahedron* **2006**, *62*, 2097.
(133) Doyle, J. J.; Ballesteros, B.; de la Torre, G.; McGovern, D. A.; Kelly, J. M.; Torres, T.; Blau, W. J. *Chem. Phys. Lett.* **2006**, *428*, 307.
(134) Rodriguez-Morgade, M. S.; Plonska-Brzezinska, M. E.; Athans, A. J.; Carbonell, E.; de Miguel, G.; Guldi, D. M.; Echegoyen, L.; Torres, T. *J. Am. Chem. Soc.* **2009**, *131*, 10484.
(135) Stöhr, M.; Wagner, T.; Gabriel, M.; Weyers, B.; Moller, R. *Adv. Funct. Mater.* **2001**, *11*, 175.
(136) Samuely, T.; Liu, S.-X.; Haas, M.; Decurtins, S.; Jung, T. A.; Stöhr, M. *J. Phys. Chem. B* **2009**, *113*, 19373.
(137) Wei, Y.; Robey, S. W.; Reutt-Robey, J. E. *J. Am. Chem. Soc.* **2009**, *131*, 12026.
(138) Calmettes, B.; Nagarajan, S.; Gourdon, A.; Abel, M.; Porte, L.; Coratger, R. *Angew. Chem., Int. Ed.* **2008**, *47*, 6994.
(139) Calmettes, B.; Nagarajan, S.; Gourdon, A.; Benjalal, Y.; Bouju, X.; Abel, M.; Porte, L.; Coratger, R. *J. Phys. Chem. B* **2009**, *113*, 21169.
(140) Yoshimoto, S.; Honda, Y.; Ito, O.; Itaya, K. *J. Am. Chem. Soc.* **2008**, *130*, 1085.
(141) Huang, H.; Chen, W.; Chen, S.; Qi, D. C.; Gao, X. Y.; Wee, A. T. S. *Appl. Phys. Lett.* **2009**, *94*, 163304/1.
(142) Gonzalez-Rodriguez, D.; Torres, T.; Guldi, D. M.; Rivera, J.; Echegoyen, L. *Org. Lett.* **2002**, *4*, 335.
(143) Gonzalez-Rodriguez, D.; Torres, T.; Herranz, M. A.; Echegoyen, L.; Carbonell, E.; Guldi, D. M. *Chem.—Eur. J.* **2008**, *14*, 7670.
(144) Gonzalez- Rodriguez, D.; Torres, T.; Guldi, D. M.; Rivera, J.; Herranz, M. A.; Echegoyen, L. *J. Am. Chem. Soc.* **2004**, *126*, 6301.
(145) Kim, J.-H.; El-Khouly, M. E.; Araki, Y.; Ito, O.; Kay, K.-Y. *Chem. Lett.* **2008**, *37*, 544.
(146) El-Khouly, M. E.; Shim, S. H.; Araki, Y.; Ito, O.; Kay, K.-Y. *J. Phys. Chem. B* **2008**, *112*, 3910.
(147) Gonzalez-Rodriguez, D.; Carbonell, E.; Guldi, D. M.; Torres, T. *Angew. Chem., Int. Ed.* **2009**, *48*, 8032.
(148) Claessens, C. G.; Torres, T. *Angew. Chem., Int. Ed.* **2002**, *41*, 2561.
(149) Fukuda, T.; Stork, J. R.; Potucek, R. J.; Olmstead, M. M.; Noll, B. C.; Kobayashi, N.; Durfee, W. S. *Angew. Chem., Int. Ed.* **2002**, *41*, 2565.
(150) Iglesias, R. S.; Claessens, C. G.; Torres, T.; Herranz, M. A.; Ferro, V. R.; de la Vega, J. M. G. *J. Org. Chem.* **2007**, *72*, 2967.
(151) Iglesias, R. S.; Claessens, C. G.; Torres, T.; Rahman, G. M. A.; Guldi, D. M. *Chem. Commun.* **2005**, 2113.
(152) Claessens, C. G.; Torres, T. *Chem. Commun.* **2004**, 1298.
(153) Claessens, C. G.; Torres, T. *J. Am. Chem. Soc.* **2002**, *124*, 14522.
(154) Li, X.; Sinks, L. E.; Rybtchinski, B.; Wasielewski, M. R. *J. Am. Chem. Soc.* **2004**, *126*, 10810.
(155) Fukuzumi, S.; Ohkubo, K.; Ortiz, J.; Gutierrez, A. M.; Fernandez-Lazaro, F.; Sastre-Santos, A. *Chem. Commun.* **2005**, 3814.
(156) Ohkubo, K.; Fukuzumi, S. *J. Porphyrins Phthalocyanines* **2008**, *12*, 993.
(157) Jimenez, A. J.; Spänig, F.; Rodriguez-Morgade, M. S.; Ohkubo, K.; Fukuzumi, S.; Guldi, D. M.; Torres, T. *Org. Lett.* **2007**, *9*, 2481.
(158) Gouloumis, A.; Liu, S. G.; Vazquez, P.; Echegoyen, L.; Torres, T. *Chem. Commun.* **2001**, 399.
(159) Gouloumis, A.; Gonzalez-Rodriguez, D.; Vazquez, P.; Torres, T.; Liu, S. G.; Echegoyen, L.; Ramey, J.; Hug, G. L.; Guldi, D. M. *J. Am. Chem. Soc.* **2006**, *128*, 12674.
(160) Gouloumis, A.; Rahman, G. M. A.; Abel, J.; de la Torre, G.; Vazquez, P.; Echegoyen, L.; Guldi, D. M.; Torres, T. *Aust. J. Chem.* **2008**, *61*, 256.
(161) Rodriguez-Morgade, M. S.; Torres, T.; Atienza-Castellanos, C.; Guldi, D. M. *J. Am. Chem. Soc.* **2006**, *128*, 15145.
(162) Ying, G.; Yu, S.-H.; Antonietti, M.; Böttcher, C.; Faul, C. F. J. *Chem.—Eur. J.* **2005**, *11*, 1305.
(163) Gonzalez-Cabello, A.; Vazquez, P.; Torres, T. *J. Organomet. Chem.* **2001**, *637*, 751.
(164) Gonzalez, A.; Vazquez, P.; Torres, T. *Tetrahedron Lett.* **1999**, *40*, 3263.
(165) Gonzalez-Cabello, A.; Claessens, C. G.; Martin-Fuch, G.; Ledoux-Rack, I.; Vazquez, P.; Zyss, J.; Agullo-Lopez, F.; Torres, T. *Synth. Met.* **2003**, *137*, 1487.
(166) Poon, K. W.; Liu, W.; Chan, P. K.; Yang, Q.; Chan, T. W.; Mak, T. C.; Ng, D. K. *J. Org. Chem.* **2001**, *66*, 1553.
(167) Gonzalez-Cabello, A.; Vazquez, P.; Torres, T.; Guldi, D. M. *J. Org. Chem.* **2003**, *68*, 8635.
(168) Soares, A. R. M.; Martinez-Diaz, M. V.; Bruckner, A.; Pereira, A. M. V. M.; Tome, J. P. C.; Alonso, C. M. A.; Faustino, M. A. F.; Neves, M. G. P. M. S.; Tome, A. C.; Silva, A. M. S.; Cavaleiro, J. A. S.; Torres, T.; Guldi, D. M. *Org. Lett.* **2007**, *9*, 1557.
(169) Sutton, J. M.; Boyle, R. W. *Chem. Commun.* **2001**, 2014.
(170) Yang, S. I.; Li, J.; Cho, H. S.; Kim, D.; Bocian, D. F.; Holten, D.; Lindsey, J. S. *J. Mater. Chem.* **2000**, *10*, 283.
(171) Miller, M. A.; Lammi, R. K.; Prathapan, S.; Holten, D.; Lindsey, J. S. *J. Org. Chem.* **2000**, *65*, 6634.
(172) Tome, J. P. C.; Pereira, A. M. V. M.; Alonso, C. M. A.; Neves, M. G. P. M. S.; Tome, A. C.; Silva, A. M. S.; Cavaleiro, J. A. S.; Martinez-Diaz, M. V.; Torres, T.; Rahman, G. M. A.; Ramey, J.; Guldi, D. M. *Eur. J. Org. Chem.* **2006**, 257.
(173) Ali, H.; van Lier, J. E. *Tetrahedron Lett.* **2009**, *50*, 1113.
(174) Kojima, T.; Honda, T.; Ohkubo, K.; Shiro, M.; Kusukawa, T.; Fukuda, T.; Kobayashi, N.; Fukuzumi, S. *Angew. Chem., Int. Ed.* **2008**, *47*, 6712.
(175) Li, J.; Diers, J. R.; Seth, J.; Yang, S. I.; Bocian, D. F.; Holten, D.; Lindsey, J. S. *J. Org. Chem.* **1999**, *64*, 9090.
(176) Li, J.; Lindsey, J. S. *J. Org. Chem.* **1999**, *64*, 9101.
(177) Liu, J.-Y.; Ermilov, E. A.; Roder, B.; Ng, D. K. P. *Chem. Commun.* **2009**, 1517.
(178) Ermilov, E. A.; Liu, J.-Y.; Ng, D. K. P.; Roder, B. *Phys. Chem. Chem. Phys.* **2009**, *11*, 6430.
(179) Rio, Y.; Seitz, W.; Gouloumis, A.; Vazquez, P.; Sessler, J. L.; Guldi, D. M.; Torres, T. Submitted for publication.
(180) Gonzalez-Rodriguez, D.; Claessens, C. G.; Torres, T.; Liu, S.; Echegoyen, L.; Vila, N.; Nonell, S. *Chem.—Eur. J.* **2005**, *11*, 3881.
(181) Xu, H.; Ng, D. K. P. *Inorg. Chem.* **2008**, *47*, 7921.
(182) Gonzalez-Rodriguez, D.; Torres, T.; Olmstead, M. M.; Rivera, J.; Angeles Herranz, M.; Echegoyen, L.; Atienza Castellanos, C.; Guldi, D. M. *J. Am. Chem. Soc.* **2006**, *128*, 10680.
(183) Medina, A. S.; Claessens, C. G.; Rahman, G. M. A.; Lamsabhi, A. M.; Mo, O.; Yanez, M.; Guldi, D. M.; Torres, T. *Chem. Commun.* **2008**, 1759.
(184) Liu, J.-Y.; Yeung, H.-S.; Xu, W.; Li, X.; Ng, D. K. P. *Org. Lett.* **2008**, *10*, 5421.
(185) Poole, C. P., Owens, F. J. *Introduction to Nanotechnology*; Wiley-Interscience: Weinheim, Germany, 2003.
(186) Lee, M.; Im, J.; Lee, B. Y.; Myung, S.; Kang, J.; Huang, L.; Kwon, Y. -K.; Hong, S. *Nat. Nanotechnol.* **2006**, *1*, 66.
(187) Borghetti, J.; Derycke, V.; Lenfant, S.; Chenevier, P.; Filoramo, A.; Goffman, M.; Vuillaume, D.; Bourgoin, J.-P. *Adv. Mater.* **2006**, *18*, 2535.
(188) Ago, H.; Petritsch, K.; Shaffer, M. S. P.; Widle, A. H.; Friend, R. H. *Adv. Mater.* **1999**, *11*, 1281.
(189) Barazouk, S.; Hotchandani, S.; Vinodgopal, K.; Kamat, P. V. *J. Phys. Chem. B* **2004**, *108*, 17015.
(190) Chaudhary, S.; Lu, H.; Müller, A. M.; Bardeen, C. J.; Ozkan, M. *Nanolett.* **2007**, *7*, 1973.
(191) Kongkanand, A.; Martínez-Domínguez, R.; Kamat, P. V. *Nanolett* **2007**, *7*, 676.
(192) Sgobba, V.; Guldi, D. M. *J. Mater. Chem.* **2008**, *18*, 153.
(193) Kam, N. W. S.; O'Connell, M.; Wisdom, J. A.; Dai, H. P. *Proc. Natl. Acad. Sci. U.S.A.* **2005**, *102*, 11600.
(194) Ijima, S. *Nature* **1991**, *354*, 56.
(195) Guldi, D. M.; Marcaccio, M.; Paolucci, D.; Paolucci, F.; Tagmatarchis, N.; Tasis, D.; Vázquez, E.; Prato, M. *Angew. Chem., Int. Ed.* **2003**, *42*, 4206.
(196) Yang, X.; Lu, Y.; Ma, Y.; Li, Y.; Du, F.; Chen, Y. *Chem. Phys. Lett.* **2006**, *420*, 416.
(197) Herranz, M. A.; Martin, N.; Campidelli, S.; Prato, M.; Brehm, G.; Guldi, D. M. *Angew. Chem., Int. Ed.* **2006**, *45*, 4478.
(198) Herranz, M. A.; Ehli, C.; Campidelli, S.; Gutierrez, M.; Hug, G. L.; Ohkubo, K.; Fukuzumi, S.; Prato, M.; Martin, N.; Guldi, D. M. *J. Am. Chem. Soc.* **2008**, *130*, 66.
(199) Murakami, H.; Nomura, T.; Nakashima, M. *Chem. Phys. Lett.* **2003**, *378*, 481.
(200) Guldi, D. M.; Rahman, G. M. A.; Jux, N.; Tagmatarchis, N.; Prato, M. *Angew. Chem., Int. Ed.* **2004**, *43*, 5526.

(201) Baskaran, D.; Mays, J. W.; Zhang, X. P.; Bratcher, M. S. *J. Am. Chem. Soc.* **2005**, *127*, 6916.
(202) Guldi, D. M.; Taieb, H.; Rahman, G. M. A.; Tagmatarchis, N.; Prato, M. *Adv. Mater.* **2005**, *17*, 871.
(203) Tanaka, H.; Yajima, T.; Matsumoto, T.; Otsuka, Y.; Ogawa, T. *Adv. Mater.* **2006**, *18*, 1411.
(204) Guldi, D. M.; Rahman, G. M. A.; Quin, S.; Tchoul, M.; Ford, W. T.; Marcaccio, M.; Paolucci, D.; Paolucci, F.; Campidelli, S.; Prato, M. *Chem.−Eur. J.* **2006**, *12*, 2152.
(205) Chitta, R.; Sandanayaka, A. S. D.; Schumacher, A. L.; D'Souza, L.; Araki, Y.; Ito, O.; D'Souza, F. *J. Phys. Chem. C* **2007**, *111*, 6947.
(206) Ehli, C.; Rahman, G. M. A.; Jux, N.; Balbinot, D.; Guldi, D. M.; Paolucci, F.; Marcaccio, M.; Paolucci, D.; Melle-Franco, M.; Zerbetto, F.; Campidelli, S.; Prato, M. *J. Am. Chem. Soc.* **2006**, *128*, 11222.
(207) Alvaro, M.; Atienzar, P.; de la Cruz, P.; Delgado, J. L.; Troiani, V.; García, H.; Langa, F.; Palkar, A.; Echegoyen, L. *J. Am. Chem. Soc.* **2006**, *128*, 6626.
(208) Yu, J.; Mathew, S.; Flavel, B. S.; Johnston, M. R.; Shapter, J. G. *J. Am. Chem. Soc.* **2008**, *130*, 8788.
(209) Guldi, D. M.; Rahman, G. M. A.; Prato, M.; Jux, N.; Qin, S.; Ford, W. *Angew. Chem., Int. Ed.* **2005**, *44*, 2015.
(210) Sgobba, V.; Rahman, G. M. A.; Guldi, D. M.; Jux, N.; Campidelli, S.; Prato, M. *Adv. Mater.* **2006**, *18*, 2264.
(211) Hasobe, T.; Fukuzumi, S.; Kamat, P. V. *J. Phys. Chem. B* **2006**, *110*, 25477.
(212) Qiu, H.; Maeda, Y.; Akasaka, T. *J. Am. Chem. Soc.* **2009**, *131*, 16529.
(213) Liu, J.; Rinzler, A. G.; Dai, H.; Hafner, J. H.; Bradley, R. K.; Boul, P. J.; Lu, A.; Iverson, T.; Shelimov, K.; Huffman, C. B.; Rodriguez-Macias, F.; Shon, Y. S.; Lee, T.; Colbert, D. T.; Smalley, R. E. *Science* **1998**, *280*, 1253.
(214) de la Torre, G.; Blau, W.; Torres, T. *Nanotechnology* **2003**, *14*, 765.
(215) Xu, H. B.; Chen, H. Z.; Shi, M. M.; Bai, R.; Wang, M. *Mater. Chem. Phys.* **2005**, *94*, 342.
(216) Yang, Z.-L.; Chen, H.-Z.; Cao, L.; Li, H.-Y.; Wang, M. *Mater. Sci. Eng., B* **2004**, *106*, 73.
(217) He, N.; Chen, Y.; Bai, J.; Wang, J.; Blau, W. J.; Zhu, J. *J. Phys. Chem. B* **2009**, *113*, 13029.
(218) Yang, Z.; Pu, H.; Yuan, J.; Wan, D.; Liu, Y. *Chem. Phys. Lett.* **2008**, *465*, 73.
(219) Dyke, C. A.; Tour, J. M. *J. Phys. Chem. A* **2004**, *51*, 11151.
(220) Georgakilas, V.; Kordato, K.; Prato, M.; Guldi, D. M.; Holzinger, M.; Hirsch, A. *J. Am. Chem. Soc.* **2002**, *124*, 760.
(221) Ballesteros, B.; de la Torre, G.; Ehli, C.; Rahman, G. M. A.; Agulló-Rueda, F.; Guldi, D. M.; Torres, T. *J. Am. Chem. Soc.* **2007**, *129*, 5061.
(222) Campidelli, S.; Ballesteros, B.; Filoramo, A.; Diaz Díaz, D.; de la Torre, G.; Torres, T.; Rahman, G. M. A.; Ehli, C.; Kiessling, D.; Werner, F.; Sgobba, V.; Guldi, D. M.; Cioffi, C.; Prato, M.; Bourgoin, J. P. *J. Am. Chem. Soc.* **2008**, *130*, 11503.
(223) Bahr, J.; Tour, J. M. *Chem. Mater.* **2001**, *13*, 3823.
(224) Wang, B. X.; Liu, Y. Q.; Qiu, W. F.; Zhu, D. B. *J. Mater. Chem.* **2002**, *12*, 1636.
(225) Hatton, R. A.; Blanchard, N. P.; Stolojan, V.; Miller, A. J.; Silva, S. R. P. *Langmuir* **2007**, *23*, 6424.
(226) Chen, R. J.; Zhang, Y.; Wang, D.; Dai, H. *J. Am. Chem. Soc.* **2001**, *123*, 3838.
(227) Kyatskaya, S.; Mascaros, J. R. G.; Bogani, L.; Hennrich, F.; Kappes, M.; Wernsdorfer, W.; Ruben, M. *J. Am. Chem. Soc.* **2009**, *131*, 15143.
(228) Khlobystov, A. N.; Britz, D. A.; Briggs, A. D. *Acc. Chem. Res.* **2005**, *38*, 901.
(229) Schulte, K.; Swarbrick, J. C.; Smith, N. A.; Bondino, F.; Magnano, E.; Khlobystov., A. N. *Adv. Mater.* **2007**, *19*, 3312.
(230) Zhang, M.; Murakami, T.; Ajima, K.; Tsuchida, K.; Sandanayaka, A. S. D.; Ito, O.; Iijima, S.; Yudasaka, M. *Proc. Natl. Acad. Sci. U.S.A.* **2008**, *105*, 14773.
(231) Cao, L.; Chen, H.; Wang, M.; Sun, J.; Zhang, X.; Kong, F. *J. Phys. Chem. B* **2002**, *106*, 8971.
(232) Cao, L.; Chen, H.-Z.; Zhou, H.-B.; Zhu, L.; Sun, J.-Z.; Zhang, X.-B.; Xu, J. M.; Wang, M. *Adv. Mater.* **2003**, *15*, 909.
(233) Dillo, A. C.; Gennett, T.; Jones, K. M.; Alleman, J. L.; Parrila, P. A.; Heben, M. J. *Adv. Mater.* **1999**, *11*, 1354.
(234) Ozoemena, K. I.; Nyokong, T.; Westbroek, P. *Electroanalysis* **2003**, *15*, 1762.
(235) Siswana, M. P.; Ozoemena, K. I.; Nyokong, T. *Electrochim. Acta* **2006**, *52*, 114.
(236) Silva, J. F.; Griveau, S.; Richard, C.; Zagal, J. H.; Bedioui, F. *Electrochem. Commun.* **2007**, *9*, 1629.
(237) Geraldo, D. A.; Chamunorwa, A. T.; Limson, J.; Nyokong, T. *Electrochim. Acta* **2006**, *53*, 8051.
(238) Porras-Gutierrez, A. G.; Gutierrez-Granados, S.; Alatorre-Ordaz, A.; Griveau, S.; Richard, C.; Zagal, J. H.; Bedioui, F. *ECS Trans.* **2008**, *15*, 133.
(239) Moraes, F. C.; Cabral, M. F.; Machado, S.A. S.; Mascaro, L. H. *Electroanalysis* **2008**, *20*, 851.
(240) Zagal, J. H.; Griveau, S.; Ozoemena, K. I.; Nyokong, T.; Bedioui, F. *J. Nanosci. Nanotechnol.* **2009**, *9*, 2201.
(241) Ozoemena, K. I.; Nyokong, T.; Nkosi, D.; Chambrier, I.; Cook, M. J. *Electrochim. Acta* **2007**, *52*, 4132.
(242) Siqueira, J. R., Jr.; Gasparotto, L. H. S.; Oliveira, O. N., Jr.; Zucolotto, V. *J. Phys. Chem. C* **2008**, *112*, 9050.
(243) Ye, J.-S.; Wen, Y.; Zhang, W. D.; Cui, H. F.; Xu, G. Q.; Sheu, F.-S. *Electroanalysis* **2005**, *17*, 89.
(244) Wang, J.; Blau, W. J. *Chem. Phys. Lett.* **2008**, *465*, 265.
(245) Nojiri, T.; Alam, M. M.; Konami, H.; Watanabe, A.; Ito, O. *J. Phys. Chem. A* **1997**, *101*, 7943.
(246) Ray, A.; Goswami, D.; Chattopadhyay, S.; Bhattacharya, S. *J. Phys. Chem. A* **2008**, *112*, 11627.
(247) El-Khouly, M. E.; Islam, S. D. M.; Fujitsuka, M.; Ito, O. *J. Porphyrins Phthalocyanines* **2000**, *4*, 713.
(248) Luo, H.; Fujitsuka, M.; Ito, O.; Kimura, M. *J. Photochem. Photobiol., A* **2003**, *156*, 31.
(249) Loi, M. A.; Denk, P.; Hoppe, H.; Neugebauer, H.; Winder, C.; Meissner, D.; Brabec, C.; Sariciftci, N. S.; Gouloumis, A.; Vazquez, P.; Torres, T. *J. Mater. Chem.* **2003**, *13*, 700.
(250) Neugebauer, H.; Loi, M. A.; Winder, C.; Sariciftci, N. S.; Cerullo, G.; Gouloumis, A.; Vazquez, P.; Torres, T. *Sol. Energy Mater. Sol. Cells* **2004**, *83*, 201.
(251) Niemi, M.; Tkachenko, N. V.; Efimov, A.; Lehtivuori, H.; Ohkubo, K.; Fukuzumi, S.; Lemmetyinen, H. *J. Phys. Chem. A* **2008**, *112*, 6884.
(252) Atienza, C.; Martin, N.; Wielopolski, M.; Haworth, N.; Clarkc, T.; Guldi, D. M. *Chem. Commun.* **2006**, 3202.
(253) Giacalone, F.; Segura, J. L.; Martin, N.; Guldi, D. M. *J. Am. Chem. Soc.* **2004**, *126*, 5340.
(254) Lemmetyinen, H.; Tkachenko, N. V.; Efimov, A.; Niemi, M. *J. Phys. Chem. B* **2009**, *113*, 11475.
(255) Loi, M. A.; Denk, P.; Hoppe, H.; Neugebauer, H.; Meissner, D.; Winder, C.; Brabec, C. J.; Sariciftci, N. S.; Gouloumis, A.; Vazquez, P.; Torres, T. *Synth. Met.* **2003**, *137*, 1491.
(256) D'Souza, F.; Gadde, S.; El-Khouly, M. E.; Zandler, M. E.; Araki, Y.; Ito, O. *J. Porphyrins Phthalocyanines* **2005**, *9*, 698.
(257) Sessler, J. L.; Jayawickramarajah, J.; Gouloumis, A.; Torres, T.; Guldi, D. M.; Maldonado, S.; Stevenson, K. J. *Chem. Commun.* **2005**, 1892.
(258) Sandanayaka, A., S. D.; Ito, O.; Zhang, M.; Ajima, K.; Iijima, S.; Yudasaka, M.; Murakami, T.; Tsuchida, K. *Adv. Mater.* **2009**, *21*, 4366.
(259) Tang, C. W. *Appl. Phys. Lett.* **1986**, *48*, 183.
(260) Yu, G.; Gao, J.; Hummelen, J. C.; Wudl, F.; Heeger, A. J. *Science* **1995**, *270*, 1789.
(261) Dennler, G.; Scharber, M. C.; Brabec, C. J. *Adv. Mater.* **2009**, *21*, 1323, and references therein.
(262) Heremans, P.; Cheyns, D.; Rand, B. P. *Acc. Chem. Res.* **2009**, *42*, 1740.
(263) Morenzin, J.; Schlebusch, C.; Kessler, B.; Eberhardt, W. *Phys. Chem. Chem. Phys.* **1999**, *1*, 1765.
(264) Tsuzuki, T.; Hirota, N.; Noma, N.; Shirota, Y. *Thin Solid Films* **1996**, *273*, 177.
(265) Tsuzuki, T.; Shirota, Y.; Rostalski, J.; Meissner, D. *Sol. Energy Mater. Sol. Cells* **2000**, *61*, 1.
(266) Ding, H.; Ram, M. K.; Zheng, L.; Nicolini, C. *J. Mater. Sci.* **2001**, *36*, 5423.
(267) Pannemann, C.; Dyakonov, V.; Parisi, J.; Hild, O.; Wöhrle, D. *Synth. Met.* **2001**, *121*, 1585.
(268) Ng, T. W.; Lo, M. F.; Fung, M. K.; Lai, S. L.; Liu, Z. T.; Lee, C. S.; Leeb, S. T. *Appl. Phys. Lett.* **2007**, *95*, 203303/1.
(269) Sullivan, P.; Heutz, S; Schultes, S. M.; Jones, T. S. *Appl. Phys. Lett.* **2004**, *84*, 1210.
(270) Heutz, S; Sullivan, P.; Sanderson, B. M.; Schultes, S. M.; Jones, T. S. *Sol. Energy Mater. Sol. Cells* **2004**, *83*, 229.
(271) Chen, L.; Tang, Y.; Fan, X.; Zhang, C.; Chu, Z.; Wang, D.; Zou, D. *Org. Electron.* **2009**, *10*, 724.
(272) Schultes, S. M.; Sullivan, P.; Heutz, S.; Sanderson, B. M.; Jones, T. S. *Mater. Sci. Eng., C* **2005**, *25*, 858.
(273) Peumans, P.; Uchida, S.; Forrest, S. R. *Nature* **2003**, *425*, 158.
(274) Rusu, M; Strotmann, J.; Vogel, M.; Lux-Steiner, M. Ch.; Fostiropoulos, K. *Appl. Phys. Lett.* **2007**, *90*, 153511/1.
(275) Gebeyehu, D.; Maennig, B.; Drechsel, J.; Leo, K.; Pfeiffer, M. *Sol. Energy Mater. Sol. Cells* **2003**, *79*, 81.
(276) Gebeyehu, D.; Pfeiffer, M.; Maennig, B.; Drechsel, J.; Werner, A.; Leo, K. *Thin Solid Films* **2004**, *451−452*, 29.
(277) Drechsel, J.; Mannig, B.; Gebeyehu, D.; Pfeiffer, M.; Leo, K.; Hoppe, H. *Org. Electron.* **2004**, *5*, 175.
(278) Maennig, B.; Drechsel, J.; Gebeyehu, D.; Simon, P.; Kozlowski, F.; Werner, A.; Li, F.; Grundmann, S.; Sonntag, S.; Koch, M.; Leo, K.;

Pfeiffer, M.; Hoppe, H.; Meissner, D.; Sariciftci, N. S.; Riedel, I.; Dyakonov, V.; Parisi, J. *Appl. Phys. A: Mater. Sci. Process.* **2004**, *79*, 1.
(279) Drechsel, J.; Mannig, B.; Kozlowski, F.; Gebeyehu, D.; Werner, A.; Koch, M.; Leo, K.; Pfeiffer, M. *Thin Solid Films* **2004**, *451−452*, 515.
(280) Meiss, J.; Leo, K.; Riede, M. K.; Uhrich, C.; Gnehr, W.-M.; Sonntag, S.; Pfeiffer, M. *Appl. Phys. Lett.* **2009**, *95*, 213306/1.
(281) Meiss, J.; Riede, M. K.; Leo, K. *Appl. Phys. Lett.* **2009**, *94*, 013303/1.
(282) Pfuetzner, S.; Meiss, J.; Petrich, A.; Riede, M.; Leo, K. *Appl. Phys. Lett.* **2009**, *94*, 223307/1.
(283) Shan, M. N.; Wang, S. S.; Bian, Z. Q.; Liu, J. P.; Zhao, Y. L. *Sol. Energy Mater. Sol. Cells* **2009**, *93*, 1613.
(284) Liu, J. P.; Wang, S. S.; Bian, Z. Q.; Shan, M. N.; Huang, C. H. *Chem. Phys. Lett.* **2009**, *470*, 103.
(285) Uchida, S.; Xue, J.; Rand, B. P.; Forrest, S. R. *Appl. Phys. Lett.* **2004**, *84*, 4218.
(286) Peumans, P.; Forrest, S. R. *Appl. Phys. Lett.* **2001**, *79*, 126.
(287) Xue, J.; Rand, B. P.; Uchida, S.; Forrest, S. R. *Adv. Mater.* **2005**, *17*, 66.
(288) Xue, J.; Uchida, S.; Rand, B. P.; Forrest, S. R. *Appl. Phys. Lett.* **2004**, *85*, 5757.
(289) Rand, B. P.; Xue, J.; Uchida, S.; Forrest, S. R. *J. Appl. Phys.* **2005**, *98*, 124902/1.
(290) Xue, J.; Rand, B. P.; Uchida, S.; Forrest, S. R. *J. Appl. Phys.* **2005**, *98*, 124903/1.
(291) Tripathi, V.; Datta, D.; Samal, G. S.; Awasthi, A.; Kumar, S. *J. Non-Cryst. Solids* **2008**, *354*, 2901.
(292) Shiokawa, H.; Hiramoto, M. *Mol. Cryst. Liq. Cryst.* **2008**, *491*, 277.
(293) Suemori, K.; Miyata, T.; Hiramoto, M.; Yokoyama, M. *Jpn. J. Appl. Phys., Part 2* **2004**, *43*, L1014.
(294) Suemori, K.; Miyata, T.; Yokoyama, M.; Hiramoto, M. *Appl. Phys. Lett.* **2005**, *86*, 063509/1.
(295) Matsuo, Y.; Sato, Y.; Niinomi, T.; Soga, I.; Tanaka, H.; Nakamura, E. *J. Am. Chem. Soc.* **2009**, *131*, 16048.
(296) Yang, F.; Forrest, S. R. *ACS Nano* **2008**, *2*, 1022.
(297) Yang, F.; Shtein, M.; Forrest, S. R. *Nat. Mater.* **2005**, *4*, 37.
(298) Zheng, Y.; Bekele, R.; Ouyang, J.; Xue, J. *Org. Electron.* **2009**, *10*, 1621.
(299) Li, N.; Forrest, S. R. *Appl. Phys. Lett.* **2009**, *95*, 123309/1.
(300) Yang, F.; Shtein, M.; Forrest, S. R. *J. Appl. Phys.* **2005**, *98*, 014906/1.
(301) Hsiao, S.; Whang, W.-T.; Suen, S.-C.; Shiu, J.-Y.; Chen, C.-P. *Nanotechnology* **2008**, *19*, 415603/1.
(302) Pfuetzner, S.; Meiss, J.; Petrich, A.; Riede, M.; Leo, K. *Appl. Phys. Lett.* **2009**, *94*, 253303/1.
(303) Yu, B.; Huang, L.; Wang, H.; Yan, D. *Adv. Mater.* **2010**, *22*, 1017.
(304) Janssen, A. G. F.; Riedl, T.; Hamwi, S.; Johannes, H. H.; Kowalsky, W. *Appl. Phys. Lett.* **2007**, *91*, 073519/1.
(305) Zhang, C.; Tong, S. W.; Jiang, C.; Kang, E. T.; Chan, D. S. H.; Zhu, C. *Appl. Phys. Lett.* **2008**, *92*, 083310/1.
(306) Yu, B.; Zhu, F.; Wang, H.; Li, G.; Yan, D. *J. Appl. Phys.* **2008**, *104*, 114503/1.
(307) Armstrong, N. R.; Wang, W.; Alloway, D. M.; Placencia, D.; Ratcliff, E.; Brumbach, M. *Macromol. Rapid Commun.* **2009**, *30*, 717.
(308) Murata, K.; Ito, S.; Takahashi, K.; Hoffman, B. M. *Appl. Phys. Lett.* **1996**, *68*, 427.
(309) Xue, J.; Uchida, S.; Rand, B. P.; Forrest, S. R. *Appl. Phys. Lett.* **2004**, *84*, 3013.
(310) Stübinger, T.; Brütting, W. *J. Appl. Phys.* **2001**, *90*, 3632.
(311) Lee, S.-H.; Kim, D.; Kim, J.; Shim, T.-H.; Park, J.-G. *Synth. Met.* **2009**, *159*, 1705.
(312) Kumar, H.; Kumar, P.; Chaudhary, N.; Bhardwaj, R.; Chand, S.; Jain, S. C.; Kumar, V. *J. Phys. D: Appl. Phys.* **2009**, *42*, 015102/1.
(313) Djurisic, A. B.; Kwong, C. Y.; Chui, P. C.; Chan, W. K. *J. Appl. Phys.* **2003**, *93*, 5472.
(314) Khodabakhsh, S.; Sanderson, B. M.; Nelson, J.; Jones, T. S. *Adv. Funct. Mater.* **2006**, *16*, 95.
(315) Bernede, J. C.; Berredjem, Y.; Cattin, L.; Morsli, M. *Appl. Phys. Lett.* **2008**, *92*, 083304/1.
(316) Yang, F.; Forrest, S. R. *Adv. Mater.* **2006**, *18*, 2018.
(317) Zhang, G.; Li, W.; Chu, B.; Chen, L.; Yan, F.; Zhu, J.; Chen, Y.; Lee, C. S. *Appl. Phys. Lett.* **2009**, *94*, 143302/1.
(318) Capobianchi, A.; Tucci, M. *Thin Solid Films* **2004**, *451−452*, 33.
(319) Terao, Y.; Sasabe, H.; Adachi, C. *Appl. Phys. Lett.* **2007**, *90*, 103515/1.
(320) Kim, I.; Haverinen, H. M.; Wang, Z.; Madakuni, S.; Kim, Y.; Li, J.; Jabbour, G. E. *Chem. Mater.* **2009**, *21*, 4256.
(321) Brumbach, M.; Placencia, D.; Armstrong, N. R. *J. Phys. Chem. C* **2008**, *112*, 3142.
(322) Placencia, D.; Wang, W.; Shallcross, R. C.; Nebesny, K. W.; Brumbach, M.; Armstrong, N. R. *Adv. Funct. Mater.* **2009**, *19*, 1913.
(323) Li, N.; Lassiter, B. E.; Lunt, R. R.; Wei, G.; Forrest, S. R. *Appl. Phys. Lett.* **2009**, *94*, 023307/1.
(324) Perez, M. D.; Borek, C.; Forrest, S. R.; Thompson, M. E. *J. Am. Chem. Soc.* **2009**, *131*, 9281.
(325) Chen, W.-B.; Xiang, H.-F.; Xu, Z.-X.; Yan, B.-P.; Roy, V. A. L.; Che, C.-M.; Lai, P.-T. *Appl. Phys. Lett.* **2007**, *91*, 191109/1.
(326) Chan, C. K.; Zhao, W.; Kahn, A.; Hill, I. G. *Appl. Phys. Lett.* **2009**, *94*, 203306/1.
(327) Hong, Z. R.; Lessmann, R.; Maennig, B.; Huang, Q.; Harada, K.; Riede, M.; Leo, K. *J. Appl. Phys.* **2009**, *106*, 064511/1.
(328) Sullivan, P; Jones, T. S.; Ferguson, A. J.; Heutz, S. *Appl. Phys. Lett.* **2007**, *90*, 103515/1.
(329) Heutz, S.; Cloots, R.; Jones, T. S. *Appl. Phys. Lett.* **2007**, *91*, 23314/1.
(330) Mutolo, K. L.; Mayo, E. I.; Rand, B. P.; Forrest, S. R.; Thompson, M. E. *J. Am. Chem. Soc.* **2006**, *128*, 8108.
(331) Gommans, H.; Cheyns, D.; Aernouts, T.; Girotto, C.; Poortmans, J.; Heremans, P. *Adv. Funct. Mater.* **2007**, *17*, 2653.
(332) Ma, B.; Woo, C. H.; Miyamoto, Y.; Fréchet, J. M. J. *Chem. Mater.* **2009**, *21*, 1413.
(333) Verreet, B.; Schols, S.; Cheyns, D.; Rand, B. P.; Gommans, H.; Aernouts, T.; Heremans, P.; Genoe, J. *J. Mater. Chem.* **2009**, *19*, 5295.
(334) Chu, C.-W.; Shrotriya, V.; Li, G.; Yang, Y. *Appl. Phys. Lett.* **2006**, *88*, 153504/1.
(335) Hong, Z. R.; Huang, Z. H.; Zeng, X. T. *Thin Solid Films* **2007**, *515*, 3019.
(336) Koeppe, R.; Sariciftci, N. S.; Troshin, P. A.; Lyubovskaya, R. N. *Appl. Phys. Lett.* **2005**, *87*, 244102/1.
(337) Troshin, P. A.; Koeppe, R.; Peregudov, A. S.; Peregudova, S. M.; Egginger, M.; Lyubovskaya, R. N.; Sariciftci, N. S. *Chem. Mater.* **2007**, *19*, 5363.
(338) Kim, J. Y.; Kim, K.; Coates, N. E.; Moses, D.; Nguyen, T.-Q.; Dante, M. A.; Heeger, A. J. *Science* **2007**, *317*, 222.
(339) Fischer, M. K. R.; Lopez-Duarte, I.; Wienk, M. M.; Martinez-Diaz, M. V.; Janssen, R. A. J.; Bauerle, P.; Torres, T. *J. Am. Chem. Soc.* **2009**, *131*, 8669.
(340) Ltaief, A.; Chaabane, R. B.; Bouazizi, A.; Davenas, J. *Mater. Sci. Eng., C* **2006**, *26*, 344.
(341) Johansson, E. M. J.; Yartsev, A.; Rensmo, H.; Sundström, V. *J. Phys. Chem. C* **2009**, *113*, 3014.
(342) Honda, S.; Nogami, T.; Ohkita, H.; Benten, H.; Ito, S. *ACS Appl. Mater. Interfaces* **2009**, *1*, 804.
(343) Vivo, P.; Ojala, M.; Chukharev, V.; Efimov, A.; Lemmetyinen, H. *J. Photochem. Photobiol., A* **2009**, *203*, 125.
(344) Cravino, A.; Sariciftci, N. S. *J. Mater. Chem.* **2002**, *12*, 1931.

CR900254Z